PHYSICS NEWS IN 1987

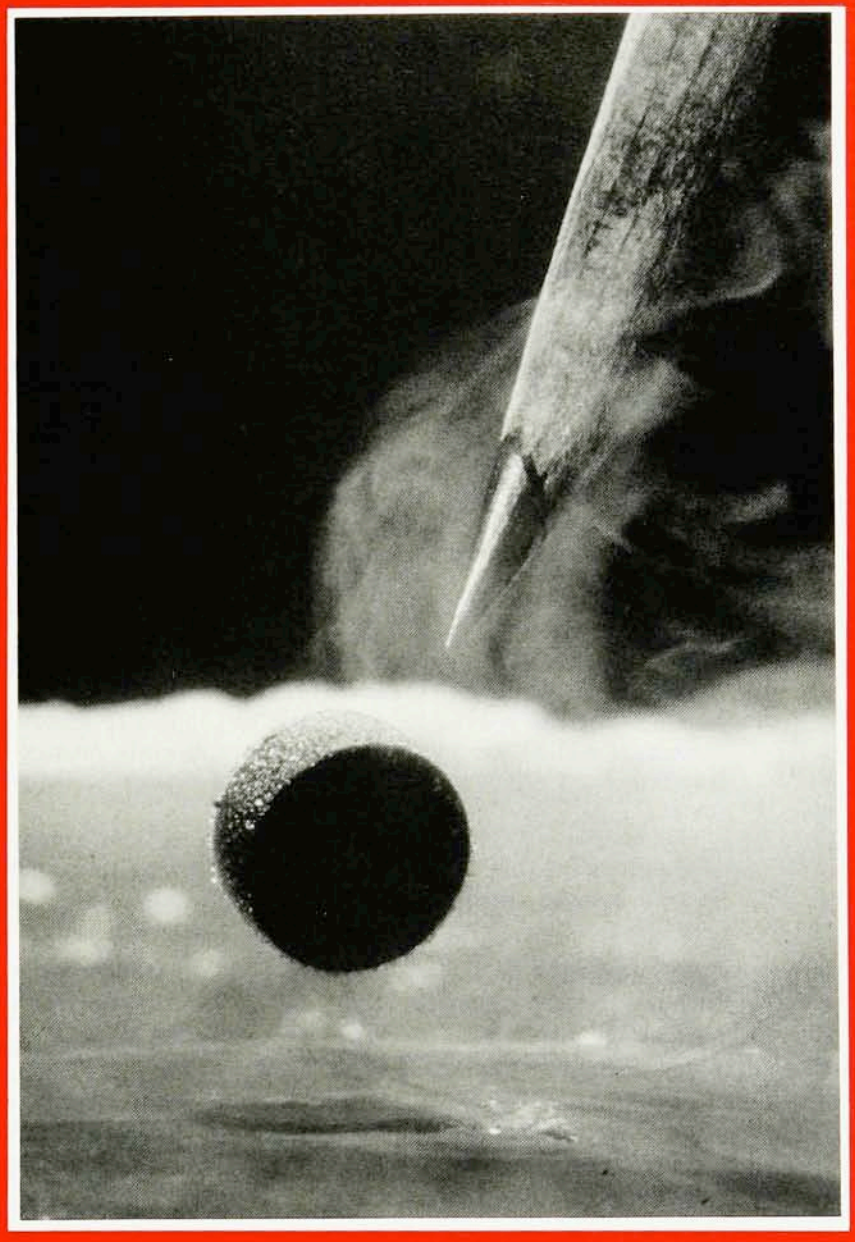

An American Institute of Physics Special Report

Phillip F. Schewe, Editor

THE AMERICAN INSTITUTE OF PHYSICS

The American Institute of Physics is a not-for-profit membership corporation chartered in New York State in 1931 for the purpose of promoting the advancement and diffusion of the knowledge of physics and its application to human welfare. Leading societies in the field of physics and astronomy are its members. AIP's activities include providing services to its Member Societies in the publishing, fiscal, and educational areas, as well as other services which can best be performed by one operating agency rather than dispersed among the constituent societies.

Member Societies arrange for scientific meetings at which information on the latest advances in physics is exchanged. They also ensure that high standards are maintained in the publication of the results of scientific research. AIP has general responsibility for the publication and distribution of journals. The Institute is expected to stay in the forefront of publishing technology and to ensure that the services it performs for its Member Societies are efficient, reliable, and economical.

The Institute publishes its own scientific journals as well as those of its Member Societies; provides abstracting and indexing services; serves the public by making available to the press and other channels of public information reliable communications on physics and astronomy; carries on extensive manpower activities; encourages and assists in the documentation and study of the history and philosophy of physics; cooperates with local, national, and international organizations devoted to physics and related sciences; and fosters the relations of physics to other sciences and to the arts and industry.

The scientists represented by the Institute through its Member Societies number more than 85,000. In addition, approximately 7000 students in over 500 colleges and universities are members of the Institute's Society of Physics Students, which includes the honor society Sigma Pi Sigma. Industry is represented through some 115 Corporate Associate members.

The purpose of the AIP's Public Information Division is to promote a public understanding of the role of physics in society and to provide an appreciation of the developments in physics by assisting Member Societies in conveying information about research, education, and manpower.

Preface

Physics News in 1987, prepared by the Public Information Division of the American Institute of Physics (AIP), is the 19th in a series of annual reviews of physics news. In past years *Physics News* was published in booklet form and was distributed to reporters, students, libraries, teachers, scientists, and to the general public. More recently *Physics News* has been published as a supplementary report in the January issue of *Physics Today*, beginning with the January 1984 issue.

The articles in *Physics News in 1987* were selected and prepared by the AIP Member Societies. The editor would like to thank the following individuals, who helped to organize the chapters and in some cases to write articles:

The American Physical Society:
Division of Chemical Physics—Stuart A. Rice, University of Chicago
Division of Condensed Matter Physics—Paul A. Fleury, AT&T Bell Labs, Murray Hill, NJ
Division of Atomic, Molecular, and Optical Physics—Stephen Chu, Stanford University
Division of Particles and Fields—Lee Pondrom, University of Wisconsin
Division of Nuclear Physics—Steven E. Koonin, California Institute of Technology
Division of Fluid Dynamics—Elaine S. Oran, Naval Research Lab
Division of Plasma Physics—Charles F. Kennell, UCLA
Division of High Polymer Physics—John F. Rabolt, IBM Almaden Research Center

Acoustical Society of America:
Daniel W. Martin, ASA Editor in Chief
Chester M. McKinney, University of Texas

Optical Society of America:
Jarus W. Quinn, OSA

American Association of Physics Teachers:
Jack M. Wilson, University of Maryland

American Crystallographic Association:
William L. Duax, Medical Foundation of Buffalo

American Astronomical Society:
Stephen P. Maran, NASA–Goddard Space Flight Center

American Association of Physicists in Medicine:
Robert L. Dixon, Wake Forest University

American Vacuum Society:
John Coburn, IBM Almaden Research Center

American Geophysical Union:
William M. Sackett, AGU

AIP Corporate Associates:
Praveen Chaudhari, IBM T. J. Watson Research Center

Phillip F. Schewe

COVER:

A magnet, made of nonsuperconducting material, floats above a sample of superconducting copper-oxide ceramic maintained at liquid-nitrogen temperatures (77 K), illustrating the Meissner effect, a phenomenon in which superconducting materials expel all magnetic fields from their interior. A pencil pointed at the magnet indicates the size scale. For more information on the subject of high-temperature superconductivity, please refer to the article on the Physics Nobel Prize and to the chapters on Condensed Matter Physics, Vacuum Physics, Crystallography, and Industrial Physics. (Photo courtesy of IBM.)

Pub. R-225.18, December 1987

Physics News in 1987
An AIP Special Report

ACOUSTICS 4
Tactile Sensory Changes in Hands Occupationally Exposed to Vibration/Arctic Ambient Noise: Ice Source Mechanics/The Coherent Scatter Boundary Wave

ASTROPHYSICS 7
Fascinating Supernova/Large Scale Streaming of Galaxies: Evidence for a Great Attractor?/A Millisecond Pulsar in a Globular Cluster/Supersonic Clumps Plow Through Cassiopeia A/Evidence for a Solar Cycle/What Makes Flares Recur at 155 or 51 Days?/Eclipses Reveal Pluto's Parameters/Very-Low-Mass Companions–Extrasolar Planets?

CHEMICAL PHYSICS 15
The Chemistry of Clusters/Two-Photon (VUV & Visible) Resonant Ionization Spectroscopy of Atoms and Molecules/Probing Unimolecular Reaction Dynamics by Vibrational Overtone Excitation/Density Functional Theory of Freezing and Solids

CONDENSED MATTER PHYSICS 18
Oxide Superconductors: An Experimenter's Dream/Oxide Superconductors: A Theorist's Challenge/Superconductivity and Magnetism in Heavy Electron Materials/Artificially Structured Magnetic Materials/Dynamics of Random Magnets/Nonlocal Quantum Transport/Membranes, Surfaces, and Microemulsions

CRYSTALLOGRAPHY 26
Biological Macromolecules/Neutron Scattering and High-T_c Superconductivity

PHYSICS EDUCATION 27
Introduction/Local Physics Alliances

ELECTRON AND ATOMIC PHYSICS 29
New Values for the Constants of Physics/Chaos in Atomic Physics/Antiprotons in an Ion Trap/Trapping Neutral Atoms

ELEMENTARY PARTICLE PHYSICS 33
Neutrinos From Supernova SN1987A/Update on the Superconducting Super Collider/The 1987 TEVATRON Collider Run/The Stanford Linear Collider/Yet Another Large Particle–Antiparticle Transition

FLUID DYNAMICS 38
The All-Wing Supersonic Plane/Dolphin Hydrodynamics/Lattice Gas Models for Fluid Dynamics

GEOPHYSICS 40
Paleoflood Hydrology/Impact Cratering/Plate Tectonic Prediction Fulfilled Dynamics of the Upper Ocean High-Pressure Experiments and the Earth's Deep Interior/The Year of Perovskite/True Polar Wander and Paleomagnetic Euler Poles

PHYSICS IN INDUSTRY 47
Progress Towards Applications of High-Temperature Superconductivity/New Approaches to X-Ray Computed Tomography/Surface Laser-Light Scattering/Low-Temperature Silicon Device Processing/Ultrashort Electrical Pulses and Their Applications

MEDICAL PHYSICS 52
Magnetic Signs of Neural Activity/Positron Emission Tomography

NUCLEAR PHYSICS 55
New Deformation Effects in Nuclei/High-Energy Nucleus–Nucleus Collisions at BNL and CERN/The Beta Decay of Tritium and the Search for Neutrino Mass/Y-Scaling in Nuclei/The M1 Scissors Mode in Nuclei

OPTICS 60
Spectral Changes and Frequency Shifts Produced by Source Correlations/External Electro-Optical Probing for High-Speed Devices and Integrated Circuits/Quantum Nondemolition Detection and Four-Mode Squeezing/Optical Associative Memories: First Step Toward Neuromorphic Optical Data Processing

PLASMA AND FUSION PHYSICS 63
Advanced Tokamaks and a Path to Ignition/Recent Progress in Laser Fusion/High-Latitude Ionospheric Structure Simulation Studies

POLYMER PHYSICS 67
Thermochromism in Long Chain Polymers/New Results on the Dynamics of Entangled Liquids

VACUUM PHYSICS 69
Thin Film Aspects of High-T_c Superconductors/Atomic Force Microscopy/Laser Surface Chemistry

PHYSICS NOBEL PRIZE 72

Tactile Sensory Changes in Hands Occupationally Exposed to Vibration

It has been known since early in this century that repeated use of hand-held or hand-guided power tools such as industrial grinders, chain saws, or rock drills may lead to adverse health effects. However, in contrast to the effects of noise on man, the consequences of exposing the hands to intense vibration have received comparatively little attention. Nevertheless, case histories and epidemiological studies have confirmed the common symptoms: periodic white fingers caused by localized arterial spasm, tingling or numbness in the hands, and a persistent reduction in tactile sensation and hand grip, often sufficient to impede the performance of fine manual tasks. This complex of vascular, neurological, and muscular disturbances has become known as the "hand-arm vibration syndrome." Its occurrence in otherwise healthy, strong men can ultimately lead to inability to continue manual work.

Quantitative assessment of the extent and degree of injury resulting from vibration exposure has proved elusive. Despite more than a decade of effort there is still no accepted, noninvasive method for determining the vascular involvement. This is thought to be a consequence of the intermittent disfunction of the blood vessels (which otherwise function within a normal range). However, considerable progress has been made during the last year in defining the tactile sensory component. This has resulted primarily from studies of vibrotactile perception in both healthy and vibration-exposed persons.

Psychophysical experiments employing selective masking and temperature control have identified four separate neural channels in the hairless skin of healthy hands operating at stimulation levels close to the threshold of vibrotactile perception.[1] With continuous sinusoidal stimulation, three of these, independently, are responsible for specific portions of the threshold-frequency function in the frequency range of 2–400 Hz.[1] The fourth channel is engaged by suprathreshold stimuli.

Neurophysiological studies of action potentials within single nerve fibers, resulting from sinusoidal vibrotactile stimulation at the fingertips, have recorded activity within four, essentially two-dimensional, matrices of tactile sensory transducers lying within 1–2 mm of the skin surface, although only three of these mechanoreceptor systems could be identified psychophysically at threshold.[2] Additional insight into the mechanisms of tactile perception has been obtained by comparing the results of vibrotactile experiments, in which the contact parameters between skin and stimulator were varied, with those of parallel studies in which the resolution of the spatial component of touch parallel to the skin surface was determined.[3]

From this work a consistent picture for the performance of normal hands has emerged. Firstly, tactual perception involving the fingers is critically dependent upon activity in one population of slowly adapting mechanoreceptors, the SAI-type receptors (so named because their action potentials persist long after a transient skin indentation), and two populations of fast-adapting receptors, FAI and FAII, which have all been identified morphologically. Secondly, vibrotactile perception at threshold can be determined by only one mechanoreceptor system through appropriate choice of frequency and contact parameters between skin and stimulator. Finally, the performance of some specific tactile tasks, such as lateral spatial resolution, is correlated with the sensitivity of one receptor matrix at the point of stimulation, in this case SAI. Hence the possibility now exists to quantify changes in mechanoreceptor performance associated with damage to the nerves and nerve endings.

The potential of such measurements for characterizing the injuries resulting from vibration exposure has recently been explored by comparing a small group of chain saw operators, all of whom report symptoms of the hand-arm vibration syndrome, with a group of healthy controls.[4] Each person was subjected to traditional neurological tests (to exclude neuropathies not related to vibration exposure) and to psychophysical measurements of vibrotactile perception thresholds and of tactile spatial resolution. Three mechanism-related patterns of threshold change have been identified.[5] The first is characterized by normal, or more sensitive than normal, thresholds in all three mechanoreceptor systems. This somewhat unexpected hypersensitivity probably reflects an initial adaptation, since subsequent measurements on one subject after an additional 20 months of exposure revealed that a rapid deterioration in threshold had occurred (to the third type of response, described below).

A second, extreme response involves abnormally insensitive thresholds in all three receptor systems. In view of the grouping of nerve fibres into bundles at a distance from the sensory transducers, it appears that this second response is indicative of damage to the nerves within the hands or arms. Such pathology has been observed in the fingers of vibration-exposed workers,[6] and is consistent with a recent analysis of sensory nerve conduction.[7] The third pattern of response involves elevated thresholds in SAI or FAII receptor systems. This response is suggestive of damage occurring at or near the sensory transducers themselves. Although pathological changes have occasionally been observed in FAII receptors,[6] the mechanisms responsible for this most common

response to vibration exposure remain to be established. Most of the workers with elevated SAI thresholds also exhibit reduced spatial discrimination, which provides an immediate measure of the potential impact on tactual function.

Anthony J. Brammer, National Research Council, Canada
and Ronald T. Verrillo, Institute for Sensory Research, Syracuse University

1. S. J. Bolanowski, G. A. Gescheider, R. T. Verrillo, and C. M. Checkosky, J. Acoust. Soc. Am. **81**, S46 (1987).
2. R. J. Lundstrom, Scand. J. Work Environ. Health **12**, 413 (1986).
3. J. E. Piercy and A. J. Brammer, J. Acoust. Soc. Am. **80**, S40 (1986).
4. A. J. Brammer, J. E. Piercy, P. L. Auger, and S. Nohara, J. Acoust. Soc. Am. **81**, S47 (1987).
5. A. J. Brammer, J. E. Piercy, P. L. Auger, and S. Nohara, J. Hand Surg. (in press).
6. T. Takeuchi, M. Futatsuka, H. Imanishi, and S. Yamada, Scand. J. Work Environ. Health **12**, 280 (1986).
7. A. J. Brammer and I. Pyykko, Scand. J. Work Environ. Health (in press).

Arctic Ambient Noise: Ice Source Mechanics

All oceans are noisy. Arctic Ocean noise originates from the ice cover, particularly from its state of stress which gives rise to fracturing. Study of noise and ice fracture processes in the Arctic has recently accelerated owing to the strategic importance of submarine operations, and to the economic importance of petroleum exploration and extraction. In this report I summarize recent progress in understanding fundamental aspects of Arctic Ocean noise as it relates to ice source mechanics.

Beyond the challenge of quantitative noise observations, there are several physical issues, such as the rheological properties of sea ice, the nature of the oceanic and atmospheric boundary layer which apply shear stresses to the ice, and the morphological features of the ice cover which may be loci for fractures. Also, while details differ, ice source mechanics bears strong resemblance to earthquake seismology and acoustic emission from dislocation motions, which are of scale much larger than and much smaller than, respectively, the scale of the ice-noise problem.

Pack ice covers the central Arctic nearly completely. It consists of first- and multi-year floes, 2–3 m thick, with joints between floes often consisting of heaped and refrozen ice blocks (known as pressure or shear ridges), or of thinner ice sheets resulting from refreezing of earlier ice openings (known as leads). Noise measured under the pack ice extends over a considerable frequency range, from 2.5 to more than 1000 Hz, with a peak at about 10–20 Hz.[1]

Considerable stresses can be accumulated in response to environmental loads, and ice can crack in response. Clues to the responsible fracture process are provided by Makris and Dyer[2] who showed that low frequency central Arctic noise correlates, over time periods of about 10 days, with stress S and stress moment M. S can be interpreted as horizontal stress acting on the ice which when multiplied by the ice sheet thickness h, gives the total horizontal force per unit width acting on an aggregate ice element of length L_s. In essence L_s is the distance between major breaks or leads in the ice, typically 100 km. Similarly, the product Mh can be interpreted as that moment around the ice's central plane acting on an element of length L_m, but here the scale is shorter, about 2 km, because flexure cannot be accumulated beyond major cracks, while horizontal forces can. S or M are the environmental clues used in seeking relevant fracture processes, at least for noise in the range 3–100 Hz.

Arctic Ocean noise is punctuated with noise events, each presumably related to ice fractures.[1,3] Is the totality of noise from 3–100 Hz explained by such events? If so, the related ice fractures should be caused by S or M, given the high correlation between them and the continuous noise. Research indicates an affirmative answer.

Central Arctic noise events have been analyzed in detail.[3] In the 20–80 Hz band the total number of noise events observed is approximately 0.5/km^2/hr. The events occur with a frequency distribution proportional to the frequency. The events can be modeled as generated by a compact stationary dipole.

The long term average spectral density, calculated from the event strengths and number density, is consistent with measured spectra; to within an order of magnitude the average noise observed at low frequencies in the central Arctic can be thought to originate from a large number of acoustic events aggregated over the entire ocean basin.[3] Since this conclusion is based on measured event data and fairly straightforward theory, I have high confidence in its validity. (The theory integrates events over the entire Arctic Ocean and includes, among others, estimates of event time duration, propagation absorption, sound speed profile, and observation depth effects.)

This result is not without controversy. The events were measured with the ice cover visually unperturbed, its usual state. When ice creates pressure or shear ridges, the action is often quite dramatic and some researchers ascribe the continuous noise over the entire Arctic to such processes.[5,6] Unquestionably ridges radiate noise when active, that is, when being formed or dramatically modified. But ridges occupy a small area of the entire ice cover[7] and only a small fraction of the ridges are active at any one time. Because of their spatial/temporal infrequency, I ascribe to them a secondary role.

A homogeneous sheet of ice will withstand environmental forcing at the levels observed without breaking. Thus fracture models must contain one or more ice inhomogeneities that produce stress concentrations. Ice morphology suggests two possibilities that have been explored in some detail.[8] One is ridge-forcing by M, the other ice-overthrusting caused by S.

In ridge forcing, ice is modeled along ridge lines as a series of bumps called hummocks. These occupy about 10^{-3} of the total ice area, or about 10^{-1} of the ridge area, and are the loci of opposing wind and current drag forces which actually

apply the environmental moment to the ice. At each hummock, ice is deformed by the moment, cracks first appear as lines radiating from the hummock, and then a circumferential crack appears at the hummock itself. Once broken at the hummock the deformed ice returns to its floating rest position. Acceleration of the mass in this unloading motion gives rise to the dipole force, and to acoustic radiation.

The ridge-forcing model works quite well. It predicts local stress sufficiently large to fracture ice, a deformation scale appropriate to the predominant wavelength of radiation, monotonic motion from deformed to rest state consistent with the observed event signature, and source strength as measured. It is important to realize that this benign process is nonetheless ubiquitous in space and time, and therefore can explain the total noise.

The overthrusting model serves to explain the correlation of noise with stress S.[8] Here the horizontal force is magnified and redirected to a vertical one by sliding upon a wedge. The model predicts local stress sufficient to break ice, block length consistent with the predominant wavelength (a finite block is formed), and source strength as observed. Unlike moment-induced deformation, the dynamic motion in this model is a damped sinusoid, the ice block acting as a free–free resonant system. Such signatures are observed in the Arctic, although less frequently than those associated with monotonic motion as in moment-induced deformation unloading.

For frequencies greater than 100 Hz other models would have to be devised. Already mentioned are crack opening or sliding noises, caused by S or M, or by heat flux.[9] Also ice diffusion is known to occur, suggesting relaxation oscillations along sliding surfaces of adjacent floes. Near the margins, where the ice transitions from continuous cover of the pack ice to ice-free water of the open oceans, bumping and gravity wave stresses can contribute as well. Thus progress summarized here is but appetizer for a rich meal yet to be served and digested.

Ira Dyer, Massachusetts Institute of Technology

1. I. Dyer, *Arctic Technology and Policy*, edited by I. Dyer and C. Chryssostomidis (McGraw–Hill, New York, 1984), pp 11–37.
2. N. C. Makris and I. Dyer, J. Acoust. Soc. Am. **79**, 1434 (1986).
3. M. Townsend-Manning and I. Dyer, submitted to J. Acoust. Soc. Am. (1987).
4. G. W. Shepard, MIT Thesis (1979).
5. R. S. Pritchard, J. Acoust. Soc. Am. **75**, 419 (1984).
6. B. M. Buck and J. H. Wilson, J. Acoust. Soc. Am. **80**, 256 (1986).
7. V. P. Gavrilo, V. D. Grishchenko, and V. S. Loschilov, in *Dynamics of Ice Cover*, edited by L. A. Timokhov (Gidrometeoizdat, Leningrad, 1974; translated by Amerind, New Delhi, 1984).
8. I. Dyer, Proceedings of the Natural Mechanisms of Surface Generated Noise in the Ocean, NATO Advanced Research Workshop, Lerici, Italy, June 1987 (to be published by Plenum Press).
9. A. R. Milne, J. Geophys. Res. **77**, 2177 (1972).

The Coherent Scatter Boundary Wave

One of the long-held beliefs of propagation physicists has been shattered by recent theoretical and experimental studies. The expectation that coherent sound which is specularly scattered from a *rough* rigid surface will be weaker than sound reflected from a *smooth* rigid surface turns out to be untrue in certain cases.

When the scattering surface is comprised of steep-sloped elements (e.g., close-packed hemispheres) a point source radiating low frequency sound at grazing incidence generates a subsonic dispersive scattered wave, the "boundary wave", which may be stronger than the incident wave. The effect is caused by multiple coherent forward scatter, which is significant when the product of the propagation constant and a typical linear dimension (e.g., the radius in the case of hemispherical bosses) is less than 1. Since the boundary wave propagates cylindrically, whereas the direct wave is spherically divergent, the boundary wave will become larger than the direct wave at sufficiently practical ranges. And the phasor sum of the boundary wave and the direct wave, which is called the rough surface wave, can also be significantly larger than the wave propagating over a smooth surface.

The boundary wave that is generated by coherent scatter was first predicted[1] by assuming that the low frequency scatter was equivalent to radiation from a surface distribution of compact elements consisting of monopoles and dipoles.[2–4] Experimental verification quickly followed for the case of hemispherical bosses[5] and other periodic surfaces.[6]

Even randomly rough natural surfaces, such as sand or gravel, experience the growth of a boundary wave at near grazing incidence, with the consequence that the acoustic pressure on the rough surface can be more than twice as great as on a smooth rigid surface.[7]

Other laboratory experiments have demonstrated that the boundary wave diffracts over a wedge in the same manner as a direct wave[6]; that the velocity dispersion near a rough boundary can cause wave refraction at a rough ocean bottom[8]; and that a rigid waveguide with steep-sloped roughness elements on one or more surfaces suffers significant changes of the eigenmodes and eigenfrequencies compared to a smooth-walled waveguide.[9]

Additional low frequency treatments have now been given for various roughness elements[10] as well as the complete behavior of the phenomenon over extended ranges to show the roles of interference and damping on the components in the Sommerfeld type uniform asymptotic presentation.[11,12]

Herman Medwin, Naval Postgraduate School, Monterey, CA

1. I. Tolstoy, J. Acoust. Soc. Am. **66** 1135 (1979).
2. M. A. Biot, J. Acoust. Soc. Am. **44**, 1616 (1968).
3. V. Twersky, J. Acoust. Soc. Am. **29**, 209 (1957).
4. M. J. Lighthill, *Waves in Fluids* (Cambridge Univ. Press, Cambridge, 1978).
5. H. Medwin, J. Bailie, J. Bremhorst, B. J. Savage, and I. Tolstoy, J. Acoust. Soc. Am. **66**, 1131 (1984).
6. H. Medwin, G. L. D'Spain, E. Childs, and S. J. Hollis, J. Acoust. Soc. Am. **76**, 1774 (1984).
7. H. Medwin and G. L. D'Spain, J. Acoust. Soc. Am. **79**, 657 (1986).
8. H. Medwin and J. C. Novarini, J. Acoust. Soc. Am. **76**, 1791 (1984).
9. H. Medwin, K. J. Reitzel, and G. L. D'Spain, J. Acoust. Soc. Am. **80**, 1507 (1986).
10. I. Tolstoy, J. Acoust. Soc. Am. **75**, 1 (1984).
11. R. J. Lucas and V. Twersky, J. Acoust. Soc. Am. **76**, 1847 (1984).
12. R. J. Lucas and V. Twersky, J. Acoust. Soc. Am. **81**, 619 (1987).

ASTROPHYSICS

If 1987 was the year of high-temperature superconductivity for physicists, it was supernova year for astronomers, and a year that saw a marked increase in their use of supercomputers too. Supernova 1987a appeared in a nearby galaxy, so far south that it passed overhead in Antarctica. It was the first supernova readily visible with the naked eye since the invention of the telescope and the nearest supernova, by a large factor, since the advent of orbiting observatories.

Supercomputers, one of the newest tools of the astronomer, have been highly publicized for grinding out elaborate theoretical calculations, but they are important to observers too. In work reported during 1987, supercomputers were used to study the remains of an earlier supernova, Cassiopeia A, and to assist in the identification of an unusual pulsar, PSR 1821-24 in the globular star cluster M 28. Since PSR 1821-24 is a superb natural clock, measurements of slow changes in its apparent 3-msec pulse rate are expected to reveal the three-dimensional space motion of the globular cluster in which it is found.

Cosmologists continued patient campaigns to map the distributions of matter and velocity on large scales. Among the significant findings was evidence pointing toward the constellations Hydra and Centaurus. Far beyond those stars is a supercluster of galaxies and beyond the Hydra–Centaurus supercluster there may be a "Great Attractor," which is perhaps a very massive supercluster but may be something much stranger. The gravitation of the G. A. may be the cause of an observed large-scale streaming of galaxies in our region of space which seem to be moving systematically with respect to the general "Hubble flow" associated with the expansion of the universe.

Closer to home, basic properties of the sun are still being sought. Here, the long-term collection of basic solar data by satellite instruments and ground-based telescopes continues to pay rich dividends. For example, independent analyses of several databases have converged on a new concept of the famous 11-year sunspot cycle. It seems that successive "cycles" are initiated at 11-year intervals, but that each may persist for at least 18 years. Thus successive sunspot cycles overlap, and a magnetic roadmap is absolutely necessary to understand the activity on the sun. "Necessary" does not mean "sufficient," however; apparently much more also must be learned about solar oscillations before the underlying phenomena of the sunspot cycle can be established with confidence. Another solar phenomenon under current investigation is an apparent 155-day (or 51-day) periodicity in the occurrence rate of solar flares, a surprising finding from the Solar Maximum Mission satellite that inspired searches through older databases with intriguing results.

Although no planet was visited by a spacecraft during 1987, Pluto let slip some secrets, thanks to an ongoing series of mutual transits and occultations of that planet and its large moon, Charon. The distant world's series of eclipse-like events occurs only once every 124 years and lasts just five years. During the current series, which will end in 1990, there is an event every three days. Astronomers are investigating the sizes, albedos, colors, surface markings, and surface constituents of the two objects and also a possible Pluto atmosphere.

Some years ago, astronomers desirous of locating planets of stars beyond the sun were advised by a noted chemist to take gas to their telescope. This advice bore fruit in 1987 when the results of six years spent monitoring starlight that was passed through a novel hydrogen fluoride gas absorption cell and into a spectrograph provided what seems to be the best evidence yet for very-low-mass companions of nearby stars. Although the suggested existence of planets around epsilon Eridani, gamma Cephei, and five other solar-type stars requires independent confirmation, the data almost surely exclude the common presence of more massive "brown dwarfs" as attendants of sunlike stars, a result expected from the theory of binary star formation, but nevertheless of considerable interest.

As usual, astronomers who teach international units to undergraduates lapse into more convenient dimensions in their writing. In the following eight articles, look out for *light year* (about 9.5×10^{17} cm), *megaparsec* or Mpc (about 3.1×10^{24} cm), *solar mass* (about 2×10^{33} g), and *jupiter* (the mass of Jupiter, about 10^{-3} solar masses).

Stephen P. Maran, NASA–Goddard Space Flight Center

Fascinating Supernova

The first supernova visible to the naked eye since Kepler's star of AD 1604 was discovered on February 23, 1987. Spotted from the University of Toronto Southern Station and the Las Campanas Observatory, both near La Serena, Chile, and from Nelson, New Zealand,[1] Supernova 1987a is in the Large Magellanic Cloud, a satellite galaxy of the Milky Way. Though not the nearest supernova since Kepler's (that distinction belongs to Cassiopeia A; see the accompanying article by Dickel), SN1987a is the brightest and nearest supernova found since astronomers began operating telescopes in space.

SN1987a is located in a region of active star formation near the bright Tarantula Nebula, about 170 000 light years from Earth (see Fig. 1). Unlike almost all other known supernovae, its progenitor star—the object that exploded—has been identified in records of past observations. The progeni-

FIG. 1. Arrow marks Supernova 1987a, photographed on February 25, 1987 from the Cerro Tololo Inter-American Observatory by Wendy Roberts of the Harvard–Smithsonian Center for Astrophysics. (Credit: National Optical Astronomy Observatories.)

tor appears to have been Sanduleak $-69°\,202$, a twelfth magnitude blue supergiant previously catalogued by Nicholas Sanduleak of Case Western Reserve University. Upon discovery, SN1987a had a visual magnitude of about 4.5. Over succeeding days, it brightened by only 0.2 magnitude, and then declined, leading some observers to fear that maximum light was over. However, it rose again from magnitude 4.5, increasing in brightness for about 80 days, to reach a peak just above magnitude 3.0 around May 20–25, 1987. It then faded in a smooth, unusual fashion until, by about July 1, the expected exponential dimming began, with a roughly 110-day *e*-folding time (see Fig. 2).

Observations of SN1987a have covered almost the whole range of the electromagnetic spectrum.[2] Promptly after its discovery, the supernova was under examination with practically every ground-based optical, infrared, and radio telescope in the Southern Hemisphere. A radio burst, detected with several Australian radio telescopes, was observed at four frequencies. From space, the International Ultraviolet Explorer, the Ginga x-ray observatory, the Kvant astrophysics module on space station Mir, and the gamma-ray spectrometer of the Solar Maximum Mission all searched for signatures of the explosion. IUE observations began within hours of the discovery, and found that an initially high luminosity in the 1200–3200 angstrom band was dropping rapidly; it decreased by a factor of 1000 within the first three days, a phenomenon attributed to the rapid expansion and cooling of the explosion photosphere.[3]

Ginga, launched in early February by Japan, monitored the supernova's emissions in the 1–40 keV region, and found the x rays to increase steadily from July to late September 1987. At the higher energies, the x-ray continuum may be produced by Compton interactions of (unobserved) gamma-ray lines with ambient electrons. On SMM, the GRS set a limit on the flux of gamma rays at energies above 1 MeV that, however, did not significantly constrain models of the supernova event. A series of balloon launches from the Southern Hemisphere, carrying larger and more sensitive payloads, have since set lower limits on the still-anticipated gamma-ray flux from SN1987a. Infrared emissions were studied from the Kuiper Airborne Observatory.

SN1987a was produced by the collapse of a massive star, and is classified as a type II supernova. (In contrast, at least some type I supernova explosions result from mass transfer onto a white dwarf star in a binary system, so that accretion precedes collapse and explosion.) However, SN1987a was dimmer than a normal type II supernova, and its light curve was unusual; perhaps a lower-mass than usual stellar envelope was responsible for these conditions. Also, it occurred in a blue supergiant progenitor, whereas conventional theory anticipates that type II supernovae occur in red supergiants. A difference in chemical composition between the Large Magellanic Cloud and the Milky Way is invoked by some astrophysicists to account for this surprise.

The most spectacular aspect of the SN1987a event was the observed outburst of neutrinos from the collapse of the core of the progenitor star (see the related article in the chapter on elementary particle physics). The neutrino data from the Irvine–Michigan–Brookhaven and the Kamioka II experiments[4,5] are in good agreement with theories of type II

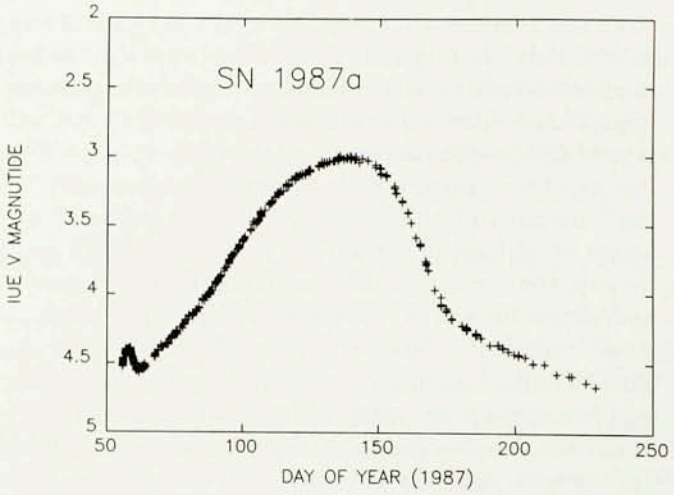

FIG. 2. Brightness variations of Supernova 1987a in visible light, as recorded by the International Ultraviolet Explorer, an orbiting observatory. Vertical scale is magnitude; horizontal scale is day of the year in 1987.

supernovae, and they may provide useful limits on the mass of the emitted neutrinos.

The most perplexing and least-anticipated phenomenon of the supernova is the reported appearance of a bright companion or "mystery spot," with a luminosity of about 10% of the supernova itself, when detected[6] on March 22, 1987 and again on April 2. The optical speckle interferometer measurements were made at Cerro Tololo Inter-American Observatory, near La Serena, and confirmed by independent work at the Anglo-Australian Observatory in Australia. While there are many theories proposed to account for the presence of this "companion," brighter than any star in the LMC galaxy except the supernova itself, and positioned just a few milliarcseconds (a projected distance of a few thousand astronomical units) from SN1987a, none yet advanced appears to be compelling and based on sound physics.

Kenneth Brecher, Boston University

1. I. Shelton, O. Duhalde, and A. Jones, International Astron. Union Circulars, No. 4316 (1987).
2. D. Helfand, Phys. Today **40** (part 1), 24 (August 1987).
3. R. Kirshner *et al.*, Astrophys. J. **320**, 602 (1987).
4. K. Hirata *et al.*, Phys. Rev. Lett. **58**, 1490 (1987).
5. R. M. Bionta *et al.*, Phys. Rev. Lett. **58**, 1494 (1987).
6. P. Nisenson *et al.*, Astrophys. J. (in press, 1987).

Large Scale Streaming of Galaxies: Evidence for a Great Attractor?

The universe is not stagnant. Galaxies are rushing away from each other with observed velocities ranging from a few hundred km/sec to 92% of the speed of light. In 1929, Edwin Hubble demonstrated that galaxies are receding from the Milky Way with a velocity that increased with distance (D) in megaparsecs (Mpc) according to the formula $v = HD$, where H is the Hubble parameter (currently believed to be between 50 and 100 km/sec/Mpc). This so-called Hubble flow is nonuniform, because the distribution of matter is inhomogeneous on scales of tens to hundreds of Mpc (and possibly on even larger scales). Matter is clumped into systems ranging from gravitationally bound small groups of galaxies to gigantic, unbound superclusters at the largest scales. The gravitational attraction of galaxies within these systems produces a departure of their velocities from those expected for uniform expansion. One can, in principle, estimate the mass of such systems by measuring the deviations of galaxy velocity from the Hubble flow.

Recently, it was reported that an enormous volume of the local universe containing at least two superclusters is systematically streaming toward a single direction as measured with respect to an inertial reference frame set by the cosmic microwave background (residue radiation from the Big Bang).[1] One interpretation of this motion is that our Milky Way Galaxy and its neighborhood are under the influence of an as-yet unidentified mass concentration, dubbed the "Great Attractor."

Evidence for such streaming can be traced in earlier work. In 1976, it was found[2] that the Milky Way has a substantial peculiar velocity, of order 500 km/sec with respect to a background of distant galaxies. In 1982, it was shown[3] that relative to spiral galaxies in ten distant clusters, the Local Group of Galaxies (which includes the Milky Way, the Andromeda Galaxy, and 15 smaller systems) is moving in a common direction. The magnitude and direction of the peculiar velocity of the Local Group may suggest that a component of this motion is toward the Virgo Cluster of Galaxies (which, together with the Local Group, forms the Local Supercluster) and that the Local Supercluster as a whole is also moving systematically, perhaps toward the next nearest supercluster in Hydra–Centaurus.[3]

In these analyses, the galaxy velocities must be measured with respect to a well-defined reference frame. The microwave background is ideal for this owing to its remarkable uniformity across the sky. Doppler shifts from the motion of our Galaxy and that of the Local Group with respect to the microwave background cause cool and hot spots in the apparent background. Thus one can determine the direction and magnitude of our motion and therefore define an absolute reference frame with respect to which galaxy streaming can be measured.

A recent study[1] extended the earlier work by enlarging the galaxy sample to encompass the entire sky. A new technique was developed to measure the distances to elliptical galaxies. This rests on the discovery of a tight correlation between the diameter of a galaxy that encloses a given integrated surface brightness (in effect, a standard candle) and the velocity dispersion of stars in the central region of the galaxy. Examination of a relatively large volume of space by this technique revealed that the Local Supercluster *and* the Hydra–Centaurus supercluster are moving at greater than 600 km/sec in the same direction with respect to the microwave background. This surprisingly large streaming motion is more than 10% of the Hubble flow velocity.

If confirmed, this observation has important consequences for the distribution of matter on very large scales. It has been suggested[4] that the streaming is caused by a "Great Attractor" that must be located beyond 120 Mpc, which is about twice the distance to the Hydra–Centaurus supercluster. Its mass would have to be twenty times larger than that of the Local Supercluster. It is unclear if the "Attractor" is simply an extraordinarily large supercluster or if it is a region of clumped dark matter, of the sort which many astronomers now believe must compose 90% of the mass of the universe.

There have been suggestions that nonuniform velocities extend to even larger scales, typical of the distances (hundreds of Mpc) between rich clusters of galaxies.[5] This would complicate the interpretation of galaxy recession velocities as being simply related to distance according to the Hubble law. Thus mapping large-scale structure becomes both more

difficult and more intriguing as a means of understanding how the universe of galaxies evolved after the Big Bang.

Jack O. Burns, The University of New Mexico

1. A. Dressler *et al.*, Astrophys. J. (Lett.) **313**, L37 (1987); Phys. Today **39**, 17 (November, 1986).
2. V. C. Rubin *et al.*, Astron. J. **81**, 687 (1976).
3. M. Aaronson *et al.*, Astrophys. J. **258**, 64 (1982).
4. A. Dressler, Sci. Am. **257**, 46 (September 1987).
5. N. A. Bahcall, R. M. Soneira, and W. S. Burgett, Astrophys. J. **311**, 15 (1986).

A Millisecond Pulsar In A Globular Cluster

The discovery of pulsating radio sources or pulsars, nearly twenty years ago, provided the first evidence for the existence of neutron stars: solar-mass stars with nuclear density. The standard model for pulsars is an isolated, rapidly rotating, highly magnetized neutron star that is converting rotational energy into relativistic particles and radiation. Thus the periods of pulsars lengthen as they age. In contrast, the evolution of neutron stars in binary systems can be more complicated. For example, mass transfer from the companion can spin up the neutron star to very high rotation rates. The recent discovery[1] of a 3-msec pulsar in the globular cluster M 28 provides strong confirmation of such "spin-up" models as well as demonstrating a strong evolutionary link between pulsars and x-ray binaries.

During the mass transfer phase, copious x rays are generated by matter falling into the deep gravitational well of the neutron star. According to the "spin-up" models, the rotation rate is limited by the magnetic moment of the neutron star. For these two reasons, the progenitors of millisecond pulsars were identified with Low Mass X-ray Binaries (LMXB).

Nearly a dozen LMXB are found in the globular clusters–dense self-gravitating star clusters containing as many as one million stars and believed to be the oldest components of our galaxy. Following the discovery of the 1.6-msec pulsar,[2] it was noted that the clusters with their extraordinary high abundance of LMXBs should be nurseries of millisecond pulsars. With this motivation, a dozen nearby globular clusters were surveyed with the Very Large Array.[3] The most promising candidate, a point source close to the center of the cluster M 28, was shown to be a weak, steep spectrum, highly polarized radio emitter[4]—attributes peculiar to pulsars. Since no pulsar was found at this location in previous searches, it was suggested that the source was a fast pulsar, which might not have been so recognized.

Proof that the point source in M 28 was indeed a fast pulsar, with a 3-msec period, or a rotation rate 11 times faster than that of the Crab pulsar, was announced in 1987 by an international team of astronomers.[1] The data were obtained with the Mark Ia 76-m radio telescope at Jodrell Bank, U.K. and were analyzed on the Los Alamos National Laboratories Cray-XMP supercomputer. A critical aspect of this work was the use of very long Fourier transforms (2^{24} points) whose development was pioneered at Berkeley and Los Alamos.

Much to everyone's surprise, the pulsar, which is designated PSR 1821–24, turned out to be a *single* star, not a binary. Theoretical models proposed to explain this pulsar take advantage of the high rate of interactions expected in the dense core of the globular cluster, including possible head-on collision of a solitary neutron star with a red giant star, disruption of a weakly bound binary by collisional perturbation, and coalescence driven by three-body encounters. All models rely upon mass transfer for spinning up the neutron star.

Timing observations have established that PSR 1821-24, like other millisecond pulsars, is an excellent clock. This property will eventually allow astronomers to obtain dynamical information about the cluster core and to determine its velocity in three dimensions and thus the space velocity of the globular cluster.

As pulsars go, PSR 1821-24 is quite bright, which suggests that a large population of fainter pulsars may exist. Many observations will be undoubtedly conducted in search of more millisecond single and binary pulsars. However, the real action will not be at the telescopes but at supercomputing centers!

The discovery of PSR 1821–24 raises new questions about the evolution of binaries in the dense environs of globular clusters. Future theoretical work will probably attempt to account for the x-ray binaries and the millisecond pulsars in one grand model. Finally, this discovery forces us once again to address the origin of neutron stars in globular clusters, the ancient regions of the galaxy.

Shrinivas R. Kulkarni, California Institute of Technology

1. A. G. Lyne *et al.*, Nature **328**, 399 (1987).
2. Phys. Today **36**, 19 (March 1983).
3. T. T. Hamilton, D. J. Helfand, and R. H. Becker, Astron. J. **90**, 606 (1985).
4. W. C. Erickson *et al.*, Astrophys. J. Lett. **314**, L45 (1987).

Supersonic Clumps Plow Through Cassiopeia A

Observations reported in 1987 brought new excitement to the study of the supernova remnant Cassiopeia A. Cas A, the brightest radio source in the sky, is the remains of a stellar explosion that probably occurred in the late seventeenth century. An international team[1] announced the first results of their detailed study of the source with the Very Large Array radio telescope (see Fig. 3). With excellent spatial resolution and a good baseline in time, they were able to follow individual features within the supernova remnant and definitively measure their motions and changes.

It appears that much of the synchrotron radio emission from Cas A arises in small, turbulent clumps that are ploughing into a roughly delineated shell, itself created by

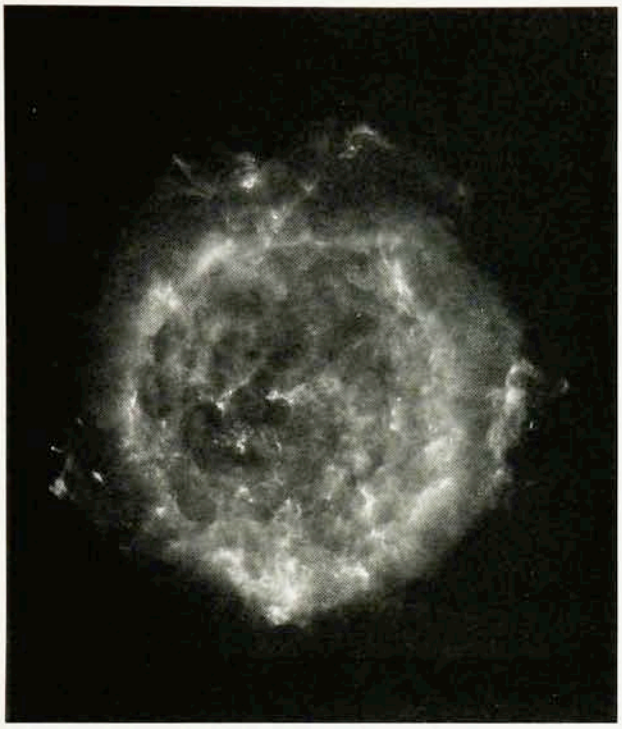

FIG. 3. Radio emission from Cassiopeia A, as observed at a wavelength of 6 cm in 1983 with the Very Large Array near Socorro, New Mexico by P. E. Angerhofer, R. Braun, S. F. Gull, R. A. Perley, and R. J. Tuffs. The data were processed on a Cray X-MP supercomputer. (Credit: National Radio Astronomy Observatory, Associated Universities, Inc.)

the deceleration of initially very rapidly moving supernova ejecta that have swept up surrounding material. The VLA observations revealed individual clumps moving supersonically through the shell. The structure around a clump appears like that of a bow shock; magnetic field draping around the clumps may produce the net radial field structure characteristic of young supernova remnants. The details are very complex, however. For example, in many places the field has an irregular orientation and the expansion is often directed at large angles to the radial direction. Fragmentation or splattering of large clumps as they encounter inhomogeneities may produce these conditions. The dynamical interaction can enhance the acceleration of relativistic particles, increasing synchrotron emissivity. Then the bigger the clump, the greater the energy delivered and the resultant radio brightness. As less dense media are encountered, a clump expands and fades. This situation is observed in several components of Cas A. The smallest features observed in the Cas A VLA maps have typical scales of about 1.3×10^{16} cm, with internal pressures that are somewhat higher than those in the average medium within the supernova remnant,[2] consistent with this scenario. Thus the small features should indeed expand adiabatically and fade.

There also are many small, denser knots in Cas A, recognized through their visible-light line emission, but unusually not coincident with radio or x-ray emitting features. A surprising new result is the spectroscopic detection of excess nitrogen in several rapidly moving visible filaments.[3] Some nitrogen-rich filaments were found earlier, but those were almost stationary and are considered to be the remains of pre-explosion mass loss from the progenitor star as it evolved toward its end as a supernova. Other previously found fast moving knots had oxygen and sulfur (not nitrogen) excesses and were assumed to be undiluted ejecta from the disrupted core of the supernova. In contrast, the fast nitrogen-rich filaments may represent fragments of the photosphere or atmospheric region of the pre-supernova star. They all are located near the outer edge of the supernova remnant, perhaps because, small and dense, they were not much decelerated by interaction with the medium encountered as they flew outward from the explosion. They remain at relatively high velocity outside most of the swept-up shell material.

The observed abundances indicate that the progenitor star of Cas A probably was a Wolf–Rayet star, of perhaps 60 solar masses. However, analysis of x-ray data plus a detailed investigation[4] of the infrared emission from dust in Cas A, as measured by the Infrared Astronomical Satellite, reveals that possibly less than 1 solar mass of ejecta and certainly less than a few solar masses have interacted with the surrounding medium. There is no evidence for a neutron star or other collapsed object in Cas A, despite careful searches, so perhaps much ejected matter has yet to manifest itself. We expect many more fascinating events in Cas A before this remarkable assemblage of exploded debris dissipates and is lost from view.

John R. Dickel, University of Illinois

1. R. Braun, S. F. Gull, and R. A. Perley, Nature **327**, 395 (1987).
2. R. G. Arendt and J. R. Dickel, Astrophys. J. **315**, 567 (1987).
3. R. A. Fesen, R. H. Becker, and W. P. Blair, Astrophys. J. **313**, 378 (1987).
4. E. Dwek *et al.*, Astrophys. J. **315**, 571 (1987).

Evidence For A Solar Cycle

The solar cycle, inferred through sunspot observations and magnetic field measurements, is an approximately 11-year periodic variation in sunspot number that is linked to the polarities of sunspot and polar magnetic fields. The standard conception that, at any given time, the sun as a whole is in some particular phase of this cycle is not compelled by the data, and a large body of new and old evidence is now forcing a change in this view. The emerging picture[1] connects the solar activity of a given cycle with a latitude zone which, in each hemisphere, originates at the pole and migrates to the equator. New zones form at each pole every 11 years; the migration takes at least 18 years: consequently, successive cycles overlap. That is, at a given time, rather than the sun as a whole being in a particular phase of the cycle, different phases of more than one cycle are present at the same time in different regions of the sun. Sunspot activity, which begins as the activity zone reaches middle latitudes, is the final phase.

For the past 30 years, observers have been reporting high-latitude zones of enhanced coronal emission that begin around the maximum of a cycle, drift equatorward and per-

sist through the minimum between cycles. These zones reach a latitude of approximately 40° in coincidence with the emergence of sunspots associated with the next solar cycle and then continue to drift toward the equator along with the spots. In the 1950s, there were several independent proposals[2] to the effect that the high-latitude emission features are early manifestations of the next cycle, but possible ambiguities in the data prevented the idea from getting much attention. A significant advance came in 1979 with the observation of small bipolar magnetic regions (ephemeral regions, "ERs"),[3] which were confined to two zones of latitude, the sunspot zone and a high-latitude zone. Those in the sunspot zone showed a statistical tendency to have a magnetic orientation appropriate to the "present" cycle, and those in the high latitude zone showed a tendency toward the opposite orientation, appropriate to the "next" cycle.

More recent evidence[1] comes from solar wind and geomagnetic data, and in particular, from the discovery of the so-called torsional oscillation,[4] a modulation of the mean solar differential rotation by a pattern of equatorward-migrating bands of faster and slower rotation. The torsional bands begin near the poles and migrate to the equator in 18–22 years. Further analysis[5] shows that the zone, between the bands, in which rotational shear enhancement is produced coincides neatly with the migrating zone of coronal emission features and ERs, and with the sunspot zone at middle-to-low latitudes. It also is a zone of apparent downflow of gases at the solar surface. Mass continuity argues against the apparent downflow being a real surface downflow and/or meridional flow. It may instead reflect a change in the surface granulation, a notion supported by a recent measurement[6] indicating that the solar surface temperature is lowered in the zone.

The migrating activity zone which characterizes the extended cycle may be the surface signature of a migrating band of strong azimuthal magnetic field. Intense deep-lying magnetic fields are thought to produce "thermal shadows" that inhibit the energy flow directly above the regions where they occur.[7] A recent model[8] proposes a large-scale pattern of counter-rotating azimuthal convective rolls near the bottom of the solar convection zone. Bands of strong azimuthal magnetic field are created at the bottoms of the rolls' subduction zones by the shear developed through the Coriolis effect. The thermal shadow created by field bands in turn reinforces and stabilizes the downflow, thereby stabilizing the rolls as well. The resulting dynamo wave propagates toward the equator, dragging the rolls along. At middle latitudes, Coriolis stresses cause the rolls to break up, allowing the azimuthal field to rise and form the active regions observed at the surface. The model invokes a transport mechanism to account for the reversal of the sun's polar magnetic field.

The original view of the solar cycle led to considerable theoretical efforts, but none of the resulting models became a paradigm.[9] Confirmation of this quite different picture of overlapping cycles is vitally dependent on the continuation of long-term synoptic observational programs such as that at Mount Wilson. Its assimilation will have a great impact on solar modeling, and might even lead to a successful theory of solar magnetism.

Herschel B. Snodgrass, Lewis and Clark College

1. P. R. Wilson *et al.*, Nature (submitted 1987); P. R. Wilson, Solar Phys. (in press, and accompanying articles 1987).
2. M. Waldmeier, *Die Sonnenkorona, Vol. II* (Basel, Birkhauser, 1957); M. Trellis, Ann. D'Astrophys. Suppl. No. 5 (1957); M. C. Bretz and D. E. Billings, Astrophys. J. **129**, 134 (1959).
3. S. F. Martin and K. L. Harvey, Solar Phys. **64**, 93 (1979).
4. R. Howard and B. J. LaBonte, Astrophys. J. (Lett.) **239**, L33 (1982).
5. H. B. Snodgrass, Astrophys. J. (Lett.) **316**, L91 (1987).
6. J. R. Kuhn, K. G. Libbrecht, and R. H. Dicke, Astrophys. J. **290**, 758 (1985).
7. E. N. Parker, Astrophys. J. **312**, 868 (1987).
8. H. B. Snodgrass and P. R. Wilson, Nature **328**, 696 (1987).
9. For an overview, see E. N. Parker, Sci. Am. **249**, 44 (August 1983).

What Makes Flares Recur at 155 or 51 Days?

Beside the sunspot cycle (see the accompanying article by Herschel Snodgrass), there are a variety of interesting time scales in solar phenomena. For example, solar physicists, struggling to understand an apparent periodicity of about 155 days in the occurrence rate of major solar flares which was suggested only in the past few years, have been confronted with the possiblity that the basic occurrence rate (if the phenomenon is real) is actually 51 days.[1] Whatever the value, such a periodicity would be an important clue to the mechanism that might make these powerful explosions occur preferentially at certain times.

Flares are short-lived outbursts of radiation and particles caused in some way by the sudden relaxation of magnetic field tension which constantly builds as magnetic flux emerges through the solar surface. Since virtually all flares occur in the vicinity of sunspots, the distribution of flares on the sun closely follows the sunspot distribution, and so the rate of occurrence of flares in general also has been expected to track the cyclic decreases and increases in the number of sunspots.

Thus the 1984 discovery[2] in data from the Solar Maximum Mission (SMM) spacecraft that the frequency of large or especially energetic flares on the sun seems to vary with a period of around 152 to 158 days was especially surprising. The effect was first found with an SMM experiment known as the Gamma-Ray Spectrometer (GRS). It was noted that flares with strong gamma-ray emission tended to occur in groups with a mean spacing of about 154 days. Similar behavior was observed for flares with high count rates as measured by SMM's Hard X-Ray Burst Spectrometer (HXRBS) and for flares with strong soft x-ray emissions as observed by the series of Geostationary Operational Environmental Satellites (GOES). An independent study[3] of a more complete set of HXRBS data yielded a consistent result, although with a period of 158 days.

The SMM database is limited, since the spacecraft was launched in 1980, during Solar Cycle 21. Therefore, the flare periodicity investigations were extended backward in time[4] by studying records of flares that produced strong microwave emission during the interval between April 1966 and December 1983, which includes Sunspot Cycle 20 (1966–1976). This revealed apparently periodic behavior (with a period of 152 days) like that found from the more recent SMM and GOES measurements, which seems to be in phase with the variations seen in Cycle 21 even though the effect was not detected during the activity minimum between the two cycles. Further support came in a report[5] that 155-day periodicity appeared to be present during Cycles 20 and 21 even in standard flare reports from ground-based H-alpha monitoring stations, as long as only major flares were considered.

At that point, the results, although still somewhat strange, at least seemed to be straightforward and fairly consistent. In fact, several authors pointed out that there was even a 1974 theoretical "prediction"[6] for the apparent period. Specifically, it had been proposed that gravity-mode oscillations of the same spherical harmonic degree (l number) coalesce to form rigidly rotating structures which produce "active longitude bands" inside the sun where the energy generation rate is enhanced. In 1983, it was further suggested[7] that when active longitude bands that correspond to different l numbers rotate past each other, strong magnetic fields are produced and hence the sunspot number increases. According to the model, the interaction between bands from the $l = 2$ and $l = 3$ gravity-mode oscillations would lead to solar activity variations with a calculated period of 155.4 days.

The latest attempt to explore the occurrence of 155-day variations in past solar cycles[1] adds new twists to the subject. To investigate the period 1955–1969, the "comprehensive flare indices" (CFI) were analyzed. The CFI's were originally computed[8] by summing up importance indices in five different aspects of solar flares, including the area of the event as observed in H-alpha as well as the microwave radio emission, and so represent the overt manifestations of solar flares very well. This study found that major flares (with CFI greater than five) apparently occurred with periodicity $P = 153$ days in Sunspot Cycle 19 (1955–1964), but only for those relatively few flares that occurred in the sun's southern hemisphere! When flares occurring over the entire disk were included, or just northern hemisphere events, the dominant period in Cycle 19 turned out to be 51 days. (Actually, there had been other reports of 51-day periodicities in measures such as the Zürich Daily Sunspot Number or the Total Solar Irradiance, but their statistical significance was unconvincing.)

A re-examination of Sunspot Cycles 20 and 21 also suggests that a periodicity of 51 days may be present, as well as one at around 77 days! Because 77 and 51 are very close to exactly one-half and one-third of 155, respectively, it has been proposed that 155 days is the fundamental period for this phenomenon. In any case, the underlying mechanism would need to be one that makes the active regions more flare productive rather than merely causing a larger number of active regions.[9] Still the question remains, are these periodicities, despite the efforts invested in documenting them, just statistical fluctuations in the enormous, changing magnetic activity of the sun? Or is there truly a periodic occurrence rate of major flares, related to some underlying global phenomenon?

Roger J. Thomas, NASA–Goddard Space Flight Center

1. T. Bai, Astrophys. J. Lett. **318**, L85 (1987).
2. E. Rieger *et al.*, Nature **312**, 623 (1984).
3. A. L. Kiplinger, B. R. Dennis, and L. E. Orwig, Bull. Am. Astron. Soc. **16**, 891 (1984).
4. R. S. Bogart and T. Bai, Astrophys. J. Lett. **299**, L51 (1985).
5. K. Ichimoto *et al.*, Nature **316**, 422 (1985).
6. C. L. Wolff, Astrophys. J. **194**, 489 (1974).
7. C. L. Wolff, Astrophys. J. **264**, 667 (1983).
8. H. W. Dodson and E. R. Hedeman, World Data Center for Solar-Terrestrial Physics Report UAG-14, Boulder: NOAA (1971).
9. T. Bai and P. A. Sturrock, Nature (in press 1987).

Eclipses Reveal Pluto's Parameters

Since Pluto was discovered in 1930, the distant planet has been an enigma. Early observations through large telescopes showed it to be unexpectedly stellar in appearance. Its orbit is also unusual, inclined to the ecliptic by 17°, and so eccentric that Pluto comes closer to the sun than Neptune for about 20 years in every 248-year orbital revolution. Pluto is closer than Neptune now, and will reach perihelion in 1989.

Little was known of Pluto until recently. Now, thanks to fortuitous geometry, the distant planet is slowly being explored. The key was the unexpected discovery of a satellite, since named Charon, in 1978. Shortly afterwards, it was realized that the orbital plane of Charon would soon line up with Earth. A series of eclipses was predicted and observations of those events began in 1985.[1] Information from the eclipses is being combined with data from other sources to home in on the diameters and other characteristics of Pluto and its moon.[2] ("Eclipse" is used informally here; technically, Charon "transits" the larger Pluto whereas Pluto "occults" Charon.)

The eclipse season comes twice in every orbit of Pluto around the sun and lasts approximately five years. The present eclipse series should extend until 1990, with an event every 3.19 days as Charon moves in its 6.38718-day orbit around Pluto.

Some recent estimates of the diameters of Pluto and Charon are derived from photometric observations made during eclipses. In the past few years, several teams of observers have published estimates, and they are beginning to approach agreement, especially on the diameter of Pluto. Early estimates range from around 2200 to 2290 kilometers, making Pluto significantly smaller than Earth's moon. For Char-

on, the estimates range from around 1160 to 1500 kilometers, so that it is about half Pluto's size. For both objects, more refined results using the accumulating eclipse event data are still forthcoming.

Although few agree on the answers, new questions are being asked about the Pluto/Charon system. For example, it is currently possible to obtain separate spectral information for Pluto and Charon. This is done by taking a spectrum of the combined light from both worlds, and then recording Pluto's spectrum alone when Charon is eclipsed. Later, the spectrum of Pluto is subtracted from the combined spectrum to yield a spectrum for Charon. Preliminary results from this technique indicate a lack of methane on Charon relative to Pluto.

Likewise, the eclipses are showing how much light Pluto and Charon each reflect back toward the sun. Early albedo measurements indicate that Charon is darker than Pluto. The relative colors of the two worlds also are being analyzed, and there is a question about whether one hemisphere of Charon is colored differently than the other.

In 1986, transits of Charon across the northern hemisphere of Pluto were monitored. By the summer of 1987, however, the satellite was making transits of the equatorial regions, and now it is beginning a series of passes across Pluto's southern hemisphere. When the eclipse season ends, and the measurements of the many events are analyzed, it will be possible to draw a crude map of the surface of Pluto, which should remain for some years to come as the best available sketch of the only planet not visited by a spacecraft in this century.

A curious feature of the eclipse studies stems from the fact that Pluto and Charon each make one rotation in the same time that Charon requires to revolve around Pluto. Consequently, a single hemisphere of Charon is locked toward the opposite hemisphere of Pluto. Thus the same hemisphere of each object always faces Earth when it is being transited or occulted.

There is special interest in data from the Infrared Astronomical Satellite, which detected weak infrared signals[3] from Pluto and Charon during its ten-month operating lifetime in 1983. Standard thermal models, which have been used successfully in the study of asteroids and the Galilean satellites, have been applied to the study of Pluto and its satellite. They indicate that the two bodies radiate heat differently, and some researchers are using isothermal models for Pluto. The question of an atmosphere for Pluto, as suggested in the 1970s, thus comes into play. An atmosphere (its existence is controversial) might cool the sunlit face of the planet and distribute the heat. It might result from the subliming of methane ice on Pluto when, as now, the planet is near its closest approach to the sun. Recent occultation data[4] suggest, in contrast, that there is water ice on Charon.

The eclipse season for Pluto and Charon comes only once every 124 years. If Charon had been discovered only a dozen years later than it was, the current season would have been missed! As it is, the eclipses are making it possible to scrutinize Pluto and Charon as separate entities, partially knowable at last.

Deborah Byrd, McDonald Observatory

1. D. J. Tholen *et al.*, Science **237**, 512 (1987).
2. J. K. Beatty, Sky & Telescope **74**, 248 (1987).
3. E. F. Tedesco *et al.*, Nature **327**, 127 (1987).
4. R. L. Marcialis, G.H. Rieke, and L.A. Lebofsky, Science **237**, 1349 (1987).

Very-Low-Mass Companions—Extrasolar Planets?

What may be the best evidence yet for planets of other stars was reported in 1987.[1,2] It was the latest in a long line of exciting announcements, none yet satisfactorily confirmed. Astronomers have been searching for very-low-mass companions of stars beyond the sun for many years. They are seeking both planets and brown dwarfs. The latter are conceived as objects intermediate in mass between planets and stars and are supposed to be the lowest-mass objects formed, like stars, by fragmentation and condensation in interstellar clouds. Brown dwarfs, if they exist, cannot maintain steady nuclear burning of hydrogen (unlike red dwarfs, the lowest-mass "true" stars) although they may pass through a brief stage of deuterium burning. Planets, in contrast, are thought to form in accretion disks around newborn or still-forming stars and of course to generate no energy at all by fusion. The hypothetical brown dwarfs, by some accounts, have masses in the range from 10 to 80 jovian masses (hereafter, "jupiters"); proven planets, of course, are confined to the solar system, and range in mass up to 1 jupiter.

The search techniques include the measurement of "wobbles" in the apparent motion of a star across the sky, attempts to detect infrared emission from putative companions of selected stars, whether by direct imaging or by speckle interferometry, and searches for low-amplitude, cyclic Doppler shifts in stellar spectra. The most famous application of the wobble technique was to Barnard's star, for which two planets have been claimed, although never independently verified. The infrared speckle method seemed to have proved itself in 1984, when a brown dwarf or massive planetary companion of the red dwarf VB8 was observed, in apparent confirmation of an earlier detection by wobble. Unfortunately, subsequent work seems to have ruled out both the speckle and the wobble results.

The 1987 announcement is the fruit of six years of patient observation by the Doppler-shift method. The 3.6-m Canada–France–Hawaii Telescope (CFHT), on Mauna Kea, was used in conjunction with a spectroscopic technique that is claimed to yield velocity measurements of unprecedented precision in such applications. The key to this precision is a hydrogen fluoride gas absorption cell. Providing that the noxious substance is safely retained in the cell, starlight collected by the CFHT can be passed through the cell and into the spectrograph. The spectrum of HF is said to be highly stable

with respect to environmental changes, so a reference grid of high reliability is impressed on the stellar spectrum. In contrast, earlier searches for small variations in the radial velocities of stars were limited by uncertain optical changes in the spectrographs used.

Earlier planet and brown dwarf searches using the Doppler technique tended to concentrate on red dwarf stars (as do some ongoing searches), since their low masses would make the velocity perturbations by accompanying planets more easily detectable. In the CFHT program, however, the targets were 16 solar-type stars. They may be of greater interest since the sun, at least, is known to have planets. In seven cases, the target stars appear to have low-amplitude velocity variations that might result from the presence of very-low-mass companions, in the range 1–8 jupiters. Whether or not these companions are real, the results are important because they seem to rule out any common presence of companion objects in the presumed brown dwarf mass range above 10 jupiters, which would have been easily detected. Current thinking about the formation of binary stars indicates that close binary pairs form with roughly equal masses; if so, sunlike stars would not be expected to have companions with masses in the brown dwarf range, unless the companions formed like planets. Thus the null result is at least consistent with theory.

If the very-low-mass companions suggested for seven stars by the HF technique indeed exist, they may constitute, at around 1–8 jupiters, the upper range of the spectrum of planetary masses, at least for planets of sunlike stars. Besides confirmation by other workers using other equipment, it is important that the HF-referenced spectra be obtained over multiple cycles of the presumed planetary orbital periods. So far, however, only one star, gamma Cephei, has been observed long enough. It appears to be a binary (its companion star was discovered in the course of the CFHT planet search), with a planet in a 2.7-year orbit. By contrast, the next best case among the seven stars is epsilon Eridani, distant only about 11 light years from Earth and best known to armchair astronomers as a target of past attempts to detect extrasolar civilizations by means of radio monitoring. There are pronounced variations in the radial velocity of epsilon Eridani, as measured at the CFHT, but it is not clear that it has been observed for as much as a full orbital period. The other five stars with possible planetary companions had each been observed for less than one-half of their respective planets' orbital period as of June 1987, according to the current interpretation of the CFHT results.

While astronomers await confirmation of these exciting findings, there is good news from the wobble and speckle fronts: a very-low-mass companion to the red dwarf star Gliese 623, which is located about 24 light years from Earth, has apparently been detected by infrared speckle interferometry and radial velocity measurements, in apparent confirmation of an earlier wobble detection. With an estimated mass of about 90 jupiters, the companion object Gliese 623B is probably one of the lowest-mass true stars known. Although neither a brown dwarf nor a planet, its detection by three methods suggests that planet seekers may now have their systematic errors under control, so that they can continue the search for very-low-mass companions with increased confidence and with several techniques.

Stephen P. Maran, NASA–Goddard Space Flight Center

1. B. Campbell, G. A. H. Walker, and S. Yang, Bull. Am. Astron. Soc. **19**, 762 (1987); also "A Search for Planetary Mass Companions to Nearby Stars," in *Bioastronomy–The Next Steps* (in press 1988).
2. D. W. McCarthy, Jr. and T. J. Henry, Astrophys. J. (Lett.) **319**, L93 (1987).

CHEMICAL PHYSICS

The Chemistry of Clusters

Recent advances in the generation, sampling, and understanding of atomic-sized clusters have been quickly followed by experiments and theories which reveal new chemical propensities characterizing these metastable materials.[1]

Ion cyclotron resonance techniques have been used to accomplish size selection of clusters and measure their bimolecular reaction rates and products under single-collision conditions. For example, positively and negatively charged silicon clusters containing up to eight atoms have been found to react with a variety of reagents including silanes, XeF_2, NO_2, and WF_6. The dependence of reaction rates and products on cluster size has been shown to correlate with two distinct types of reactivity related to the different types of dangling bonds on the clusters.[2]

Sequential clustering reactions with silane have been discovered to form larger hydrogenated silicon particles, in analogy to chemical vapor deposition growth of silicon.[3] Crucial bottlenecks occur early in the clustering sequences which limit the rate of cluster growth. The mechanism and

energetics for the individual steps of the sequential addition of SiD_2 to Si^+, leading to a highly branched terminal structure of $Si_4D_6^+$, have been derived using an interplay between *ab initio* electronic structure theory and phase space theory.[4]

Comparable insights into bare metal cluster ion chemistry have resulted from low-energy ion-beam techniques which have been used to select Al cluster sizes and examine their reactivity. Cationic clusters containing up to 26 atoms are shown to chemisorb oxygen molecules and then undergo highly exothermic reactions which primarily result in units of Al_2O being expelled from the cluster.[5] In contrast, activation barriers of 1–2 eV for chemisorption are encountered in the reactions of aluminum cluster cations with deuterium.[6] The chemistry unique to heterogeneous catalysis has been further elucidated using monodispersed transition metal cluster ions. Chemisorption on nickel clusters shows pronounced size-dependent saturation coverage.[7] The extent of dehydrogenation and cracking of hydrocarbons has been found to vary considerably amongst nickel, palladium, and platinum clusters.[8]

Mark Cardillo, AT&T Bell Labs

1. Physics News in 1984, p. S16.
2. M. L. Mandich, W. D. Reents, Jr., and V. E. Bondybey, J. Phys. Chem. **90**, 2315 (1986); M. L. Mandich, V. E. Bondybey, and W. D. Reents, Jr., J. Chem. Phys. **86**, 4245 (1987); W. D. Reents, A. M. Mujsce, V. E. Bondybey, and M. L. Mandich, J. Chem. Phys. **86**, 5568 (1987).
3. M. L. Mandich, W. D. Reents, Jr., and M. F. Jarrold (submitted to J. Chem. Phys.).
4. K. Raghavachari (submitted to J. Chem. Phys.).
5. M. F. Jarrold and J. E. Bower, J. Chem. Phys. **85**, 5373 (1986); L. Hanley and S. Anderson, Chem. Phys. Lett. **137**, 5 (1987).
6. M. F. Jarrold and J. E. Bower, J. Am. Chem. Soc. (in press).
7. P. Fayet, M. J. McGlinchey, and L. H. Woste, J. Am. Chem. Soc. **109**, 1733 (1987).
8. T. F. Magnera, D. E. David, and J. Michl, J. Am. Chem. Soc. **109**, 936 (1987).

Two-Photon (VUV & Visible) Resonant Ionization Spectroscopy of Atoms and Molecules

The laser is responsible for the discovery and investigation of many nonlinear spectroscopic processes. Of increasing interest among these is two-photon resonant absorption[1,2] which allows the examination of atomic and molecular states that lie in a higher-energy region not normally accessible by a one-photon process (owing to parity considerations). Two-photon resonant spectroscopy tends to be less sensitive to fluctuations in the laser light source and therefore yields more easily reproduced data than nonresonant multiphoton spectroscopy.

The third harmonic (355 nm) from a Nd:YAG laser is used to simultaneously pump a dye laser and produce coherent vacuum ultraviolet light (VUV) in the generation cell. The dye laser is tuned so that visible and VUV photons (at a wavelength of 118 nm) excite the species of interest in the detection cell. The excited species is subsequently ionized by an additional photon and the ejected electron is detected by charge collection on parallel plates.[3]

With commercially available narrow-bandwidth pulsed lasers, the energy levels of many gaseous atoms and molecules can be measured as accurately as with the longest VUV monochromators. The results we obtained with broad bandwidth lasers agree well with measurements by other researchers.[4]

Two-photon rates were also obtained in this experiment. These results agree well with theoretical estimates.[5] Two-photon rates are therefore useful parameters for predicting the signal size in future experiments.

The two-photon rates that have been measured thus far can now be used for relative measurements of other atoms and molecules. Presently the method is being employed with hydrogen. In the future we plan to use this technique together with a pulsed nozzle source to measure energy levels and two-photon rates in cooled molecules.

M. P. McCann, C. H. Chen, and M. G. Payne, Oak Ridge National Laboratory

1. R. G. Bray, R. M. Hochstrasser, and J. E. Wessel, Chem. Phys. Lett. **27**, 156 (1974).
2. J. Burris and T. J. McIlrath, J. Opt. Soc. Am. **B2**, 1307 (1985).
3. M. P. McCann, C. H. Chen, and M. G. Payne, Appl. Spectrosc. (March–April 1987).
4. C. E. Moore, *Atomic Energy Levels, Vol. I and II* (National Bureau of Standards, Washington, D.C. 1971), pp. 169–172, 211–215.
5. M. P. McCann, C. H. Chen, and M. G. Payne (to be published).

Probing Unimolecular Reaction Dynamics by Vibrational Overtone Excitation

The decomposition of an isolated, energized molecule is an elementary chemical process that constitutes a crucial intermediate step in many complex chemical transformations. Statistical theories, which have been very successful in describing unimolecular reactions, are based on the notion that the redistribution of energy deposited among the internal degrees of freedom is rapid compared to the reaction rate. In the context of these theories, the course of the reaction is determined only by the total energy, regardless of its manner or site of deposition into the molecule and, in some versions, the total angular momentum.

Current selective excitation experiments, in which energy is deposited in a highly specific manner, are stringently testing these assumptions. One of several informative laser preparation schemes[1] excites weak transitions that involve overtones of stretching vibrations of the electronic ground state. The spectroscopy of these highly vibrationally excited molecules is an excellent means of determining reaction rate information. For example, extensive spectral analyses[2] and theoretical treatments[3] have uncovered the role that nonlinear interactions, such as Fermi resonances, play in the flow of energy among the degrees of freedom in highly vibrationally excited molecules. This understanding has set the stage for detailed studies of unimolecular reactions in which the nature of the initially prepared state is well defined.

One example of the close interplay of theory and experiment is the work being performed on the vibrational overtone-induced dissociation of hydrogen peroxide (HOOH) into two OH fragments.[4–9] This prototypical bond fission process is amenable both to vibrational overtone-induced dissociation and to detailed theoretical modeling. The experimental approach is to excite the fifth overtone of the OH stretching vibration, thereby depositing more than enough energy to break the relatively weak O–O bond, and to determine the populations of individual OH quantum states using laser-induced fluorescence.[4] In addition, picosecond laser techniques make it possible to monitor the product time evolution directly.[5] The resulting lifetime of about 6 ps is very long on the timescale of molecular vibrations.[7] This implies that individual transitions in the spectrum of the dissociating molecule should be about 1 cm^{-1} wide, a prediction that is experimentally confirmed for HOOH cooled in a free-jet expansion.[8] This calculation also predicts that because of the absence of low-order nonlinear resonances, not all vibrations are classically energized prior to dissociation.

These theoretical studies demonstrate the complexity of intramolecular energy transfer processes even in a molecule as apparently simple as hydrogen peroxide. The numerous nonlinear resonances and couplings that lead to complex intramolecular dynamics often produce the efficient, although not necessarily perfect, energy redistribution that makes statistical theories so successful in polyatomic systems. This is particularly apparent in analyzing the overtone-induced dissociation of HOOH. A modified statistical calculation predicts lifetimes and product state distributions that agree with experimental results,[9] but the dynamical quasiclassical trajectory calculation, which finds nonstatistical behavior (in that the energy redistribution is incomplete prior to reaction), produces a comparable lifetime.[7] Close contact between theory and experiment promises to continue revealing even more details of intramolecular energy sharing and its consequences for unimolecular reactions.

Turgay Uzer, Georgia Institute of Technology and
F. Fleming Crim, University of Wisconsin

1. H. Reisler and C. Wittig, Ann. Rev. Phys. Chem. **37**, 307 (1986).
2. For example, J. Segall, R.N. Zare, H.-R. Dubal, M. Lewerenz, and M. Quack, J. Chem. Phys. **86**, 634 (1987); J. E. Baggot, D. W. Law, P. D. Lightfoot, and I. M. Mills, *ibid.*, **85**, 5414 (1987); J. S. Wong, W. H. Green, C.-K. Cheng, and C. B. Moore, *ibid.*, **86**, 5994 (1987); G. J. Scherer, K. K. Lehmann, and W. Klemperer, *ibid.*, **81**, 5319 (1985); J. W. Perry, D. J. Moll, A. Kupperman, and A. H. Zewail, *ibid.*, **82**, 1195 (1985).
3. For example, D. W. Oxtoby and S. A. Rice, J. Chem. Phys. **65**, 1676 (1976); E. L. Sibert III, W. P. Reinhardt, and J. T. Hynes, *ibid.*, **81**, 1115; 1135 (1984); J. S. Hutchinson, J. T. Hynes, and W. P. Reinhardt, *ibid.*, **90**, 3528 (1986).
4. T. R. Rizzo, C. C. Hayden, and F. F. Crim, J. Chem. Phys. **81**, 4501 (1984); T. M. Ticich, T. R. Rizzo, H.-R. Dubal, and F. F. Crim, *ibid.*, **84**, 1508 (1986).
5. N. F. Scherer, F. E. Doany, A. H. Zewail, and J. W. Perry, J. Chem. Phys. **84**, 1932 (1986); N. F. Scherer and A. H. Zewail., *ibid.*, **87**, 97 (1987).
6. B. G. Sumpter and D. L. Thompson, J. Chem. Phys. **82**, 4557 (1985).
7. T. Uzer, J. T. Hynes, and W. P. Reinhardt, Chem. Phys. Lett. **117**, 600 (1985); J. Chem. Phys. **85**, 5791 (1986).
8. L. J. Butler, T. M. Ticich, M. D. Likar, and F. F. Crim, J. Chem. Phys. **85**, 2331 (1986).
9. L. Brouwer, C. Cobos, J. Troe, H.-R. Dubal, and F. F. Crim, J. Chem. Phys. **86**, 6171 (1987).

Density Functional Theory of Freezing and Solids

The phenomena by which a fluid freezes into a solid when the pressure is increased or the temperature is lowered is a universal property of matter. The freezing phase transition is geometrical in nature, strongly first-order in three dimensions, and is characterized by discontinuities in thermodynamic quantities such as entropy and density. The correlations have a short range nature and do not diverge near the transition point.

One might thus conclude that there are no universal features of freezing. This is not so. For example, computer simulations[1] of hard-sphere fluids, Lennard–Jones fluids, one-component plasmas, as well as experimental results on Ar, Rb, and Na all exhibit similar solidification parameters.

A statistical mechanical theory of the solid–liquid transition has recently been developed[2] which addresses the following basic question: given the intermolecular potential for a system, how do the thermodynamic properties change when melting occurs? The basic ingredient of the freezing theory, first formulated by Ramakrishnan and Yussouff, is to project the thermodynamic potential difference between the solid and the liquid onto an order-parameter space, the order parameters being proportional to the lattice periodic components of the one-particle density. The total potential is the sum of any externally imposed potential and the response potential set up as a result of forces between the particles in the now inhomogeneous system. The response potential of the system is a function of the one-particle density. Solutions of the integral equations for the solid singlet density show[3] how correlations in the fluid self-consistently generate a nonuniform density of crystalline symmetry and periodicity.

Both experiments and computer simulations[1] indicate that at the melting point the atomic motions in a solid are still small (less than 0.2 of the nearest-neighbor distance) and approximately harmonic. This suggests that the one-particle solid density can be expressed as a sum of narrow gaussian distributions centered on the sites of a crystal lattice. This observation has been exploited in developing a remarkably simple and accurate theory of freezing.[4] The only input is the structure factor of the liquid and the symmetry of the crystal lattice. The gaussian approximation[4] to the one-particle density has also been successfully applied to study glassy and disordered systems[5] as well as the interface between a perfect crystal and the liquid.[6] More recently a density functional formalism of polyatomic molecules and freezing of molecular[7] liquids has been introduced.

This opens up the exciting possibility that properties of a deformed solid can be explored. In a recent work, Jaric *et al.* have extended the order-parameter theory to obtain the elastic moduli for hard spheres[8] and Lennard–Jones crystals,

elastic moduli of quasicrystals, and the Debye–Waller factors and the thermal diffuse broadening of the diffraction patterns. Elastic constants of nematics[8] have been obtained. The core region of a screw dislocation has also been theoretically analyzed.[9]

Udayan Mohanty and Udai P. Singh, Boston College and Gerald Jones, University of Notre Dame

1. D. Frenkel and J. P. McTague, Ann. Rev. Phys. Chem. **31**, 491 (1980).
2. T. V. Ramakrishnan and M. Yussouff, Phys. Rev. B **19**, 2775 (1979).
3. P. Tarazona, Mol. Phys. **52**, 81 (1984); B. Bagchi, C. Cerjan, U. Mohanty, and S. A. Rice, Phys. Rev. B **29** , 6222 (1983); M. Baus, Mol. Phys. **51**, 211 (1984); M. Baus, Mol. Phys. **51**, 211 (1984); A. Haymet, J. Chem. Phys. **78**, 4541 (1983); W. Curtin and N. W. Ashcroft, Phys. Rev. A **32**, 2909 (1985); R. Hall and P. Wolynes, J. Chem. Phys. (in press).
4. G. Jones and U. Mohanty, Mol. Phys. **54**, 1241 (1985).
5. Y. Singh, J. Stossel, and P. Wolynes, Phys. Rev. Lett. **54**, 1059 (1985); S. Sachdev and D. Nelson, Phys. Rev. B **32**, 4592 (1985).
6. U. Mohanty and G. Jones, Bull. Am. Phys. Soc. **31**, 619 (1986); D. Oxtoby and A. Haymet, J. Chem. Phys. **76**, 6262 (1982); P. Harrowell and D. Oxtoby, J. Chem. Phys. **80**, 1639 (1984).
7. D. Chandler, J. D. Mccoy, and S. Singer, J. Chem. Phys. **85**, 5971 (1986); U. P. Singh and Y. Singh, Phys. Rev. A **33**, 2725 (1986); U. P. Singh and U. Mohanty (unpublished).
8. M. Jaric and U. Mohanty, Phys. Rev. Lett. **58**, 230 (1987); M. Jaric, U. Mohanty, and D. Nelson (preprint); G. Jones (preprint); M. D. Lipkin, S. A. Rice, and U. Mohanty, J. Chem. Phys. **82**, 472 (1985); T. V. Ramakrishnan, Pramana (1985); Y. Singh and K. Singh, Phys. Rev. A **33**, 3481 (1986).
9. M. Rajlakshmi, H. R. Krishnamurthy, and T. V. Ramakrishnan (unpublished); U. Mohanty (unpublished).

CONDENSED MATTER PHYSICS

By far the biggest news in condensed matter physics during 1987 was the astounding increase in the maximum superconducting transition temperature from 23 K where it had stood for 13 years to well over 90 K, breaking the long-intimidating "liquid nitrogen" barrier and setting off an unprecedented wave of scientific, technological, and media excitement. After struggling for 75 years to increase T_c by just over 19 K, physicists and materials scientists nearly quadrupled this increment in about 75 days. In the months following, thousands of scientists all over the world were engaged in trying to reproduce, modify, improve, and most importantly to understand the remarkable copper oxide superconductors. The stakes, both scientific and economic, are clearly enormous, as are the number of advances which have already been made and the challenges which remain.

The articles here by Bertram Batlogg on the experimental physics and by Elihu Abrahams and Seb Doniach on the theory, convey clearly the flavor of this scientific enterprise. There have been so many kinds of experiments on so many compounds and so many theoretical suggestions that any attempt at a complete list, let alone a complete reference set would vastly exceed our space limitations. Instead these authors have distilled what we presently understand to be the key points and remaining issues, referring to conferences or summaries published elsewhere for details. (Articles on high-temperature superconductivity can be found as well in the article on the 1987 Physics Nobel prize and in the chapters on physics in industry, crystallography, and vacuum physics.)

The major points are that high T_c superconductivity is special (if not unique) to the copper oxide materials; the superconductivity arises from pairs of carriers (holes); is very sensitive to oxygen content and unforgiving of substitution for copper; the rare earth identity is relatively unimportant, but the structure is dependent upon doping content. Experiments suggest that BCS-like pairing accounts for the penetration depth, tunneling gap, specific heat, and ultrasonic velocity behavior with temperature. Optical and infrared and isotope effect experiments, however, call into serious question the adequacy of phonons as the pairing mechanism. These facts together with the tendency toward magnetic order in the undoped (semiconducting) counterparts of the copper oxide superconductors points strongly toward an electronic mechanism.

It is intriguing that this association between magnetism and superconductivity is also evident in the other major class of exotic superconductors—the heavy fermions—where it is much better understood. Indeed as Zachary Fisk points out, the heavy electron materials appear to owe their superconductivity to a magnetic parentage. There is strong and growing evidence that the superconducting pairs are mediated by spin fluctuations rather than phonons. Equally fascinating are the anomalous normal-state properties of these materials. Both their thermodynamic and transport behavior suggests the inadequacies of normal one-electron band theory for the *f*-shell electrons. The effective electronic masses as high as several hundred are still incompletely understood. How much is due to band mass and how much to quasiparticle correlations? Is there a connection perhaps via the malleable Hubbard model between the heavy electron and the Cu-O superconductors?

Magnetism appears on the research forefront in yet another context with our newfound ability to structure metallic multilayers with the kind of atomic scale control formerly possible only in semiconductors. Myron Salamon points out that we can now make entirely new artificially structured magnetic materials which exhibit magnetic ordering found nowhere in nature. Controlling composition on the same submicroscopic length scales as the range of interatomic interactions themselves not only permits new magnetic structures, but offers unprecedented opportunity to explore interfaces and surfaces and to one day perhaps marry semiconductor, metallic, and magnetic epitaxial materials to fabricate new types of devices.

Magnets have traditionally served as important systems for advancing our understanding of condensed matter systems through the combined power of sophisticated theoretical models and incisive experimental technique. Indeed, much of the past decade's success in understanding phase transitions and critical phenomena was achieved on the playing field of magnetism. Magnetic materials also serve as prototypes for attack on the structure and dynamics of random systems. Daniel Fisher discusses the remarkable recent progress on both aspects of the random-field and spin-glass problems. We now know that three-dimensional long-range order does exist in the random field magnets. And for spin glasses evidence is mounting that there is indeed an equilibrium phase transition in three dimensions. Perhaps even more exciting has been the new understanding of the origin of hysteretic and relaxational dynamic phenomena in random magnets. Important new ideas about the exponential growth with scale length of equilibration times point toward an explanation of a wide variety of heretofore puzzling phenomena. The generality of these arguments suggests their applicability to a much broader class of random systems like fluid mixtures and perhaps even real structural glasses.

Disorder manifests itself in unexpected ways even in simple situations like the transport of charge through a very small wire. In the past few years experiments have shown that quantum effects become important on spatial scales of thousands of angstroms, far larger than the electronic de Broglie wavelength. Disorder is known to induce electron localization and to alter dramatically the nature of electron transport. But the discovery of such strong quantum effects as large conductance fluctuations even in the presence of weak disorder was initially surprising. Richard Webb summarizes the continued progress in understanding these effects, exquisitely enhanced by our ability to fabricate multiterminal devices with internal structures much smaller than the phase coherence length of the electronic wave function. Thus for electrons which are elastically scattered in traversing the structure, substantial interferences cause large fluctuations in received signal which appear random, but are rigorously reproducible for a given sample and are of universal strength. Furthermore the addition of any appendages to a quantum device changes the details, so that the electrical leads themselves must be considered as part of the sample. These concepts are important not only to the physics of mesostructures but to the technology which might be based on them as IC design rules shrink well below the present one-micron scale.

Fluctuations and randomness are also key concepts for another area of mesophysics. Long the province of chemists and biologists, membranes, films, and microemulsions are beginning to engage the attention of physicists as well, with some remarkable progress already resulting. Stanislas Leibler's account of static structures, dynamic fluctuations, and transitions draws conceptual connections between phenomena across the scientific spectrum from cell biology to quantum field theory. Both experimental and theoretical techniques from the arsenal of condensed matter physics are beginning to provide quantitative insight into the behavior of complex and heterogeneous fluid systems. This is indeed a rapidly emerging field.

The small sampling of news items described below can only hint at the vitality of effort and excitement of discovery which continue to characterize condensed matter physics.

Paul A. Fleury, AT&T Bell Laboratories

Oxide Superconductors: An Experimenter's Dream

In the quest for elucidating the physics of the new copper-oxide-based superconductors launched by the discovery of Bednorz and Müller[1] hundreds of solid state scientists, both experts and novices in the mature field of superconductivity, have directed their efforts to these compounds. Within the last several months nearly every one of the standard superconducting experiments has been performed on the new ceramic superconductors, resulting in a wealth of new information.[2,3]

The "barrier to entry" to this worldwide endeavor, a sample with a sharp resistive transition, appears deceptively low and universally affordable. But the significance of any result must be weighted by the quality of the material studied. In the hectic pace of the past year, with the number of publications on this subject exceeding 1000, careful assessments of the sample quality through x-ray diffraction, magnetic measurements, and oxygen content analysis has often been neglected. Nevertheless, a clear picture has begun to emerge of at least the basic parameters describing the normal and superconducting states.

The high T_c compounds, represented here by $(La,Sr)_2CuO_4$ (abbreviated LSCO) and by $Ba_2YCu_3O_7$ (BYCO) and its many substitutional relatives, have much in common, both crystal-chemically and electronically. Their essential structural element is an oxygen-copper network. In LSCO, the "40 K material," layers of corner-linked oxygen octahedra with Cu in the centers, are separated by two layers of LaO. This K_2NiF_4 structure is reminiscent of a perovskite with its three-dimensional arrangement of corner-linked octahedra. The "90 K material," BYCO, crystallizes in a new

structure of orthorhombic symmetry. Two corrugated Cu-O planes and a linear Cu-O chain are the significant parts of the structure. Substitutions for the various elements, such as transition metals for Cu or magnetic rare earths for Y, and their influence on superconductivity clearly identify the Cu-O network as the electronically essential ingredient. The Y site is so decoupled from superconductivity that substituting the strongly magnetic Gd ion does not affect superconductivity, even though the fully substituted material orders magnetically at 2.2 K. Any replacement of Cu, however, drastically reduces T_c both in LSCO and BQCO. Of the utmost importance is the strongly covalent character of the Cu-O bands and the oxidation state of Cu, which is intermediate between two and three.

The materials' structural anisotropy is reflected in the electronic properties, which are distinctly different in directions parallel and perpendicular to the Cu-O planes. Compared to ordinary metals, the carrier concentration is quite low (10^{21}–10^{22} cm^{-3}), which partly accounts for the dull black appearance of the ceramic compounds. They are poor metals indeed. The electrical resistivity is high, several hundred micro-ohm-centimeters at T_c, and exhibits a remarkable nearly linear increase with temperature without saturation at highest temperatures. The magnetic susceptibility in the normal state of BYCO is essentially temperature independent when samples are carefully prepared to avoid the formation of local Cu^{2+} moments. Similarities with rare earth intermediate valence compounds are present.

The low carrier concentration also results in large magnetic penetration lengths of about 1000 Å for BYCO and 2500 Å for LSCO. Together with the very short (and anisotropic) coherence length of order 10–20 Å, this characterizes these compounds as extreme type II superconductors. The upper critical fields reach record values with slopes near T_c of about 1 T/K in LSCO and in BYCO of 3 T/K (0.1 T/K) for fields parallel (perpendicular) to the Cu-O planes.

The critical current density is of crucial importance for applications. Encouraging values in excess of $10^6 A/cm^2$ at 77 K have been achieved in oriented thin films. The current carrying capacity of bulk ceramic samples, however, is inferior by orders of magnitude, and is further suppressed by modest magnetic fields of few kOe. Although links are most likely the reason for this, their nature remains to be understood.

Much of the research has focussed on revealing the origin of the high T_c's. Cu-O and $Ba(Pb, Bi)O_3$ superconductors form a class, distinctly different from the intermetallic compounds in that their transition temperatures are much higher than expected given their relatively small electronic density of states at the Fermi level. The transition temperatures of these oxides are three to five times higher than those of intermetallics with comparable densities of states. Isotope effect studies in which phonon frequencies were reduced through replacement of oxygen by its heavier isotope, revealed no shift of T_c in the 90 K compounds. For the 40 K material a very weak isotope effect was observed.

Far-infrared and tunneling spectroscopy in BYCO and LSCO indicate superconducting values that are somewhat larger than expected from weak coupling BCS. Site specific measurements of the nuclear relaxation rates in BYCO suggest the gap in the "chains" to be three to four times larger than in the "planes". The importance of the chains becomes evident also when oxygen is selectively removed from the chains resulting in a precipitous drop of T_c to 60 K, speculatively assigned to the T_c of the planes.

Microscopic understanding of the crystal-chemical aspects and ever more sophisticated experiments on high-quality samples will be necessary not only to solve the problem of limited critical densities in bulk material, but also ultimately to understand the very high T_c's. An exciting chapter in solid state science has been opened.

Bertram Batlogg, AT&T Bell Laboratories

1. J. E. Bednorz and K. A. Müller, Z. Phys. B Condensed Matter **64**, 189 (1986).
2. Proc. Symp. S, 1987 Spring Meeting of the MRS; edited by D. U. Gubser and M. Schlüter (1987).
3. *Proceedings of the Int'l. Conference on New Mechanisms of Superconductivity, Berkeley*, edited by V. I. Kresin and S. A. Wolf (Plenum, New York, 1987).

Oxide Superconductors: A Theorist's Challenge

The modern understanding of superconductivity began with the development of the BCS (Bardeen, Cooper, Schrieffer) theory in 1957. Superconductivity is now understood as a phase transition to a coherent state of correlated electron pairs. Originally, the theory was worked out with a weak short-range attractive interaction between the electrons which was taken as a model for the electron–electron coupling arising from exchange of lattice phonons. A vast body of experimental data on weak coupling superconductors came into spectacular agreement with the detailed predictions of BCS theory. Strong-coupling extensions of BCS soon followed: the dynamics of phonons and Coulomb repulsion were included and data on strong-coupling superconductors with somewhat higher transition temperatures were explained.

The search for high T_c superconductors of course antedates the BCS theory. However, it was the existence of the BCS framework which enabled theorists to make a contribution to this search. Proposals for different pairing interactions to go into the BCS theory appeared as experimental T_c's moved up to 23 K and stopped there in the mid 1970's. At this time strong arguments appeared which indicated that the phonon exchange mechanism could never produce a T_c much higher than about 30 K. However, it is expected that if the pairing could be effected by a purely electronic mechanism, then the characteristic energy scales could be much larger, allowing correspondingly higher supercon-

ducting T_c's as large as those in other electronic transitions. Hope for such a possibility was reinforced by the observation of superfluidity in liquid ^{3}He, where the pairing is indeed driven by excitations of the particles themselves.

Following the discovery of superconductivity in heavy-electron intermetallic compounds in 1979, various anomalies were observed which indicate that the pairing mechanism is not the conventional phonon one. There is now both experimental and theoretical evidence that the pairing is mediated by electronic excitations, namely antiferromagnetic spin fluctuations. Unfortunately, in these materials the strong electron–electron correlation effects result in T_c's of around 1 K or less.

A prototype for an electronic system with strong interaction is the Hubbard model which dates from the early sixties. It is a model of itinerant electrons with a large, short-range repulsion called U. The model has resisted all but analytic mean-field and computational-variational solutions. Furthermore, depending on the values of U and the electron density, it possesses a rich variety of phases: antiferromagnetic, ferromagnetic, paramagnetic, insulating, conducting, and perhaps superconducting. Intense interest in the Hubbard model accompanied experiments on the heavy electron compounds.

The discovery of high- T_c superconductivity in the rare earth copper-oxide compounds has further stimulated investigations of purely electronic mechanisms for superconductivity.[1] The absence of an isotope effect in the higher T_c (greater than 90 K) materials encourages this view. The new superconductors have the peculiarity that they arise by doping (with holes) a parent compound which is a Mott insulator and probably antiferromagnetic, as in the large-U Hubbard model with one electron per site.

One view is that the same interaction (U) responsible for the magnetism in the parent material produces superconductivity in the doped compound. This is the basis of the recently formulated resonating valence bond (RVB) proposal. It is an example of a rather new approach to understanding the superconducting ground state. Alternative interactions based on the Hubbard model and its extensions, such as charge transfer excitation exchange and coupling invoking antiferromagnetic spin fluctuations are being considered.[1]

Some experimental data suggest that the superconducting hole carriers in these compounds may have correlation-induced several-fold mass enhancements. The effective Fermi energy would then be significantly less than 1 eV. Consequently, much of the conventional theoretical apparatus which involves certain simplifications and perturbative approximations is no longer applicable. The resulting paucity of small parameters indicates difficult problems for calculations of T_c in the oxide superconductors.

Theorists are thus faced with a tough problem in which electron correlations dominate the physics of superconductivity. Certainly, to understand the Hubbard model it has become clear that new ways of describing the physics are needed. The traditional language of Hubbard bands which barely gives lip service to the central role played by correlation has so far not yielded the solution. If the oxide materials are indeed in the strong correlation class, the search for a quantitative understanding may require totally new methods. It is possible that some truly novel adaptation of phonon-mediated pairing or another mechanism such as plasmon or exciton exchange might prove correct.[1] In any event, there remain important questions of how any of the simplified theoretical models are related to the structure and chemistry of the actual compounds. What is the role of defects and oxygen vacancies? What are the limits on T_c? How can the 100 K barrier be overcome and higher temperature superconductors (if they exist) be stabilized? The lure of enormous scientific and technological impact following from these new discoveries will keep condensed matter theorists and experimentalists busy for years to come.

Elihu Abrahams, Rutgers University and
Sebastian Doniach, Stanford University

1. Detailed discussions of the physics of these materials can be found in the *Proceedings of the Int'l. Conference on New Mechanisms of Superconductivity, Berkeley*, edited by V. I. Kresin and S. A. Wolf (Plenum, New York, 1987).

Superconductivity and Magnetism in Heavy Electron Materials

Heavy electron materials[1] are distinguished by the development at helium temperature of a large electronic specific heat coefficient γ of order 1 J/mole K^2. These large γ's are found only in f-electron materials (primarily Ce and U intermetallics), although there appears no good reason for not finding similar d-metal compounds. It is useful to think about these materials in terms of the Kondo model, in which conductor electron spins are correlated with the rare earth ions.

What is new here is that in these atomically ordered lattices the electronic state at low temperature becomes "coherent." The loss of incoherent scattering[1] characteristic of the high-temperature state is seen as a rapid drop in the electrical resistivity and in the Hall constant. The effective masses observed in these experiments are heavy: the largest, about 90 times the mass of free electron, being seen in the compound UPt_3.

Much of the interest in the heavy electron materials derives from the fact that superconductivity is observed near 1 K in $CeCu_2Si_2$,UPt_3, and UBe_{13}, despite the magnetic parentage of their unusual normal state properties. The major challenge is deciding whether the pairing or the mechanism are new. There is growing evidence that the superconducting state in UPt_3 and DBe_{13} is an anisotropic singlet. Evidence[1] comes variously from non-BCS temperature dependence below T_c in ultrasonic attenuation, specific heat, thermal conductivity and penetration depth as well as unusual anisotropy in the ultrasonic attenuation in DPt_3 and a peak below T_c in the ultrasonic attenuation of UBe_{13}.

In Th-doped UBe_{13} there is a second phase transition[1] seen in specific heat below the 0.6 K superconducting transition. Muon spin resonance (μSR) experiments suggest that the lower state possesses a small magnetic moment. Detailed measurements on pressure effects in this alloy system suggest that the lower phase involves a different symmetry superconducting state, a possibility which has been addressed by theorists.

μSR also suggested a small ordered moment in UPt_3. Recent neutron experiments[2] bear this out: an ordered moment of about 0.02 μ_B and the build-up order parameter for this state appear to be arrested by the establishment of superconductivity at 0.5 K. Magnetic order below 5 K has also been observed in Pd- and Th-doped UPt_3. Superconductivity has also been found[3] to coexist with small moment ordering in the case of URu_2Si_2.

Extensive neutron experiments have been reported[1] for UPt_3 and U_2Zn_{17}. In UPt_3, strong antiferromagnetic correlations have been shown to develop as coherence develops, and their presence in the superconducting state makes a magnetic mechanism for T_c in this case plausible. For the antiferromagnet U_2Zn_{17}, the magnetic fluctuations are found to be highly localized in reciprocal space.

Zachery Fisk, Los Alamos National Laboratory

1. M. Brian Maple, Phys. Today **39**, 72 (March 1986); recent experimental and theoretical results can be found in: Proceedings of the International Conference on Valence Fluctuations, Bangalore, India (1987).
2. G. Aeppli, C. Broholm, J. Kjems, and E. Bucher (preprint).
3. C. Broholm, J. K. Kjems, W. J. L. Buyers, P. Matthews, T. T. M. Palstra, A. A. Menovsky, and J. A. Mydosh, Phys. Rev. Lett. **58**, 1467 (1987).

Artificially Structured Magnetic Materials

The ability to tailor-make materials on the atomic scale has long been possible in organic chemistry. Recently developed "epitaxial" methods, however, permit solid state physicists to deposit materials, atomic layer by atomic layer, on a suitable crystalline substrate. When atomic registry is achieved (epitaxy), the quality of the artificial structure can rival that of natural crystals. This art is most fully developed for semiconductors, but has recently been demonstrated for a wide variety of metallic systems.[1-6] An intriguing aspect of epitaxially grown multilayers is the ability to introduce new periodicities on the atomic scale. In the past year, entirely new magnetic materials have been produced by growing rare-earth-based multilayers whose artificial periodicities are comparable with the natural magnetic periodicities occurring in bulk phases of the elements themselves. The key to this advance was the development of techniques to control the growth[1] of Nb on sapphire substrates with choice of growth axis followed by the discovery[2] that Y(001) would grow on Nb(110).

Consider, for example, Y/Gd multilayers.[3,4] Yttrium has no *f* electrons and is normally nonmagnetic, while bulk gadolinium becomes ferromagnetic near room temperature. The Y/Gd multilayers can be either ferromagnetic or antiferromagnetic, depending on the Y thickness, with the magnetization lying in the hexagonal basal plane rather than along the *c* axis as in bulk Gd. Careful analysis of the magnetization density shows that it lies entirely within the Gd sheets, and that interdiffusion is minimal. These results demonstrate the existence of alternating ferro/antiferromagnetic coupling through the Y layer which can be correlated with oscillations in conduction electron spin density in the Y.

Richer systems[5,6] result when Gd is replaced by Dy or Er, elements that exhibit long-period helical or *c*-axis modulated structures. Dy/Y multilayers order in the same basal plane spiral as elemental Dy, although at a lower temperature. The spiral is, however, amplitude and "frequency" modulated by the Y layers, resulting in a complex structure in magnetic neutron scattering. The spiral retains its coherence over many multilayer periods, implying that the phase and chirality of the spiral is propagated through the Y layers. One may thus regard the spin polarization in the Y as an induced spin-density wave. The overall coherence length of the spiral decreases inversely with the thickness of the Y layer. Further, bulk magnetic properties, such as the spin-wave gap and magnetization curve, change with Y thickness. The ferromagnetic phase transition in bulk elemental Dy, which is driven by magnetostriction, does not occur in the multilayer. Epitaxial constraints on the basal plane lattice constants have been shown to suppress the ferromagnetism. However, ferromagnetism in Dy is recovered in sufficiently thick, epitaxially grown films. Even in the multilayers, the application of a magnetic field at low temperatures induces a metastable ferromagnetic state, accompanied by *c*-axis magnetostriction. The spiral phase can be recovered only by heating the multilayer sample to approximately 50% of its critical temperature.

An Illinois/NBS team[7] has also been studying Er/Y multilayers. These exhibit a sharp transition to *c*-axis ferromagnetism at low temperatures in an applied field of approximately 2 T. Bulk Er spontaneously tranforms to the same phase at 20 K in zero field. The complicated sequence of changes in helical period observed in elemental Er is absent in the multilayer; only a single, temperature independent period is found in several superlattices with Er thicknesses spanning the range of observed periodicities. More recently, a Bell Labs/Brookhaven group[4] has studied quasiperiodic sequences of Y and Gd layers (which do not produce a quasiperiodic spin arrangement) and multilayers of Gd and Dy. Both systems exhibit complicated spin arrangements whose details have yet to be worked out.

This new ability to make tailored magnetic structures holds promise for the integration of magnetic structures with semiconductors and for new types of thin-film recording. Control of magnetic coupling distance, magnetostriction, and coercive fields has already provided important insight into the nature of magnetic coupling in the rare earths and the role of magnetoelastic energy in determining magnetic phases.

Myron B. Salamon, University of Illinois

1. S. M. Durbin, J. E. Cunningham, and C. P. Flynn, J.Phys. **F12**, L75 (1982).
2. J. Kwo, D. B. McWhan, M. Hong, E. M. Gyrogy, L. C. Feldman, and J. E. Cunningham in *Layered Structures, Epitaxy and Interfaces*, edited by J. H. Gibson and L. R. Dawson (Material Research Soc., Pittsburgh, 1985), Vol. 37, p. 509.
3. J. Kwo, E. M. Gyorgy, D. B. McWhan, M. Hong, F. J. DiSalvo, C. Vettier, and J. E. Bower, Phys. Rev. Lett. **55**, 1402 (1985).
4. C. Vettier, D. B. McWhan, E. M. Gyorgy, J. Kwo, and B. M. Buntschuh, Phys. Rev. Lett. **56**, 757 (1986); C.F.Majkrazac *et al.*, Phys. Rev. Lett. **56**, 2700 (1986).
5. M. B. Salamon, S. Sinha, J. J. Rhyne, J. E. Cunningham, R. Erwin, and C. P. Flynn, Phys. Rev. Lett. **56**, 259 (1986).
6. R. W. Erwin, J. J. Rhyne, M. B. Salamon, J. Borchers, S. Sinha, R. Du, and C. P. Flynn, Phys. Rev. Lett. **B35**, 6808 (1987).
7. J. Borchers, M. B. Salamon, R. Du, C. P. Flynn, R. W. Erwin, and J. J. Rhyne, Proc. Third International Conf. on Superlattices, Microstructures, and Microdevices, Chicago, 1987 (to be published).

Dynamics of Random Magnets

Random magnetic systems have provided challenges to experimentalists and theorists for quite some time. Until recently, attention had focused on the question of whether or not equilibrium thermodynamic phase transitions exist in either random field magnets or spin glasses. Following recent progress in this direction, the focus has shifted to the fascinating dynamic properties of these systems. It is hoped that random magnets will form a cornerstone for the understanding of other random systems in the same way that conventional magnets served as a model for critical phenomena.

The most striking way in which many random magnets differ from their nonrandom counterparts is in the sudden onset of hysteretic behavior below a sharp dynamic "freezing" temperature. Experiments on random field magnets, realized as randomly diluted antiferromagnets like Fe-Zn-F, indicate that the presence or absence of antiferromagnetic order at low temperatures depends on the history of the system.[1,2] If an applied magnetic field is turned on before the system is cooled, no long-range order occurs and the correlations saturate at a scale of a few hundred angstroms. Conversely, if the field is turned on after cooling, long-range antiferromagnetic order is found.[2] For several years the source of this irreversible behavior was not understood even in this deceptively simple system.

Another more complicated class of random magnetic systems, spin glasses, have long been known to exhibit hysteretic behavior, such as irreversible "remanent" magnetization, and frozen-in anisotropy.[3] In spin glasses, random magnetic alloying, such as in Cu-Mn, causes competing ferro- and antiferromagnetic interactions which give rise to "frustration" and causes the system to seek complex ground states in which the spins are frozen in random directions without either ferro- or antiferromagnetic order. For many years the question of whether either random field magnets or spin glasses had equilibrium phase transitions at all aroused considerable controversy.[1,3] Recently, convincing answers have been found in both cases.

John Imbrie has rigorously proved that equilibrium long-range order exists at low temperatures in three-dimensional random-field magnets.[4] For spin glasses, although the situation is by no means as settled, Monte Carlo simulations, other numerical techniques and experiments on a variety of systems all show a nonlinear magnetic susceptibility which diverges at a critical temperature T_c, indicating an equilibrium phase transition in three dimensions.[3]

Following this progress in understanding the static equilibrium behavior, the primary questions have centered upon the dynamics: why do random magnets have such difficulty reaching equilibrium, and why do they exhibit such marked hysteretic behavior? A key to understanding this issue is the fact that nonrandom systems have no such difficulties. In nonrandom systems, the time scale for relaxation of processes involving correlations on a length scale L typically grows as a power of L. This implies that, both near phase transitions and in ordered phases, macroscopic size regions can be equilibrated in macroscopic times:

The first theoretical arguments for radically different behavior in random systems showed[5] that in the ordered phase of random field magnets, the time scale for domains of size L to develop grows exponentially with L. This very slow dynamical behavior is due to the presence of free energy barriers caused by the randomness whose magnitude grows as a power of L. Villain and Fisher[6] argued that similar exponentially activated dynamics occurs as the phase transition to the ordered phase is approached from above, so that even with macroscopic experimental measuring times, the system will fall out of equilibrium on cooling at a sharp freezing temperature just above T_c.

In spin glasses, a picture has been developed[7] of the ordered phase in which exponentially slow relaxation as a function of length scale also leads to hysteretic behavior qualitatively similar to that seen in recent experiments.[3,8] This predicts that the spin glass ordered phase has a remarkable property which plays an important role in preventing establishment of macroscopic equilibrium on macroscopic time scales: an extreme sensitivity to temperature which causes the relative orientation of distant spins to change randomly with even small temperature changes![7,9]

The validity of this scaling picture of the ordered phase remains highly controversial, especially in its prediction of the absence of a phase transition in a magnetic field,[7] which contrasts with earlier theories.[3] It has very recently been shown,[7,9] however, that in a magnetic field there should be a sharp dynamic freezing line—as in random field magnets—even if there is no true phase transition, so it may turn out that for many experiments whether or not a transition actually occurs is somewhat moot.

Although we now have a qualitative understanding of some aspects of freezing in random magnetic systems, many open questions remain, especially concerning the role of anisotropy and various types of magnetic interactions. In the

meantime, however, the ideas of "activated dynamic scaling"[7] have found their way into at least one other random system—two fluid phase separation in porous media[10]—and may facilitate an understanding of the slow dynamics of many other systems, such as dipolar glasses, strongly localized electronic systems, and perhaps even "real" glasses.

Daniel S. Fisher, Princeton University

1. R. J. Birgeneau, Y. Shapira, G. Shirane, R. A. Cowley, and H. Yoshizawa, Physica **137B**, 83 (1986) and references therein.
2. A. R. King, V. Jaccarino, D. P. Belanger, and S. M. Rezende, Phys. Rev. B **32**, 503 (1985); A. R. King, J. A. Mydosh, and V. Jaccarino, Phys. Rev. Lett. **56**, 2525 (1986).
3. For a recent review of spin glasses, see K. Binder and A. P. Young, Rev. Mod. Phys. **58**, 801 (1986).
4. Y. Imry and S.-K. Ma, Phys. Rev. Lett. **35**, 1399 (1975); J. Z. Imbrie, Phys. Rev. Lett. **53**, 1747 (1984).
5. J. Villain, Phys. Rev. Lett. **52**, 1543 (1984); G. Grinstein and J. Fernandez, Phys. Rev. B **29**, 6389 (1984).
6. J. Villain, J. Phys. (Paris) **46**, 1843 (1985); D. S. Fisher, Phys. Rev. Lett. **56**, 416 (1986).
7. D. S. Fisher and D. A. Huse, Phys. Rev. Lett. **56**, 1601 (1986) and a second article to be published; D. S. Fisher, J. Appl. Phys. **61**, 3672 (1987).
8. M. Alba, M. Ocio, and J. Hammann, Europhys. Lett. **2**, 45 (1986); P. Refrigier, E. Vincent, J. Hammann, and M. Ocio, J. Phys. (Paris) (to be published).
9. A. J. Bray and M. A. Moore, Phys. Rev. Lett. **58**, 57 (1987); A. J. Bray and M. A. Moore, in *Heidelberg Colloquium on Glassy Dynamics*, edited by J. L. Van Hemmen and I. Morgenstern (Springer, Berlin, 1987).
10. S. B. Dierker and P. Wiltzius, Phys. Rev. Lett. **58**, 1865 (1987); M. C. Goh, W. I. Goldburg, and C. M. Knobler, Phys. Rev. Lett. **58**, 1008 (1987); D. A. Huse, Phys. Rev. B **36** (in press).

Nonlocal Quantum Transport

The study of quantum interference corrections to the low-temperature electrical conductivity of normal metals has been an important part of condensed matter research during the last decade. It has long been recognized that the semiclassical approach toward calculating transport properties of metals can not properly describe the physics at the microscopic level. The surprising discovery was that, in some cases, these quantum corrections were readily observable at size scales more than a million times larger than what we normally consider to be the separation between the microworld of quantum mechanics and the macroworld of classical physics. Even in the presence of strong elastic scattering, the distance over which electrons maintain complete quantum-mechanical phase coherence can be hundreds of times larger than this average scattering length.

Perhaps the most striking examples of these quantum interference phenomena in condensed matter systems occur when the sample size is comparable to the phase coherence length of the electrons. Under these conditions, the conductance of a ring oscillates periodically (see *Physics News in 1985*, p. S19) as a function of magnetic field with a flux period equal to h/e (where h is Planck's constant and e is the charge of the electron), and the conductance of a line exhibits sample-specific but reproducible aperiodic fluctuations as a function of magnetic field. Both are quantum interference effects and both have a universal root-mean-square (RMS) value for the conductance fluctuation amplitude of approximately e^2/h (see *Physics News in 1986*, p. S16).

In the last two years it has become possible to fabricate multiterminal devices with an average spacing between voltage probes that is much less than the phase coherence length L_ϕ of the electrons. Transport measurements[1-4] in this regime have clearly demonstrated the nonlocal properties of the electronic wave functions. No matter where the voltage probes are located, interference effects from classically forbidden regions of the sample are measured. Perhaps the clearest demonstration of these nonlocal effects is an experiment using two nearly identical 2 μm long and 0.1 μm wide polycrystalline gold lines.[2] A 0.7 μm diameter loop is located 0.2 μm outside the classical current paths on one of the devices. The phase coherence length of the electron in both samples was approximately 2 μm. The conductance of both devices (as a function of magnetic field) exhibits slow random fluctuations with the same characteristic magnetic field scale and peak-to-peak variations, on the order of $2e^2/h$. However, the sample with the ring located outside the classical current path exhibits large h/e oscillations of exactly the expected period based on the normal metal Aharonov–Bohm effect. These observations emphasize the wavelike nature of the electronic transport phenomena being measured as well as demonstrating convincingly that the region between the voltage probes is not the actual sample being measured. The real sample dimensions are determined by the phase coherence length of the electrons, and the addition of any leads changes the details of the quantum interference phenomena. This nonlocal signal attenuates exponentially[5] as the separation between the ring and classical current path increases.

As a consequence of these nonlocal effects, experiment[3,4] and theory[6-9] have shown that the RMS value of the voltage fluctuations measured as a function of magnetic field using voltage probes separated by distances L much less than L_ϕ is constant, independent of L. This is simply another manifestation of the fact that the actual sample length is always on the order of L_ϕ, independent of where the voltage probes are placed within this length. These length independent voltage fluctuations translate into conductance fluctuations which appear to diverge as $(L_\phi/L)^2$ with reported values many orders of magnitude larger than e^2/h. However, when L_ϕ is substituted for the sample length, the universal value of e^2/h for the conductance fluctuations is recovered.

This work on multiprobe devices in the diffusive regime of electrical transport has shown that the electrons can propagate into any of the attached leads and therefore these leads must be considered as part of the sample. The addition of any appendage to a quantum device changes the details of the electron wave functions and can no longer be thought of as just some local nonevasive chemical potential probe. In the near future it should be possible to gain access to the quantum coherent regime of transport by measuring the effects of leads placed within elastic scattering length (the ballistic regime). By changing both the size of the attached leads or the capacitive coupling to the sample, important new information on the role of the measurement process in quantum mechanical systems should emerge from additional work on small structures.

R.A. Webb, IBM T.J. Watson Research Center

1. H. A. Webb, S. Washburn, A. U. Benoit, C. P. Umbach, and R. B. Laibowitz, *Proc. 2nd Int. Symp. on Foundations of Quantum Mechanics*, edited by M. Nmiki *et al.* (The Physical Society of Japan, Tokyo, 1987), Vol. 193, p. 193.
2. C. P. Umbach, P. Santhanam, C. van Haesendonck, and R. A. Webb, Appl. Phys. Lett. **50** 1289 (1987).
3. A. D. Benoit, C. P. Umbach, R. B. Laibowitz, and R. A. Webb, Phys. Rev. Lett. **58**, 2343 (1987).
4. W. J. Skocpol, P. M. Mankiewich, R. E. Howard, L. D. Jackel, D. M. Tennant, and A. D. Stone, Phys. Rev. Lett. **58**, 2347 (1987).
5. R. A. Webb, S. Washburn, H. H. Haucke, C. P. Umbach, and A. D. Benoit (submitted for publication).
6. M. Buettiker, Phys. Rev. B **35**, 4123 (1987).
7. Y. Isawa, H. Ebisawa, and S. Maekawa, J. Phys. Soc. Japan **55**, 2523 (1986).
8. Y. Imry (to be submitted); P. A. Lee *et al.* (to be submitted).
9. B. Doucot and R. Rammal, J. Phys. (Paris) **47**, 973 (1986); and a second article to be published.

Membranes, Surfaces, and Microemulsions

When amphiphilic molecules are brought into contact with water they tend to assemble so as to orient their polar hydrophilic "heads" towards the water and their oily hydrophobic chains away from it. Among the simplest structures formed in this way are two dimensional films and membranes, common examples of which are soap films (in which a water layer is "sandwiched" between two monolayers of soap), surfactant monolayers (as found at water–oil interfaces in microemulsions), and bilayer lipid membranes.

Chemists and biologists have long studied amphiphilic systems, mainly because of their biological and technological importance. In recent years these systems have also attracted the attention of physicists, thanks to their variety of phase behavior and the fascinating (micro)structures. Membranes and films can be found in the form of isolated sheets or closed vesicles, three-dimensional (liquid) crystals or "random," topologically complex assemblies (microemulsions).

The recent progress made in understanding many aspects of films, membranes, microemulsions, and lyotropic liquid crystals is largely due not only to the notable refinements of experimental techniques, but also to unusual convergence of interests among different groups of scientists. In February 1987 a remarkable conference in Les Houches, France[1] gathered physicists and physical chemists interested in films and membranes. Quantum field theorists exchanged ideas with specialists in the applications of vesicles in the cosmetic and pharmaceutical industries.

An excellent example of such convergence of interests lies in the problem of bending elasticity of films and membranes, and the role it plays in the thermodynamic behavior of amphiphilic systems. It was recognized long ago that the shapes and fluctuations on unswollen vesicles (even red blood cells) are governed to a large extent by the curvature energy of their membranes. A series of elegant experiments using micromechanical methods and high-contrast video microscopy elucidated the different shapes assumed by such vesicles and the characteristics of their thermal fluctuations, allowing quantitative comparisons with thermodynamic theories. An important consequence of the elastic properties of membranes is the existence of a strong, long-range entropic repulsion between two adjacent sheets. Quantitative measurements of this repulsion have recently been performed in lamellar phases of lyotropic liquid crystals (which can be viewed as stacks of interacting membranes). Moreover, new theoretical studies predict that these fluctuation-induced interactions can lead to a continuous transition at which the membranes separate completely even in the presence of finite molecular attraction. Observation of this critical "unbinding" transition constitutes a major experimental challenge and could lead to better understanding of analogous phenomena on other domains of condensed matter physics, such as the wetting transitions.

Another interesting question connected to elastic properties of membranes is how thermal fluctuations modify the rigidity of a single sheet. It has been argued that in fluid membranes fluctuations decrease the bending rigidity, and thus decrease the persistence length (i.e., the correlation length for the surface orientation). This effect may be important for an understanding of the stability of microemulsion phases and is now being intensively studied by various experimental techniques such as light and neutron scattering and NMR. Even more striking are theoretical predictions for solid, hexatic, or polymerized sheets. In these systems a so-called crumpling transition has indeed been observed in a recent Monte Carlo simulation. Polymerized membranes appear to be good candidates for the experimental observation of this interesting phenomenon.

Fluidity is only one example of the many possible internal aspects of membranes. Important progress in several experimental techniques (including fluorescence microscopy, x-ray synchrotron scattering from surfaces, second harmonic generation) has permitted the observation of many fascinating static and dynamic phenomena taking place inside monolayer films and single bilayers, including formation of spiral crystals of chiral molecules. These phenomena, however, are still poorly understood from both experimental and theoretical points of view.

Finally, it is worth mentioning the astonishing formal connections between the problem of fluctuating membranes or films (which can be viewed as a two-dimensional generalization of the random walks problem) and other topics in theoretical physics and mathematics. For example, it seems that: (i) microemulsions are good experimental systems to explore the problem of random surfaces with varying topology, which arises naturally in theoretical particle physics; (ii) the theory of hexatic membranes is formally equivalent to a renormalizable theory of strings; (iii) the structure of cubic phases in lyotropic liquid crystals is connected to the theory of periodic embedded minimal surfaces, a subject actively studied in differential topology and geometry. Many connections have also recently begun to emerge with cellular biology (for instance in the field of membrane fusion), though one should not overestimate the pertinence of these simple physical concepts to the real biological systems.

Stanislas Leibler, Cornell University
and CEN-Saclay, France

1. *Proceedings of the Les Houches Conference on Amphiphilic Films and Membranes*, edited by D. Langevin and J. Meunier (Springer Verlag, New York, 1987), references therein.

CRYSTALLOGRAPHY

Biological Macromolecules

The recent congress of the International Union of Crystallography in Perth, Australia, illustrated how rapidly the study of macromolecule crystallography has progressed just in the past year. In this article I shall focus on some of the latest advances.

Obtaining an adequate supply of pure sample. Gene manipulation and cloning have revolutionized the availability of pure samples. Not only can relatively large quantities of samples be obtained, but they can also be specifically modified for investigating the effects of amino acid substitutions on molecular function or stability.

Crystallization. The problem of crystallization has received a great deal of long overdue attention lately, with the aim of making systematic a process that has historically been a "black art". Theoretical investigations currently underway hold great promise for the future of crystallization, but practical improvements are here now. For example, computers have been programmed to design the crystallization experiments and robots have been programmed to execute them. A plate for crystallization experiments that is well adapted for both manual use and automated use by robots has been designed, manufactured, and is now available.

Measurement of intensity data. Three years ago, area detectors for the rapid simultaneous measurement of intensity data were only available at a national resource; one had to apply for access and usually had to wait before time was scheduled. Today area detectors are commercial products and are already installed in many individual laboratories. In addition, it has recently been shown that protein crystals can be flash-frozen and that data can be measured from frozen crystals that shows little, if any, radiation damage. More than any other recent advance, the ability to measure accurate data rapidly has changed the face of macromolecular crystallography.

Phasing. Genuinely "direct methods" of phasing macromolecular structures are not with us yet, but the Perth meeting did witness the first report of a protein structure phased by means of anomalous dispersion data measured at multiple wavelengths. There were also many reports at Perth of structures phased using molecular replacement, a phasing technique that becomes more widely applicable as our data base of known structures increases.

Fitting and refinement of a model. The future of both model fitting and refinement lies in eliminating the manual intervention of the crystallographer that is now required by the development of computer programs capable of accomplishing each task completely automatically. At Perth, Alwyn Jones described his progress with computer programs that use the data base of known structures both as a guide in the map fitting procedure and as a check on the structure once it has been fit. The breakthrough in refinement has not come yet, but work is underway on several different approaches to the problem.

These technical and computational advances, and many others, have greatly increased the complexity of problems now being investigated. In the past year we have seen reports of three structures of complexes between antibody and an immunoglobulin fragment specific for that antibody, structures of antiviral drugs of intact ribosomal subunits that diffract to at least five a resolution. But perhaps the best illustration of the increased pace in the field was a slide that Brian Matthews presented at Perth, showing the superimposed results of 13 structure determinations of the phage T4 lysozyme, each with a different amino acid at residue 157. Consider that each structure determination required engineering of the gene, production and isolation of sample, crystallization, data collection and refinement: all summarized in a single slide. Macromolecular crystallography has indeed entered a new era.

Paula Fitzgerald, University of Alberta

Neutron Scattering and High-T_c Superconductivity

The recent discovery of high-temperature superconductivity in Cu-based mixed oxide systems provides an excellent example of the application of a variety of neutron scattering techniques to the determination of crystal structures, phase equilibria, magnetic order, lattice dynamics and spin fluctuations. X-ray powder and single-crystal diffraction experiments quickly established the positions of the cations in $Ba_2YCu_3O_{7-\delta}$ but did not provide definitive information about the oxygen content and positions because of the relatively weak scattering from oxygen and the presence of domains which hampered the single crystal studies. It is generally believed that the oxygen atoms play a critical role in the superconducting properties.[1]

Neutron powder data do not suffer from these disadvantages, and in addition the well-established and powerful technique of profile analysis introduced by Rietveld[2] is particularly well suited to this kind of structural study. In a very short time, precise details of the oxygen positions were independently determined by at least seven groups[1] working at Argonne, the National Bureau of Standards, Brookhaven, McMaster University, the Institute Laue–Langevin, Grenoble, the Rutherford–Appleton Laboratory, Didcot, and the Japanese National Laboratory for High Energy Physics. Three of these are pulsed neutron sources and four steady-state reactors.

The measurements were carried out on independently prepared samples, yet the agreement among the seven sets of results is remarkably good. As is now well documented, the structure has an orthorhombic cell and can be viewed as a heavily distorted, oxygen-defective, ordered derivative of the cubic ABO_3 perovskite structure. An important feature is the ordering of one of the seven oxygens in the basal plane midway along the *b* axis, whereas the analogous site midway along the shorter *a* axis is essentially vacant. One-third of the Cu atoms have a fourfold planar coordination in the *bc* planes, and form chains linked through this set of oxygens. The remaining two-thirds form a dimpled two-dimensional network approximately in the *ab* planes. Further structural studies carried out at some of the above institutes on the related compound $Ba_2YCu_3O_6$, which is tetragonal and non-superconducting, show that the basal plane oxygen has been lost, leaving isolated CuO_2 pairs in these planes.

The application of neutron powder techniques to phase equilibria studies is well illustrated by some very detailed structural studies carried out at the pulsed neutron source at Argonne,[3] where it is possible to obtain complete data sets in as little as two hours. As $Ba_2YCu_3O_7$ is heated, some oxygen is first lost from the basal plane site, while at about 600 °C, the remaining oxygens begin to disorder into the vacant site. At about 700 °C in pure oxygen the composition is roughly $Ba_2YCu_3O_{6.5}$, basal plane disorder is complete and the structure becomes tetragonal. These results demonstrate the importance of annealing temperatures, atmospheres, and cooling rates in determining the superconducting properties of these materials.

The existence of a magnetic transition in $La_2CuO_{4-\delta}$ to an ordered antiferromagnetic state has been demonstrated in a number of experiments at Brookhaven.[4] That the small peaks are indeed magnetic in origin has been unequivocally confirmed by neutron polarization analysis techniques.[5] The occurrence of long-range magnetic ordering indicates the importance of electron spin correlations, which may be a vital clue in the detailed understanding of the mechanism of superconductivity in high T_c materials. Inelastic neutron scattering measurements have also been performed on La_2CuO_4 single crystals.[6] A very interesting and unusual feature of this material is the existence of a novel kind of two-dimensional antiferromagnetic behavior well above the magnetic transition temperature[7]: the spins are ordered instantaneously over long distances, but there is no detectable time-averaged staggered magnetic moment. The energy scale of the spin fluctuations is quite large and lends support to models of superconductivity which invoke magnetic interactions for the pairing.

D. E. Cox, Brookhaven National Laboratory

1. D. O. Welch *et al.*, Nature **327**, 278 (1987) and references therein.
2. H. M. Rietveld, J. Appl. Cryst. **2**, 65 (1969).
3. J. D. Jorgensen *et al.*, Phys. Rev. B **36**, 3608 (1987).
4. D. Vaknin *et al.*, Phys. Rev. Lett. **58**, 2802 (1987); T. Freltoft *et al.*, Phys. Rev. B **36**, 826 (1987); B. X. Yang *et al.*, J. Phys. Soc. Jap. **56**, 2283 (1987).
5. S. Mitsuda *et al.*, Phys. Rev. B **36**, 822 (1987).
6. R. J. Birgeneau *et al.*, Phys. Rev. Lett. **59**, 1329, (1987).
7. G. Shirane *et al.*, Phys. Rev. Lett. **59**, 1613 (1987).

PHYSICS EDUCATION

Introduction

The renewed interest in undergraduate physics education has resulted in several new programs at the National Science Foundation (NSF), some of which fell under the new Office of Undergraduate Programs while others were under the individual research directorates. The American Institute of Physics (AIP) has also reinstituted the Visiting Scientists Program which matches speakers to primarily undergraduate institutions.

The ferment in undergraduate physics[1,2] resulted in a number of programs. One is the project on the new introductory physics sponsored jointly by the American Association of Physics Teachers (AAPT), The American Physical Society (APS), and the AIP.[3] The Introductory University Physics Project (IUPP), funded by a grant from the NSF, is being led by John Rigden, Director of Physics Programs at AIP. The Maryland University Project in Physics and Educational Teaching (MUPPET) is in its third year of a project analyzing the physics curriculum in the light of contemporary physics, computers, and the cognitive sciences. A similar situation in mathematics is being addressed in a like fashion. The first workshop on the introductory calculus course was held at Tulane University and resulted in a call for major changes in the curriculum.[4] Another conference on related topics was held in October at the National Academy of Sciences.

The use of computers in physics continues to be one of the most important concerns at all levels. AIP has introduced a new journal, *Computers in Physics*, to address these issues in research and in graduate and advanced undergraduate education. The second international meeting on Computers in Physics Teaching was held at Dickinson College in January 1987. Plans were laid for future activities, including a large open international meeting to be held at North Carolina State University in August 1988. In 1987 two efforts to review and distribute educational software were announced. AAPT will be doing so through its newly established Instructional Media Center, which will also be reviewing videotapes, videodisks, and other media. AIP will review MS-DOS software under terms of a grant from IBM.

International cooperation on physics education was also evident in 1987. A series of papers on issues in Japanese physics education resulted from the 1986 Tokyo Conference. U.S. participation was coordinated by AAPT under a grant from the NSF. The InterAmerican Conference on Physics Education, meeting in July 1987 in Oaxtepec, Mexico, led to the formation of networks which should continue their work over the coming years.

The International Physics Olympiad, involving 25 countries, was held in Jena, East Germany in July 1987.[7,8] The United States team participated for the second time. The five-member team brought home three bronze medals and an honorable mention. The Canadian team, participating for the third time, brought home three awards.

The Physics Teaching Resource Agents program trained another 50 teachers and continued its regional outreach program. There are now about 250 PTRA's. In this program (see *Physics News in 1986,* p. S56) over 873 local workshops, reaching more than 23 000 teachers, have been held since 1985.[9] Most of these teachers are in high schools, but some PTRA programs have also been held at the junior-high and elementary school level as well.

The AAPT released two position papers on physics teaching: "The Role, Education, and Qualifications of the High School Physics Teacher" and "Course Content in High School Physics." Each was the product of years of effort on the part of several committees; each paper is addressed to decision makers and the general public. The National Science Teachers Association is trying a different approach to similar issues. They have begun a national program of certification of physics teachers. AAPT was invited to join the program but declined to do so after several months of study.

Although there have been incremental improvements in physics education over the last few years, the United States continues to lag behind most of the developed world. American physicists have often conceded the difficulties found in our secondary education system, but have relied upon the universities and graduate schools to make up the difference. It is no longer clear that this is the case. Research and graduate education, particularly in Europe and Japan, have advanced rapidly in the last decade. American institutions are experiencing difficulties in finding qualified native-trained students for graduate study and in getting them through the doctoral programs. One might expect considerable attention to be directed to these issues in 1988.

Jack M. Wilson, AAPT and The University of Maryland

1. J. S. Rigden, Am. J. Phys. **55**, 681 (1987); 491 (1987).
2. J. Wilson, AAPT Announcer **17**, 18 (1987); **15** 120 (1985); **14** 91 (1984).
3. D. Holcomb, R. Resnick, and J. Rigden, Phys. Today **40**, 87 (May 1987).
4. *Toward a Lean and Lively Calculus*, edited by R. Douglas (Mathematical Association of America, **City**, 1987).
5. J. Wilson, "Microcomputers as Learning Tools," in *Proceedings of the InterAmerican Conference on Physics Teaching*, (Publisher, Oaxtepec, Mexico, 1987).
6. *Quarks, Quasars, and Quandries*, edited by G. Aubrecht (AAPT, College Park, MD, 1987).
7. "The Physics Olympiad," AAPT Announcer **17**, 20 (1987).
8. Phys. Today **40**, 71 (September 1987).
9. J. Nelson and Y. Van Hise, Phys. Today (to be published).

Local Physics Alliances

The College–High School Interaction Committee (CHIC), a joint committee of APS and AAPT, has helped initiate a program of "Local Physics Alliances," professional collaborations between teachers of physics from schools and nearby colleges. Under a grant from the National Science Foundation, the APS will run regional how-to-do-it workshops for high school teachers and college faculty interested in closer cooperation. The grant provides for consultant advice and support to local groups as they build alliances. John Russell of Southeastern Massachusetts University and Brian B. Schwartz of APS will act as co-principal investigators.

Taking as its model county bar and medical associations, the program encourages teachers of physics at all levels—like lawyers and physicians—to meet regularly to update their physics knowledge and to improve the quality of physics teaching in their area. The alliances also offer both college faculty and school teachers a glimpse of the other's teaching environment. The school teachers and college faculty better appreciate one another as professional colleagues and their students benefit from the increased sharing of knowledge between them.

For physics teachers the need is especially great. Most teachers of physics in schools are isolated professionally; a recent NSTA survey shows that 85% of high school physics teachers have only one physics class. Generally they must also teach another subject to sustain their commitment to teaching physics. In elementary and middle schools those who teach physics as part of the science curriculum, and who so strongly shape students' early attitude about science, generally have no contact with other professional physics instructors and little stimulation to expand their knowledge of physics.

Most college physics departments want to cooperate more closely with physics teachers in their local schools.

Nearly 500 physics departments across the country have joined in a network formed by the CHIC committee to share information on local school–college cooperative projects. The CHIC Newsletter, edited by Professor Peter Lindenfeld of Rutgers, enables departments which already are cooperating with nearby schools to publicize their efforts and to stimulate others to emulate them. All departments are anxious to increase the number of students studying physics and to maintain high quality in the physics instruction students receive. Many, however, need more active support and encouragement in finding out what teachers in their area need and in building a relationship of professional equality through which to meet those needs. That is what the Local Physics Alliances program will provide. The first workshops are being planned for spring 1988 and will be co-chaired by Don Barron of Wheaton High School, Maryland, and by Karen Johnston of North Carolina State.

John Russell, Southeastern Massachusetts University
Brian B. Schwartz, The American Physical Society and Brooklyn College

ELECTRON AND ATOMIC PHYSICS

New Values for the Constants of Physics

The speed of light in vacuum c, the Planck constant h, and the rest mass of the electron m_e are examples of the fundamental constants of physics. They are important ingredients in basic theories of physics.

It has long been and remains a principal goal of physics to determine the values of the fundamental constants with ever greater accuracy. This is not because adding another decimal point has intrinsic value, but because doing so may lead to the discovery of a heretofore unknown inconsistency in our physical description of nature. The fundamental constants play a key role in the basic theories which connect all of the diverse fields of physics together, and the careful comparison of their numerical values as obtained from various experiments in these different fields can critically test the validity of the basic theories themselves.

It is often necessary to re-examine and revise the recommended values of the fundamental physical constants even when a new value for only one particular constant becomes available because of the complex relationships which exist among them; a significant change in one can lead to significant changes in many others. This re-examination and revision is done by "combining" the available data using a mathematical technique known as least-squares. The resulting values of the constants are thus known as least-squares adjusted values.

A new and significantly more accurate set of recommended values for the fundamental physical constants became available in early 1987. An important milestone for all of science and technology because of the pervasiveness of these fundamental quantities, the new set was published in a report of the CODATA (Committee on Data for Science and Technology) Task Group on Fundamental Constants.[1] The report summarizes the 1986 least-squares adjustment of the constants and gives the new set of self-consistent values of the constants derived from that adjustment. Recommended for international use by CODATA, the 1986 set replaces the set of constants established by CODATA in 1973.[2]

The 1986 adjustment was motivated by the extraordinary experimental and theoretical advances made since the 1973 adjustment in almost all areas relevant to the fundamental constants. Examples are the high-accuracy, direct measurement of infrared and optical frequencies, culminating in the redefinition of the meter in terms of the distance traveled by light in a given time; the accurate, direct determination of an atomic lattice spacing in terms of an optical wavelength leading to a more accurate value of the Avogadro constant; the significantly improved measurement of the anomalous magnetic moment of the electron and quantum electrodynamic calculation of its theoretical value in terms of the fine-structure constant α; and the discovery in 1980 by K. von Klitzing of the integral quantum Hall effect resulting not only in a highly accurate value of α from solid-state physics, but the 1985 Nobel prize for physics as well.

As in previous least-squares adjustments of the constants, the data for the 1986 adjustment were divided into two groups; auxiliary constants and stochastic input data. Auxiliary constants are either defined constants such as c that have no uncertainty or constants with uncertainties sufficiently small in comparison with the uncertainties of the stochastic input data that their values cannot be significantly affected by the least-squares adjustment. In the present case the uncertainty of each auxiliary constant was no greater than 0.02 parts per million, or ppm. In contrast, the uncertainty assigned the 38 items of stochastic input data considered in the 1986 adjustment were in the range 0.065–9.7 ppm.

Each of these 38 items was expressed, using the auxiliary constants as necessary, in terms of five quantities that served as the unknowns or variables of the 1986 adjustment. "Best" values in the least-squares sense for these five quantities, with their uncertainties, are thus the immediate output of the adjustment. After an exhaustive analysis using a number of least-squares algorithms, the initial group of 38 items of stochastic input data was reduced to 22 items by deleting those that were either highly inconsistent with the remaining data or had assigned uncertainties so large that they carried negligible weight. The adjusted values of the five unknowns and all the other 1986 recommended values that were subsequently derived from them are thus based on this final input set of 22 items. As a result of the enormous advances made throughout the precision measurement-fundamental constant field since 1973, the 1986 adjustment represents a major advance over its 1973 counterpart; the uncertainties of the recommended values have been reduced by roughly a factor of ten!

The 1986 adjustment provides a good example of how the fundamental constants can be used to test physical theory. If the quantum Hall effect (QHE) data are deleted from the final set of 22 items of input data and a new adjustment using the remaining data is carried out, and if the resulting new adjusted value of α is compared with that directly obtained from the deleted QHE data, then one finds that the two values of α differ by only (0.043 ± 0.085) ppm. One may therefore conclude that the theory of the QHE, which predicts that this macroscopic solid-state physics phenomenon can be used to determine to high accuracy the basically microscopic fine-structure constant α, is indeed correct.

Barry N. Taylor, National Bureau of Standards

1. E. R. Cohen and B. N. Taylor, CODATA Bull. **63** (Pergamon Press, Nov. 1986); Rev. Mod. Phys. **59**, 4 (Oct. 1987).

2. CODATA Bull. **11** (Intl. Council Sci. Unions, Paris, Dec. 1973); E. R. Cohen and B. N. Taylor, J. Phys. Chem. Ref. Data **2**, 663 (1973).

Chaos in Atomic Physics

In the last ten years our understanding of irregular dynamics in nonlinear classical systems has been progressing rapidly. Of greatest importance has been the realization that even very simple mathematical models, described by a few nonlinear differential or difference equations, can exhibit behavior as complex as a random process. In particular the word "chaos" has emerged as a technical term with a precise mathematical meaning to refer to the irregular behavior of these deterministic models.[1] However, since the microscopic description of strongly perturbed and strongly coupled systems in atomic, molecular, and solid-state physics is governed by the linear equations of quantum mechanics, much recent attention has been focused on the question of whether the effects of classical chaos persist on the quantum level.[2]

Initial theoretical studies of this issue were confined to simple models of nonlinear oscillators subject to periodic perturbations or models of molecules with an anharmonic potential. The classical dynamics of these systems exhibits a dramatic transition from regular to chaotic behavior as the nonlinearity is increased, either by raising the strength of the perturbation or by increasing the energy of the molecule. Moreover, because of the simplicity of these models, direct numerical integration of the corresponding Schrödinger equation has been used to investigate the quantum dynamics. These studies have resulted in a large number of papers with a variety of provocative results which have sparked a lively debate over the problem of "quantum chaos."[2]

Ultimately, experimental studies of real quantum systems which correspond to classically chaotic systems are required to resolve this controversial issue. In the last few years experimental investigations of two very simple atomic systems have provided the first detailed pictures of how the classical nonlinear dynamics can affect the behavior of real quantum systems. Specifically, the measurements of the microwave ionization of highly excited hydrogen atoms by Koch[3] at Stony Brook and Bayfield[4] at Pittsburgh provide a means of investigating the quantum behavior of a periodically, perturbed nonlinear oscillator. The photoabsorption spectroscopy of highly excited hydrogen atoms in strong static magnetic fields by Welge[5] at Bielefeld in West Germany, provides a means of studying quantum behavior of a two-dimensional anharmonic oscillator. Moreover, because of the relative simplicity of the mathematical models which describe these physical systems, considerable insight has been gained into the problem of "quantum chaos" through the detailed classical, semiclassical, and quantum analyses of the experimental results.

For example, Koch has measured the threshold microwave fields for the sharp onset of ionization for hydrogen atoms prepared in initial quantum states ranging from an n of 32 up to 90. Remarkably, these experimental results for the threshold fields are in excellent agreement with the predictions for the onset of chaos in the corresponding classical model of a periodically perturbed Kepler orbit.[6] The quantum theory for these experiments is very difficult, since roughly 100 photons are required for ionization and the threshold fields correspond to 10% of the Coulomb binding field. Nevertheless, numerical solutions of the time-dependent Schrödinger equation for a one-dimensional model of the experiments indicate that for the present experimental parameters the wave functions exhibit an abrupt transition from a localized to a delocalized wavepacket, which rapidly ionizes, when the threshold field is exceeded.[7,8] Although these numerical calculations reveal the mechanism whereby the quantum evolution can mimic the onset of classical chaos, these calculations also predict that for other ranges of experimental parameters the quantum system will remain localized,[8] through a mechanism related to Anderson localization,[9] even when the classical system is fully chaotic. The experiments are expected to explore this new regime, where the classical and quantum theories disagree, in the very near future.

In addition, Welge's measurements of the photoabsorption spectrum near the ionization energy for a hydrogen atom in a strong magnetic field reveals a spectrum of modulations which can be associated directly with individual classical periodic orbits.[5,10] Despite the fact that the classical phase space is almost fully chaotic at these energies, the quantum mechanics appears to cling to these unstable periodic orbits. These remarkable results provide another example of how the quantum mechanics can remain more regular than the classical dynamics.

As both experiments and theory progress, this work will continue to enhance our understanding of the nature and limitations of the quantum manifestations of classical chaos and, perhaps more importantly, will reveal the rich new structure of quantum physics for strongly perturbed and strongly coupled systems which promises to have important applications in the interaction of intense radiation with matter, in chemistry, and in solid-state and nuclear physics.[2]

Roderick V. Jensen, Yale University

1. R. V. Jensen, Am. Sci. **75**, 168 (1987).
2. *Chaotic Behavior in Quantum Systems*, edited by G. Casati (Plenum, New York, 1985).
3. K. A. H. van Leeuwen *et al.*, Phys. Rev. Lett. **55**, 2231 (1985).
4. J. N. Bardsley, B. Sundaram, L. A. Pinnaduwage, and J. E. Bayfield, Phys. Rev. Lett. **56**, 1007 (1986).
5. A. Holle, G. Wiebusch, J. Main, B. Hager, H. Rottke, and K. H. Welge, Phys. Rev. Lett. **56**, 2594 (1986).
6. R. V. Jensen, *Atomic Physics 10*, edited by H. Narumi and I. Simamura (Elsevier, Amsterdam, 1987).
7. R. Blumel and U. Smilansky, Z. Phys. **D6**, 83 (1987).
8. G. Casati, B. V. Chrikov, and D. L. Shepelyansky, Phys. Rev. Lett. **53**, 2525 (1984); G. Casati, B. V. Chrikov, D. L. Shepelyansky, and I. Guarneri, Phys. Rev. Lett., **57**, 823 (1986).
9. R. E. Prange, D. R. Grempel, and S. Fishman, in *Chaotic Behavior in Quantum Systems*, edited by G.Casati (Plenum, New York, 1985), p.205.
10. D. Wintgen and H. Friedrich, Phys. Rev. A **36**, 131 (1987).

Antiprotons in an Ion Trap

Antiprotons are the antimatter counterparts of protons, which together with neutrons and electrons make up most of our universe. The unique Low Energy Antiproton Ring (LEAR) operating at the European Center for Nuclear Research (CERN) decelerates antiprotons created in huge accelerator facilities at GeV energies to kinetic energies as low as 21 MeV and 5 MeV. To go to much lower energies, our TRAP collaboration[1] obtained 150 nsec bursts of approximately 10^8 antiprotons at 21 MeV from LEAR. As many as 1 in 10^4 of these antiprotons were slowed to below 3 keV by collisions within 3 mm of beryllium, when the thickness was optimally adjusted.

The slowed antiprotons traveled along magnetic field lines from a strong 6 Tesla solenoid and within a series of three cylindrical metal electrodes which together comprised a crude ion trap. A rapid application of -3000 volts to one electrode completed the ion trap while the antiprotons were inside. After a prearranged time, the antiprotons were released from the trap, after which they hit a wall of the apparatus and annihilated. The highly energetic pions which were produced traveled easily through the vacuum walls of the apparatus and produced light pulses in surrounding plastic scintillators. These were counted to ascertain that nearly 10^3 particles were confined in the trap for more than 1 msec from a single burst of antiprotons as described. The number of antiprotons slowed and confined could eventually be increased by as much as a factor of 10–100.

The time that antiprotons can be held in the trap determines the type of experiments which can be done. Antiprotons readily annihilate via collisions with background gas atoms. So far, antiprotons were twice held for 10 min, and each time only five antiprotons remained. With improved vacuum, however, prospects are excellent for holding the antiprotons for a much longer time, ideally for longer than 10 months as was done with a single electron.[2] The vacuum requirements are indeed stringent, a pressure less than 10^{-14} Torr is required to keep the annihilation rate below one per day under the desired conditions for the mass measurement. This pressure will be achieved by submerging a closed vacuum vessel in liquid helium.

One possible cooling scheme for going below 3 keV is to let a cold buffer gas of electrons in the same trap collide with the antiprotons. At a later stage, oscillations of the antiprotons will lose energy as they produce a current in a cold resistor attached to the trap, until they reach thermal equilibrium with the resistor. With cold antiprotons, at 4.2 K, a goal is to measure the ratio of the antiproton to proton masses by comparing measured cyclotron frequencies. This ratio is now known to be unity to within a few parts in 10^5 from comparisons of the calculated and measured x-ray energies in exotic atoms, which have an antiproton orbiting a nucleus. We hope to improve the accuracy by four orders of magnitude or more.

The theoretical expectation, of course, is that the proton and antiproton will have the same mass, because of the invariance of local, relativistic field theories under a charge conjugation, parity, and time reversal transformation (*CPT*), which transforms a particle into its antiparticle. Experimental confirmations of *CPT* invariance are surprisingly scarce, however.[3] The most accurate comparison is for the K°meson and its antiparticle, each of which is made up of a quark and antiquark. Accurate comparisons of the masses and magnetic moments of leptons have also been made, for electrons and muons. No other experimental tests exceed one part per million in accuracy. In fact, the antiproton to proton mass comparison would be the first test of *CPT* invariance done with a baryon (three bound quarks) which exceeds this precision.

In the future it may be possible to produce "antihydrogen" via recombination of cold positrons and antiprotons within various ion traps. To study its properties, it would be nice and perhaps necessary to capture antihydrogen as it is formed in a surrounding neutral particle trap. Since we have

been contemplating this difficult scenario, copious amounts of hydrogen have been confined in a neutral particle trap,[4] and there is increasing interest in slowing and trapping hydrogen as a means for doing more precise spectroscopy. With trapped and cooled antihydrogen, it would be possible to measure the gravitational acceleration of a neutral antihydrogen atom by observing how the gravitational force shifts the location of an antihydrogen atom in a magnetic trap. Such effects were recently observed with trapped sodium atoms.[4]

Gerald Gabrielse, Harvard University

1. G. Gabrielse, X. Fei, K. Helmerson, S. L. Rolston, R. Tjoelker, T. A. Trainor, H. Kalinowsky, J. Haas, and W. Kells, Phys. Rev. Lett. **57**, 2504 (1986).
2. G. Gabrielse, H. Dehmelt, and W. Kell, Phys. Rev. Lett. **54**, 537 (1985); see also Phys. Today **38**, 17 (May 1985).
3. Particle Data Group, Rev. Mod. Phys. **56**, S1 (1984).
4. See accompanying item on neutral particle trapping by D. Pritchard.

Trapping Neutral Atoms

The three new traps for neutral atoms which have been demonstrated this year open the way for significant experiments on trapped atoms. Over 10^{12} atoms have been trapped, densities of $10^{11}/cm^3$ have been reached, and trapping times of many minutes have been observed. These represent orders of magnitude improvement over the previous atom traps.[1] In addition to demonstrating new technology, atom trap experiments are beginning to yield measurements of intrinsic physical interest.

The first new trap confines Na atoms to a local magnetic field minimum. In this trap, built by D. Pritchard's group at MIT, laser light pressure is used to slow and load atoms continuously into the trap; more than 10^9 atoms have been trapped and cooled to a few millikelvin.[2] The effect of gravity on the trapped atoms is large, displacing the trapped atoms several cm from the exact field minimum. The apparatus can be described as a "gravitational–magnetic state separator": atoms in different hyperfine states have different effective magnetic moments and are confined at different vertical positions in the trap.

The second new trap, demonstrated at AT&T Bell Labs in a collaborative effort between S. Chu's group and Pritchard's group, uses light forces to confine the atoms.[3] Its most novel feature is that the trapping force arises from light forces originating from near-resonant scattering of the photons in the laser beams, rather than the gradient light forces used in earlier traps. As a result, traps of about 1 cm^3 size can be constructed. The key breakthrough is the use of a very weak magnetic field to differentially shift the atoms' magnetic sublevels across the trap so that the atoms preferentially scatter photons which force them toward the field center. This trap has compressed about 10^8 atoms to densities in excess of $10^{11}/cm^3$. The trapping light force has also been used to cool the atoms to a fraction of a millikelvin. Under these conditions Doppler broadening is negligible, and the width of the absorption line is close to the natural linewidth.

The third new trap is a magnetic field minimum trap, but it is novel in two important respects: it traps H atoms, and the atoms are cooled using a helium-3 dilution refrigerator rather than laser cooling. The trap, constructed at MIT under the supervision of T.Greytak and D.Kleppner, is loaded with a puff of cold, spin-polarized H atoms.[4] The trap depth is several times greater than the atoms' thermal energy, so escaping atoms must remove an energy equal to several times the average thermal energy per atom, cooling the remaining atoms. This evaporation process leaves behind more than 10^{12} atoms which have been cooled to about 40 millikelvin, where their evaporation rate becomes insignificant.

The attainment of dense, cold atom samples opens up the interesting new area of ultracold atomic collisions physics. At Bell Labs, an excited-state collisional loss mechanism has been observed which shortens the storage time at high densities. The collisional loss mechanism may reflect the attainment of a new regime (for atomic collisions), one in which the spontaneous decay time is shorter than the lifetime of the collision so that decay during the collision is highly probable. Two collision processes have been observed in the MIT hydrogen trap: spin exchange which initially expels atoms with the "wrong" nuclear spin from the trap, and depolarization which arises from the long range dipole–dipole coupling between the electron spins of the colliding atoms.

In addition to ultracold collisional phenomena, neutral atom traps open possibilities for high-resolution spectroscopy, better atomic frequency standards, fundamental physical tests using trapped atoms, and the study of cooperative effects such as super-radiance and Bose condensation. With this year's generation of new traps, some of these possibilities should become reality.

David E. Pritchard, Massachusetts Institute of Technology

1. *Physics News in 1985*, p. S31; *Physics News in 1986*, p. S25.
2. V. S. Bagnato, G. P. Lafyatis, A. G. Martin, E. L. Raab, R. N. Ahmad-Bitar, and D. E. Pritchard, Phys. Rev. Lett. **58**, 2194 (1987).
3. E. L. Raab, M. Prentiss, A. Cable, S. Chu, and D. E. Pritchard (to be published in Phys. Rev. Lett.).
4. H. F. Hess, G. P. Kochanski, J. M. Doyle, N. Masuhara, D. Kleppner, and T. J. Greytak (to be published in Phys. Rev. Lett.).

Neutrinos From Supernova SN1987A

On February 23, 1987, at 7:35 Universal Time, a burst of neutrinos produced interactions in two large underground detectors, the Kamiokande II detector[1] operated by a Tokyo-KEK-Niigata-Pennsylvania collaboration near the village of Kamioka, Japan, and the Irvine-Michigan-Brookhaven (IMB) detector[2] near Cleveland, Ohio. Both detectors were unattended at the time, but the interactions were recorded on magnetic tape. Several hours later, optical astronomers in the southern hemisphere observed the first supernova visible to the naked eye since the invention of the telescope. The supernova, known as SN1987A, was initiated by the gravitational collapse of a star 170,000 years ago in the Large Magellanic Cloud, a dwarf galaxy which is a satellite of our own galaxy. The supernova and the detection of the associated neutrinos is a major event for astrophysicists and elementary particle physicists alike (see the corresponding article on the supernova in the chapter on astrophysics).[3]

The systematic study of supernovae is a half-century old. In recent years they have been detected at the rate of about one per month by optical astronomers looking at galaxies beyond the Milky Way. Type I supernovae are believed to be produced when a white dwarf star accretes matter from a binary companion. The mass accretion increases the pressure and the temperature causing the carbon-oxygen core to ignite, producing a thermonuclear deflagration or detonation which destroys the star. In contrast, the progenitors of Type II supernovae such as SN1987A are believed to be massive stars with iron cores. When the mass of the inert iron core reaches a certain critical mass, "the Chandrasehkar mass," it can no longer support itself against gravity, and it collapses. The core collapse proceeds until it reaches a density slightly greater than nuclear density. Infalling material then "bounces" and creates a shock wave which propagates through the outer layers of the star producing the optical pyrotechnics of the supernova. The residual core cools to a neutron star, or if the core mass is large enough, a black hole.

The role played by neutrinos in Type II supernovae is fundamental. As the collapse progresses, electron capture of free and bound protons produces a burst of electron neutrinos of average energy about 10 MeV lasting a fraction of a second, and involving no more than 10^{51} ergs. When the bounce shock breaks out of the "neutrinosphere" at the periphery of the core, an additional few times 10^{51} ergs is liberated. Most of the neutron star's prodigious binding energy of a few times 10^{53} ergs (0.1–0.2 solar masses) is subsequently released in neutrino–antineutrino pairs of all flavors (electron, muon, and tau types) in roughly equal numbers over some seconds. The electron neutrinos and antineutrinos have average energies of 10–15 MeV. The total energy output in neutrinos of all types can be compared with the optical output of the supernova, which for a year is only about 10^{49} ergs.

The preceding description of a Type II supernova is highly schematic and ignores the interplay of general relativity, hydrodynamics, and the strong and electroweak interactions used to calculate the collapse of the progenitor and the cooling of the residual core.[4]

Both the Kamiokande II and IMB detectors are large volume (2140 and 5000 tons, respectively) water vessels viewed by a uniform surface array of photomultiplier tubes sensitive to Cerenkov light emitted by charged particles traveling faster than the speed of light in the water (see Fig. 1).

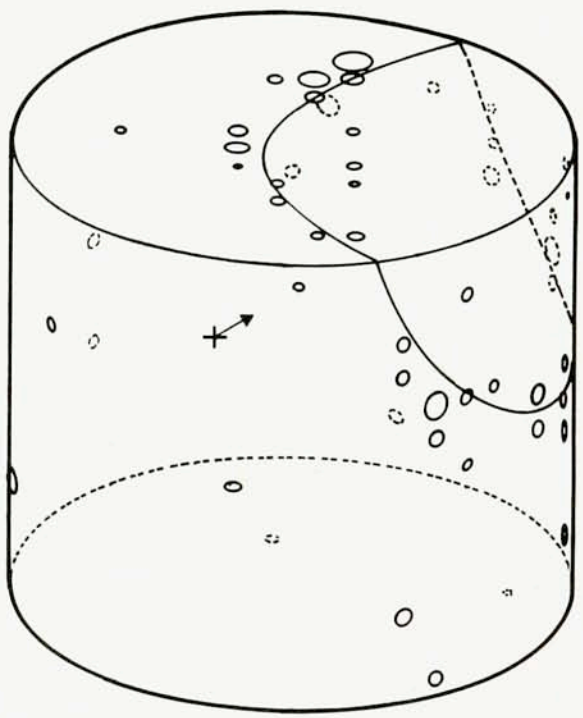

FIG. 1. Schematic representation of event 9 of the neutrino burst from SN1987A as recorded in the Kamiokande II detector. The detector is a 16 meter diameter by 16 meter high cylindrical water vessel viewed by 0.5 meter diameter photomultipliers mounted on a 1.0 meter grid on the inner surface of the vessel. The small circles on the surface of the cylinder in the figure represent photomultipliers which participated in the event. The area of the small circles represents the energy deposition viewed by the photomultiplier. The cross and arrow near the center of the cylinder represent the event vertex location and electron trajectory. The irregular solid line on the surface of the cylinder is the projection of the ring of Cerenkov light for the measured electron vertex and direction on the cylinder surface. Multiple scattering of the electron and Rayleigh scattering of the Cerenkov light by the water cause some photomultiplier tubes far from the nominal Cerenkov ring to be illuminated.

The neutrinos may interact with the free protons in the water, atomic electrons, and oxygen nuclei. The largest interaction probability is associated with the absorption of electron antineutrinos by free protons producing neutrons which are almost at rest, and positrons. The kinetic energy of the positrons is 1.8 MeV less than that of the incident neutrino, and they are distributed almost isotropically with respect to the antineutrino direction. The only other important interaction is the elastic scattering of neutrinos from atomic electrons in the water. All flavors of neutrinos and antineutrinos scatter from electrons. Although electron neutrinos dominate this scattering probability, this probability varies from about 10–40 times less than electron antineutrino absorption on protons at the energies of interest. Electrons recoiling from scattered neutrinos carry little information about the neutrino energy, but are kinematically constrained to trajectories close to that of the incident neutrino. Measurement of the intensity of the Cerenkov light determines the energy of the electron or positron, while the distribution of Cerenkov light over the surface of the vessel determines the direction of the particle. Electron neutrino and antineutrino absorption by oxygen can be ignored below neutrino energies of about 35 MeV.

The neutrino burst of February 23, 1987 produced eleven events in thirteen seconds in the Kamiokande II detector, and simultaneously produced eight events in six seconds in the IMB detector. The absolute time with respect to the optical light curve and the identification of the progenitor star as a blue giant, the time duration of the burst, the energy spectrum of the observed events, the angular distribution with respect to the direction of the supernova, and the absence of any background process which explain the data all lead to the conclusion that the gravitational collapse of a stellar core and the subsequent birth of a neutron star have been observed directly for the first time in history!

Thirty years of laboratory research on neutrinos have provided the input for model calculations of supernovae which agree remarkably well with the statistically limited data. It is interesting to note that the difference between the total electron antineutrino energy inferred from the measurements and the typical binding energy of a neutron star implies that the bulk of the binding energy is carried away by mu and tau neutrinos and antineutrinos created solely by the neutral-current weak interaction, a mechanism first observed only fifteen years ago.

The supernova event has also had a direct impact on our understanding of neutrinos. Owing to the great distance to the Large Magellanic Cloud the lower limit on the lifetime of electron neutrinos and antineutrinos has been extended by three orders of magnitude, ruling out neutrino decay as an explanation of the solar neutrino problem. The long distance to the source and the low energy threshold of the Kamiokande II detector (7.5 MeV) also permit an upper limit of 20 eV to be placed on the mass of the electron antineutrino.[5] This result is comparable to the best results obtained in terrestrial laboratories to date. The data also place a limit of about seven on the number of flavors of light neutrino; adding more flavors reduces the expected flux of each flavor until the observation disagrees with the expectation.[6] Finally, many exotic mechanisms to transport the gravitational binding energy out of the core can be excluded: Our present knowledge of physics seems adequate to describe the data available.

The new science of neutrino astronomy awaits the next Type II galactic supernova.

Eugene W. Beier, University of Pennsylvania

1. K. Hirata *et al.*, Phys. Rev. Lett. **58**, 1490 (1987).
2. R. M. Bionta *et al.*, Phys. Rev. Lett. **58**, 1494 (1987).
3. David Helfand, Phys. Today **40**, 24 (August 1987); Adam Burrows, Phys. Today **40**, 28 (September 1987).
4. S. A. Colgate and R. H. White, Astrophys. J. **143**, 626 (1966); S. E. Woosley, J. Wilson, and R. Mayle, Astrophys. J. **302**, 19 (1986); and A. Burrows and J. M. Lattimer, Astrophys. J. **307**, 178 (1986).
5. E. W. Kolb, A. Stebbins, and M. Turner, Phys. Rev. **35D**, 3598 (1987).
6. D. N. Schramm, Proc. XXII Recontre de Moriond (in press, 1987).

Update on the Superconducting Super Collider

The Superconducting Super Collider (SSC) will provide high energy physics with unsurpassed research opportunities from the time of its projected completion around 1996 well into the twenty-first century. The collisions of its oppositely rotating 20-TeV proton beams will explore a domain far beyond that accessible at the Tevatron Collider, which is just now beginning to produce results at Fermilab.

The potential for discoveries at the SSC will be determined by the energy of the machine and the intensity of its beams. The energy cannot be increased arbitrarily because maintaining the beam in its closed orbit requires intense magnetic fields. Extensive work carried out at Brookhaven, Fermilab, Lawrence Berkeley Laboratory, and elsewhere has demonstrated that 6.6 Tesla superconducting magnets can be relied on to provide the required bending field. With this quantity fixed, the radius of the machine is proportional to the beam energy.

The SSC is designed to yield an enormous number of proton–proton collisions, about 10^8 per second. This corresponds to a "luminosity" of 10^{33} cm^{-2} s^{-1}. It is impossible to record the result of each of these collisions, most of which will produce a hundred or more particles. In fact, only a small fraction of the collisions are of interest for any particular investigation. It is essential then to be able to identify these events rapidly, to "trigger" on them, and to read out electronically the data that will allow their features to be reconstructed. A typical event may have 200 or so particles produced by the collision of the two protons. Since the interesting events are rare, it is desirable to generate as many events as possible, while still retaining the capability to identify the needles in the enormous haystack. At a total energy of 40 TeV, a luminosity of 10^{33} cm^{-2} s^{-1} appears an effective choice, balancing the desire to maximize useful output from the detector against the difficulty of handling 10^8

events per second and the radiation damage higher rates would cause sensitive electronic components.

What new discoveries are within reach of a machine with a center-of-mass energy of 40 TeV and a luminosity of 10^{33} cm^{-2} s^{-1}? Precisely because the SSC will explore a new domain, it is impossible to predict what it will find. However, our understanding of fundamental interactions is sound enough to permit us to say whether or not a particle could be discovered once we hypothesize its existence. Five quarks are already known: the *u*, *d*, *s*, *c*, and *b*. It is nearly certain that there is a sixth, whose mass seems to be greater than about 50 times the mass of a proton. This *t* quark is likely to be produced copiously at the SSC. There may be additional quarks, and if their masses are less than about 1–2 TeV/c^2, they could be discovered at the SSC. Similarly, three charged leptons, the electron, the muon, and the tau are known. Additional charged leptons, up to a mass of about 0.5 TeV/c^2 could be found at the SSC.

Even more exciting would be the discovery of a new "gauge boson." Gauge bosons are the carriers of forces, the most familiar being the photon, which carries the electromagnetic force. The W and the Z discovered at the European Laboratory for Particle Physics, CERN, in Geneva, Switzerland are gauge bosons responsible for weak interactions like nuclear beta decay. The discovery of a new gauge boson would indicate the existence of a hitherto unknown force. A more enigmatic particle is the Higgs boson, which is intimately connected to the origin of the masses of all particles. Although it is uncertain exactly what form the Higgs boson might take, if it conforms to the simplest possibility and if its mass is too great to permit it to be found earlier at $e^+ e^-$ machines, the SSC will be ideally suited to discover it. Even if there is not a simple Higgs boson, the SSC will be able to explore whatever lies at the heart of the difference between the electromagnetic and weak interactions. Reducing the planned energy or the luminosity would dramatically reduce this capability. One exciting speculation is that in addition to all the known particles, there is an entirely new, more massive set, with each new particle related to a known particle but having spin (intrinsic angular momentum) differing by one-half unit. This proposal is known as supersymmetry and its realization would yield a bonanza of particles for the SSC to study.

During the past year, SSC research and development and related efforts have centered on three areas: design of the accelerator itself, design of detectors to measure particle collisions at the SSC, and theoretical investigations of physics that might be uncovered at the SSC. At the same time, important progress has been made on the practical issue of obtaining approval and funding for the project. On January 30, 1987, Secretary of Energy John S. Herrington announced President Reagan's decision to support the construction of the SSC. The determination of the site for the SSC will be made on the basis of the proposals submitted by various states by September 1987. The proposals will be narrowed to a small set by a Select Panel appointed by the National Academy of Science and the National Academy of Engineers.[1] The Department of Energy plans to pick a preferred site from the list during the summer of 1988. The final choice will be announced by the Secretary of Energy in January 1989, with site preparation beginning directly afterwards. All of this is dependent, of course, on the support of the Congress. The projected spending shows the annual construction cost climbing rapidly to a figure around $600 million to $700 million, maintained from FY 90 through FY 94, then dropping during the two final years of construction.

While spending on the SSC was modest during 1987 (about $20 million), important R&D was carried out across the country, directed by the Central Design Group located at the Lawrence Berkeley Laboratory. More than two dozen model superconducting magnets have been constructed, with lengths between 1 and 4.5 meters. In addition, a number of full-scale 17-m dipole magnets have been built.

The exciting discovery of a class of oxide superconductors with considerably higher critical temperatures raised the question of whether much higher magnetic fields and so much smaller size and easier operating conditions might transform the supercollider, but it appears that the new materials will not provide a shortcut to the SSC.[2] Quite apart from the uncertainties about their properties, important limitations from mechanical strength considerations, the need for quench protection, and the necessity of maintaining an extremely good vacuum reduce the impact that the new superconductors could have on the design of the SSC. While the use of the new high-temperature superconductors in the primary focusing and bending magnets of the machine seems quite unlikely, efforts have begun to see if 90K superconductors could be exploited for special purposes.

The demands placed on detectors at the SSC will be far greater than at any earlier accelerator. The enormous event rate and extreme complexity of the events require very fast response time and fine segmentation of the detector. Fast, sophisticated electronics will be needed to collect information from as many as several thousand channels. In July 1987 over 260 physicists from 84 institutions, including 24 from outside the United States, met for two weeks in Berkeley to discuss possible detector designs, in a continuation of workshops held in Snowmass, Colorado in 1982, 1984, and 1986.[3]

Interest in a high-energy hadron collider has spread worldwide, including ongoing construction of a 3 TeV + 3 TeV collider in the Soviet Union and discussion in Europe of a collider in the LEP tunnel.[4] Many Europeans participated in the Berkeley detector workshop and indeed a workshop on the physics of high-energy colliders was held earlier at La Thuile, Italy in January 1987.

Robert N. Cahn, Lawrence Berkeley Laboratory

1. Phys. Today **40**, 52 (August 1987).
2. Phys. Today **40**, 50 (August 1987).
3. Stephen Adler, *Physics News in 1986*, p. S28.
4. Phys. Today **40**, 71 (September 1987).

The 1987 TEVATRON Collider Run

The top energy available for experiments in high-energy physics increased significantly in 1987 with the commissioning and first data runs of the Fermilab TEVATRON proton–antiproton collider. The run, which took place between January and early May, saw steady progress in the accelerator performance and achieved the goals of exceeding 10% of the full design luminosi-

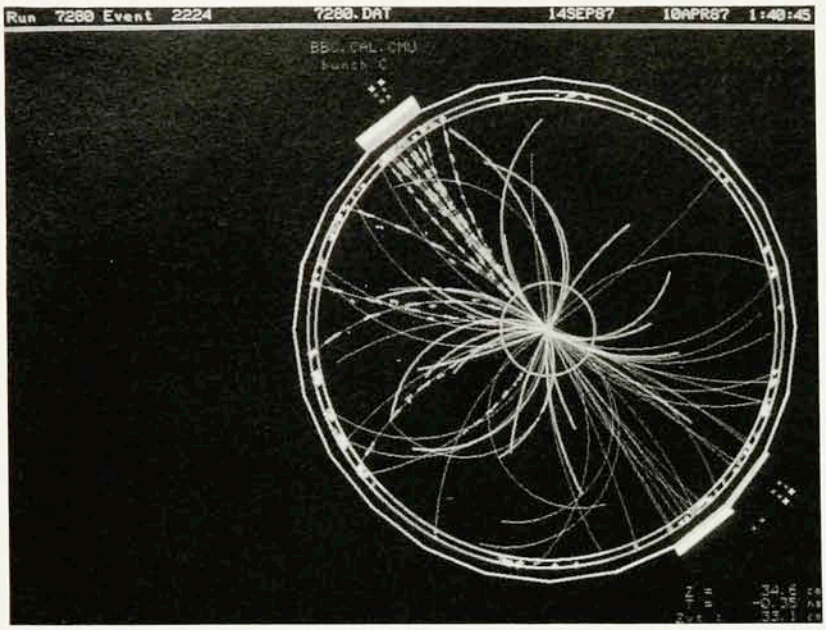

FIG. 2. A two-jet event observed by the CDF experiment.

ty at a collision energy of 1.8 TeV and providing colliding beams for detector checkout and initial physics running. The Collider Detector at Fermilab (CDF) collected many events (see Fig. 2) containing W and Z bosons, the carriers of the electroweak force, previously seen only at the CERN SPS collider in proton–antiproton collisions up to 0.63 TeV. CDF also detected examples of quark and gluon interactions at energies higher than observed previously. Along with the general purpose CDF, two other, more specialized, experiments took preliminary data.

The Fermilab TEVATRON is the first high-energy accelerator based on superconducting magnets. It was operated as a source of beams for fixed target experiments since October 1983. In 1986, modifications to the accelerator to permit colliding beams experiments and commissioning of the antiproton source (another major accelerator achievement) were completed, paving the way for the 1987 collider run. The principal challenge to the Fermilab accelerator physicist was to orchestrate the complex actions of the TEVATRON, the original Fermilab Main Ring, the antiproton source, and other machines in the system so that sufficient antiprotons would be produced, transferred efficiently to the TEVATRON, brought into collision with protons, and stored for several hours of experimental data taking while the next batch of antiprotons was accumulating. By May, the typical antiproton accumulation rate exceeded 10^{10}/hr, the typical starting luminosity was greater than 10^{29} cm^{-2} s^{-1}, and the beam storage times were several hours. The accelerator physics objectives of the run had been met.

The goals for the CDF Collaboration, a consortium of physicists, students, and staff from 10 U. S. universities, 3 U. S. national laboratories, 2 Italian institutions, and 2 Japanese institutions, were to test its large general purpose detector and to take a first look at 1.8-TeV physics. Essentially all of the hardware components of the 4500-ton device had been installed by the time of the 1987 run. CDF comprises charged particle tracking detectors, electromagnetic shower counters, hadron calorimeters, and muon detectors covering a large solid angle where the most energetic collisions are expected to emerge. It has more than 50 K channels of analog information to provide data on events selected by a trigger system. These data are assembled by a control system involving clustered computers, FASTBUS data communications, and distributed microprocessors for correction and compaction. The first priority for the 1987 was to test all of these pieces together as a system. By the middle of February, most simple problems had been uncovered and the running was interrupted for one week to effect repairs and fixes. After that, the TEVATRON and CDF ran essentially continuously until May 10 without significant interruption.

By the end of March, the first convincing example of a W event was found by CDF. Also, hundreds of beautiful examples of jet events were recorded, giving vivid representations of the underlying quark–gluon structure of the proton. The detector was working well enough then to concentrate on accumulating data for physics studies. By the end of the run, CDF recorded over half a million collision events, including approximately 50 vector boson (W and Z) candidates, and hadron jets having energies higher than previously detected. These data are being studied offline to monitor detector performance and learn new physics.

With the data collected during the 1987 run, the CDF group intends to measure the general properties of 1.8-TeV collision events, to verify predictions of the Standard Model of quark and lepton interactions, and to begin to look for phenomena beyond the Standard Model. Many analyses will follow from this data; for example, approximately 20 Ph.D. theses are expected from this first round of data! The next data run will begin in early 1988. More than ten times the integrated luminosity is anticipated in that run which should allow the CDF group to make a serious search for the top quark and to accumulate more W and Z events than have been observed to date by the pioneering experiments at the CERN collider. With some luck one will begin to see the outlines of physics beyond the Standard Model.

The productivity of the 1987 TEVATRON collider run should be exceeded in the relatively near future, but the satisfaction experienced by the physicists, engineers, students, and staff

who had labored for so many years to make it possible cannot be surpassed.

Roy F. Schwitters, Harvard University

1. Argonne, Brandeis, Chicago, Fermilab, INFN-Frascati, Harvard, Illinois, KEK-Japan, Lawrence Berkeley, Pennsylvania, INFN-Pisa, Purdue, Rockefeller, Rutgers, Texas A&M, Tsukuba, Wisconsin.

The Stanford Linear Collider

Final installation of the components of the Stanford Linear Collider (SLC) was completed early in March of this year, and commissioning of the machine as a unit was begun then. The commissioning has gone very well with one major exception—the arc AG magnet system (described below). The linac operates reliably at 47 GeV (enough energy to produce Z bosons), and has been run as high as 53 GeV. Beams of both positrons and electrons can be accelerated simultaneously to the end of the linac. Electron intensities of several times 10^{10}/pulse have been attained at the end of the linac with good emittance. Positron beams of some 10^{10}/pulse have been brought through the damping ring, but so far no major effort has been devoted to accelerating high-intensity positron beams through the linac. This is not expected to be difficult. In order to keep down radioactivity in the arc sections of the accelerator and final focus systems, commissioning has proceeded using electron beams of 2×10^{9} per pulse at a repetition rate of five pulses per second. In summary, all of the systems up to the arcs themselves have now been working well, and with beam intensities and qualities more than adequate for the first year of the experimental program.

Early attempts to bring the electron beam through the arc and final focus were almost immediately successful; in fact, beams of both electrons and positrons were brought simultaneously to the interaction point at the end of March 1987. The beam spot sizes were very large, however, and when attempts were made to bring the beam size down to the order of magnitude required for physics, it became clear that there was a problem in the arc system. This problem was diagnosed as being caused by a focussing error which is magnified where the magnets are "rolled" to bend the beams up or down in the nonlevel tunnel. It was found that this effect could be corrected empirically using the beam. The diagnosis was made difficult because of a simultaneous misbehavior of magnet movers and their position read-out devices. The problem has been resolved, and during July, attempts were successful in getting a good beam of electrons at the end of the arc. In July the electron beam was brought into the final focus, and was observed at the interaction point with a radius of some five microns—quite adequate for physics although not yet down to the design specification of 1–2 μm.

The present plan is to continue to refine the tuning of the north (electron) arc and final focus system while simultaneously bringing the positron beam through the south arc and final focus. It is expected, now that the beam dynamics of the north arc are reasonably well understood, that the south arc tuning will go relatively quickly, and that collisions will be obtained soon. The present schedule calls for turning everything off after collisions have been obtained in order to start installation of the MARK II detector at the interaction point. This installation (along with a considerable amount of other work to be done in parallel) will take several months, so the startup for physics should come early in 1988.

D. R. Getz and R. Stiening, SLAC

Yet Another Large Particle–Antiparticle Transition

A recent experiment conducted by the so-called ARGUS group at the electron–positron collider at DESY in Hamburg, West Germany has shown that the B meson occasionally turns into its own antiparticle (the $\bar{B}$ meson), at a rate much higher than previously expected.[1] If such a transformation is permitted by the standard model of particle physics (the transformation of the neutral K meson into its antiparticle was observed as early as the 1950s), then why are the new ARGUS results so interesting?

The particle–antiparticle transformation, it seems, is a quantum effect which often serves as a microscope for observing particles which are too heavy to be produced at accelerators. For example, original theoretical models lead to very large K^0–$\bar{K}^0$ transformation rates which disagreed with the data. In order to remedy this situation the charm quark was postulated and the value of its mass predicted. Subsequently, the charm quark was found at the right mass. In this sense K^0–$\bar{K}^0$ transitions played a crucial role in the formulation of the standard model.

In addition, the attempt to extend the standard model—that is, to search for a more fundamental theory which includes the standard model as a special case—often has resulted in a new prediction for the K^0–$\bar{K}^0$ transformation rate. In this way, for example, the supersymmetric models and composite models have been greatly constrained.

We are certain that the measurement of the B–$\bar{B}$ transition will provide additional constraints which will help us toward a correct extension of the standard model. In fact, it has already yielded new information about the mass of the postulated top quark. The existence of B–$\bar{B}$ transitions had been predicted soon after the discovery of the B meson. The present surprise, however, is that the observed mixing effect is about 20–100 times larger than most theoretical predictions. Most calculations assumed a top-quark mass less than 50 GeV, based upon a preliminary value reported at various conferences by the UA1 group performing an experiment at $p\bar{p}$ collider at CERN. The ARGUS result requires the top quark to be heavier than 50 GeV.

Immediate implications of a top-quark mass greater than 50 GeV are these: first, the creation of the top quark will not be possible at TRISTAN, the highest energy circular e^+e^- collider which recently came into operation at KEK in Tsukuba, Japan; secondly, the Z boson will not decay into a $t\bar{t}$ pair. (This will be tested soon at SLC, which is being built at Stanford.)

The most exciting aspect of the ARGUS discovery is its implications on *CP* violation in the B system. While the *CP* violating effect for K mesons is small, only 0.2%, such effects for B mesons are predicted to be bigger. Indeed, with the observed B–$\bar{B}$ transition, the effect is as large as 10–60%. This makes it 20–100 times easier to detect compared to our previous expectations.

In about six months, the CLEO group working at the CESR e^+e^- colliding beam machine at Cornell will have an indepen-

dent measurement for B–$\bar{B}$ mixing. There is much more work to be done along this line. Presently, the possibility of studying B mesons produced at SSC is being considered (SSC would produce about 10^4 BB pairs a second). Further study of B mesons at $e^+ e^-$ colliders, at the VEPP-4 machine at Novosibirsk in the Soviet Union, and TRISTAN, are being planned. There is also a proposal to build a B factory at the SIN laboratory in Villigen, Switzerland.

If the B system is anything like the K system, it will be extremely useful in understanding the fundamentals of particle physics and it will be an active area of research in 1990s and beyond.

A.I. Sanda, Rockefeller University

1. Phys. Today **40**, 17 (August 1987).

FLUID DYNAMICS

The All-Wing Supersonic Plane

The laws of aerodynamics favor flight in the subsonic speed range. This becomes evident if we consider a simple measure of aerodynamic efficiency, the lift/drag (L/D) ratio, which reflects the fact that energy expended in flight is just about equal to the drag of the aircraft times the flight distance. For example, test wings in idealized two-dimensional flows can have an L/D of better than 100. More practical, passenger-carrying 747s have an L/D of about 20. The 747 flying at 500 mph at 40,000 ft gets 60 seat-miles per gallon, which is about the same as an automobile although it travels ten times as fast. The Concorde, which flies at twice the speed of sound with an L/D of 7.5, needs 200,000 lbs of fuel (or 2000 pounds per passenger) to cross the Atlantic. Because the Concorde has a short wing span, it is not very efficient at low speeds. About 40% of its fuel is used for take-off and low-velocity maneuvering around the airport. The advantages of supersonic flights for long intercontinental flights and the high cost of the Concorde leads us to seek more optimum shapes for supersonic aircraft.

One model for a supersonic wing is that of an arrowhead traveling with the point forward. This intuitive picture is countered by an interesting feature of the mathematics of aerodynamics: the drag of a wing, whatever its shape, is unchanged by reversing the direction of motion. In fact, the optimum wing shape should look the same going in either direction, thus ruling out the arrowhead shape as the optimal form. The analysis shows that a long narrow elliptic wing is optimum compared to a wide class of other shapes. However, at supersonic speeds this wing must be flown at a large angle of yaw relative to the oncoming flow, so that from above, this oblique wing looks nearly the same in either direction. Another interesting result of this analysis is that the optimum wing shape for supersonic speed is basically the same as for subsonic speed.

These concepts lead to an alternative to conventially shaped aircraft, one that is made entirely of a long, narrow elliptic wing that is steered with rudders to change its angle of yaw to suit the Mach number. An elliptic wing with a 10:1 axis ratio can achieve L/D ratios better than 20 at all subsonic speeds. Flying at twice current jet speed, the wing must be turned to 60°, and at Mach two to 70° to the direction of flow. Such an all-wing supersonic transport could fly across the Pacific at Mach two without refuelling.

Does the oblique wing actually show the benefits indicated by theory? In the 1970s an elliptic wing with a 10:1 axis ratio and mounted on a small body was tested in a wind tunnel at the NASA Ames Research Center.[1] When the wing was straight and the velocity was subsonic (0.6 the speed of sound), the L/D was 30. Turning the wing to 45° at Mach one produced L/D of 20. At 60° and Mach 1.4, the L/D was 11. These values show a dramatic loss of L/D going to supersonic speed, but they are higher than those obtained with other wing shapes.

If the wing is to contain passengers, it must be large. The minimum is about 400 ft, about twice that of the 747, with a 50-ft width at the center. The load is distributed along the span so that bending loads are not large. Recent advances in automatic stability and aircraft control also make such a design more practical. Almost any aerodynamic configuration can be made stable in pitch by getting the center of gravity far enough forward. The practical problem with this is that it leaves a large part of the wing volume unavailable for carrying a load. A better solution is to provide stability automatically by using a computer-controlled narrow flap along the trailing edge. Such an automatic control could smooth out the path while descending through turbulence.

It is unlikely that any supersonic transport could compete with present-day airplanes if fuel efficiency is the only criterion. However, the cost of fuel and transporting it are not the only items in the price of a ticket. The advantages of quickly

traveling intercontinental distances, which would increase use of a supersonic airplane, would compensate for some of the lost efficiency and make the supersonic wing airplane an economically competitive aircraft.

Robert T. Jones, NASA Ames Research Center and Stanford University

1. L. A. Graham, R. T. Jones, and F. W. Boltz, Experimental Investigations of the Oblique Wing and Body Combinations at Mach Numbers between 0.6 and 1.4, NASA TMX-62256, Ames Research Center, Moffet Field, 1973.

Dolphin Hydrodynamics

The dolphin's reported ability to reach and maintain high swimming speeds has long been of interest to scientists and engineers. Particular interest has been paid to the possibility that dolphin's speed and endurance abilities are related to physical adaptations that reduce its drag. As early as 1936, Sir James Gray spoke of possible drag-reduction adaptations in the dolphin.[1] In his paper, Gray recounts E. E. Thompson's observation of a dolphin swimming at an estimated speed of 10.2 m/s alongside his ship. Gray estimated the drag of the dolphin and compared it to an estimate of the metabolic energy available to the dolphin for propulsion. To Gray's surprise, there was an order of magnitude discrepancy between the two figures. The estimated drag on the dolphin was ten times that of the energy available to it for propulsion. This discrepancy became known as the "Gray Paradox" and led Gray to postulate that the dolphin might incorporate some form of drag-reduction during swimming.

In the early 1960s, Thomas Lang and co-workers performed a series of experiments with live dolphins.[2,3] Lang demonstrated that speed and duration reports for swimming dolphins were too high. Consequently, when Gray used these speeds to calculate the drag of the swimming dolphin, the estimate of the drag was too high. Lang's data, coupled with the fact that Gray's energy availability analysis was not based on dolphin physiology, led him to believe that there was no order of magnitude drag reduction. Lang's results did not indicate that the dolphin did not significantly reduce its drag, just that Gray's original estimates were wrong.

In recent years, a renewed interest by the scientific community in dolphin hydrodynamics has provided some new insights into the existence extent and nature of possible drag reduction by the dolphin. The recent work has been multidisciplinary, involving such varied disciplines as fluid dynamics, physiology, behavioral science, and veterinary medicine.

Gray originally proposed that the dolphin might somehow maintain a laminar boundary layer around its body. Lang's studies indicated otherwise because he did not measure large drag reductions. However, this did not preclude the existence of laminar flow over a large portion of the dolphin's surface, which would provide some drag reduction. Techniques of turbulent drag reduction such as skin compliance and polymer addition could also be used by the dolphin to reduce drag on its body. Skin compliance means that the dolphin's skin dynamically responds to the flow around it and absorbs some of the energy in the flow that would have been converted to drag. Polymers reduce drag by providing an energy absorber in the form of long-chain molecules which uncoil (like an extending spring) and absorb energy from the flow. Both of these techniques need to be considered when studying the dolphin as a drag reducing system.

The results of recent studies of dolphin drag reduction do in fact indicate a drag reduction capability, but they are as yet inconclusive. The biopolymers present in the dolphin's eye secretions have been identified as a possible contributor to the drag-reduction system. A two-component biopolymer system involving skin and eye secretions and possible interactions between biopolymer and other drag-reduction mechanisms are still being studied. The discovery of fat globules in the dolphin's skin is significant as a second component of a two-component biopolymer system.[4] Studies of the dolphin's skin have shown that there is potential for an active or passive skin response to pressure fluctuations in the boundary layer which might provide a turbulent skin friction drag reduction.[4,5]

Most of the work to date in dolphin hydrodynamics has not been done by fluid dynamicists, although that is now changing. Very recently, Willis[6] showed that drag on a flat plate can be reduced with a compliant coating very similar to a dolphin skin. The object of research being performed at the Naval Ocean Systems Center (NOSC) is to obtain accurate estimates of metabolic energy available to the dolphin and locate laminar to turbulent transition on a swimming dolphin. At the Naval Research Laboratory, the flow field around a swimming dolphin is being simulated numerically. Although the solution to the mysteries of the dolphin's swimming speed appear to be at hand, much careful work is still required before the secrets of the dolphin are ours.

Jeffrey E. Haun, Naval Ocean Systems Center and Eric W. Hendricks, Naval Research Laboratory

1. J. Gray, J. Exp. Biol. **13**, 192 (1936).
2. T. G. Lang and K. Pryor, Science **152**, 531 (1966).
3. T. G. Lang and K. S. Norris, Science **151**, 588 (1966).
4. J. E. Haun, E. W. Hendricks, N. K. Chun, and F. R. Borkat, Dolphin Hydrodynamics NOSC TR 935, Naval Ocean Systems Center, San Diego, CA 1983.
5. W. M. Madigosky, F. R. Borkat, and R. W. Kataoka, J. Acoust. Soc. Am. **79**, 153 (1986).
6. G. H. K. W. Willis, PhD. Thesis, Cambridge University (1986).

Lattice Gas Models for Fluid Dynamics

A "lattice gas" computer model consists of many point particles that are allowed to move about on a lattice (a regular array of points or cells in space). A few simple rules determine the motion of the particles. One rule is that each particle can have only one of a few allowed velocities. Another rule is that each particle moves to the next lattice site in the direction of its velocity at each time step. A third rule, which

varies from model to model, describes how particles scatter at each lattice site. Considerable progress has been made recently in applying such simple methods to the solution of the equations of fluid dynamics.

Lattice gas models developed recently apply to a variety of fluid problems. One-dimensional models of shock formation have been shown to produce the same solutions as well-known shock-forming equations.[1] Two-dimensional hydrodynamic flows around plates,[2] through channels,[3] and with thermal and gravitational effects[4,5] have been modeled with these techniques. Three-dimensional hydrodynamic lattice gas models[6] have recently been generated that promise new high-resolution insight into turbulence. Conducting fluids in magnetic fields have been modeled as well.[7] An important focus of present research is the determination of what can and cannot be modeled efficiently with lattice gas methods.

Several features of lattice gas methods have stimulated recent interest. One feature is the efficient use of computer memory. In two-dimensional fluid models, for example, the complete information for ten cells can be packed into each 64-bit computer word. This allows computations containing 5,000,000,000 cells to fit into the 512-million-word SSD (solid state disk) produced by CRAY Research.

Another feature is the considerable computer speed at which the methods operate. The CRAY X-MP-416 will process 200,000,000 cells each second. The most attractive aspect related to speed is the fact that the methods are completely parallel: N processors will solve problems N times faster than one processor. Studies indicate that special purpose lattice gas computers with several hundred thousand processors are feasible. Inexpensive special computers that model two-dimensional hydrodynamics for 130,000 cells have already been built.

A strong advantage of lattice gas models is that complicated boundaries are easily incorporated into the methods with very little extra computer time required. The computer programs for lattice gas methods are enormously simpler than standard computer programs. Usually only a few dozen FORTRAN lines are required. In addition, the conservation laws for mass, energy, and momentum are satisfied exactly. Throughout the calculations, no roundoff errors ever occur for these conserved quantities.

In spite of their considerable long-term promise, lattice gas methods will probably remain a research tool in the near term. One problem is that with only a few particle speeds allowed, the range of velocities is severely limited. A second problem is that because the lattice gas equation of state depends on velocity, real-world problems are only approximated instead of being solved exactly. A third problem is that the results tend to be noisy, with significant density and velocity fluctuations occurring. These problems can be surmounted by adding to the models a greater variety of speeds. However, as the models become more complicated, their speeds and memory efficiencies will be reduced.

Gary D. Doolen, Los Alamos National Laboratory

1. B. M. Boghosian and C. D. Levermore, Complex Systems **1**, 17 (1987).
2. D. d'Humieres, Y. Pomeau, and P. Lallemand, C.R. Acad. Sci. Paris II **301**, 1391 (1985).
3. D. d'Humieres and P. Lallemand, C. R. Acad. Sci. Paris II **302**, 983 (1986).
4. P. Clavin, D. d'Humieres, Y. Pomeau, and P. Lallemand, C. R. Acad. Sci. Paris II **303**, 1169 (1986).
5. C. Burgess and S. Zaleski, "Buoyant Mixtures of Cellular Automaton Gases," Complex Systems **1**, 31 (1987).
6. U. Frisch, D. d'Humieres, B. Hasslacher, P. Lallemand, Y. Pomeau, and J. Rivet, Complex Systems (August 1987).
7. D. Montgomery and G.D Doolen, Phys. Lett. A **120**, 229 (1987).

GEOPHYSICS

Paleoflood Hydrology

Knowledge of the occurrence, flux, and redistribution of water and sediment on Earth is based primarily on engineering time-scale (less than 100 years) measurements and recordings. Some recorded hydrologic data extend back thousands of years in such centers of early civilization as the Nile Valley and China. However, most of the water and sediment data used in planning, supply, and design throughout the world depend on a relatively short, recent period of direct measurements, and the hope that these data are representative of longer term means and variances. This problem presents an opportunity for unique and innovative approaches to flood hazard investigations; one of these is paleoflood hydrology.

Paleoflood hydrology is the study of the movements of water and sediment in channels before the time of continuous hydrologic records or direct measurements. Elapsed time since the floods of interest can range from several years to thousands of years. The most commonly used indirect evidence includes vegetation, landforms, and sediment deposits. Paleoflood hydrology is primarily a development of botanists, geologists, and geomorphologists interested in flood hydrology, using techniques from dendrochronology, sedimentology, stratigraphy, and geomorphology.

Trees growing on floodplains are commonly scarred, broken, or toppled by floodwaters, but rarely are killed. New wood will grow over scars, and the number of annual tree rings that have grown since scarring of the tree will be an accurate measure of the number of years that have passed since the flood occurred. Also, when trees are inclined or toppled by flood waters, new sprouts grow vertically, and their annual rings can be used to determine the length of time that has elapsed since the flood damage to the vegetation. If a tree survives partial burial by flood sediments, new wood formed in the buried part of the trunk resembles root wood more than stem wood. This allows measurement of the year and amount of sedimentation from a particular flood.[1] Scars on trees may also reflect maximum levels of floodwaters.[2]

The size and spacings of tree rings formed during times of historical gauging-station records in a region correlates well with streamflow data. These results indicate that studies of tree-ring series can be a good surrogate for long-term streamflow data beyond historical time.[3] The occurrence of single floods and inundation periods leaves recognizable anomalies in intra-ring morphology, that can be dated to within a few weeks of the event.[4]

Along stream channels, vegetation patterns and associations are sensitive to flood levels and flood frequency. Individual plants or plant associations have been shown to have consistent relationships to frequency of flooding.[5]

Morphological characteristics of stream channels are related to the frequency and magnitude of past flood flows. Stream channel properties used to derive previous flood discharges including bankfull width, depth, cross-sectional area, width/depth ratio, slope, and meander geometry. Because stream channels can be overwhelmed during extraordinary floods, geomorphic evidence for paleofloods usually can only be used to reconstruct floods of relatively low recurrence intervals (usually less than 50 years).[6]

In some areas, it can be assumed that the largest particles present in flood deposits represent the maximum competence of the stream during the flood. This situation occurs in upland areas with highly jointed or fractured bedrock, or in valleys filled with coarse surficial deposits, such as glacial outwash. Such studies relate hydraulic properties of modern floods, such as shear stress, stream power, depth, or velocity, to the sizes of particles thought to have been transported. This information is then transferred to deposits of unknown flood magnitude. Large errors exist with competence investigations, but the simplicity and broad applicability of the method make it appealing. Results could have a possible error of about a factor of 2, but under the best circumstances, reconstructed results could be as close as about 30%.[7]

The most consistent and accurate sedimentological paleoflood reconstructions involve the use of slackwater deposits, which consist predominantly of sand and silt that settle relatively rapidly from suspension in backwater or quiet-water locations during major floods. Slackwater sediments are likely to contain organic material, such as driftwood or leaf litter. Radiocarbon dating of organic material is the primary dating tool of paleoflood hydrology. With tandem accelerator mass spectrometry, samples of elemental carbon as small as 1 to 2 mg, can be dated between the year 1950 and 10,000 years ago, with an error less than 100 years. Samples from between 1950 and the present can be dated to the precise year by using known concentrations of radioactive carbon in the Earth's environment from nuclear bomb testing.[8]

With knowledge of the maximum flood level in a valley one can calculate the peak discharge for a paleoflood in stable bedrock river reaches by indirect-discharge estimation methods.[9] It is also possible to actually construct flood-frequency curves for paleofloods extending back thousands of years with flood-level computations and radiometric-dated organic materials in slackwater sediments.[10] When coupled with new quantitative techniques, such as maximum likelihood estimators, reliability of flood-frequency estimates increase dramatically.[11]

Paleoflood hydrology has many practical aspects. Knowledge of flood frequency and magnitudes well beyond short historic records is desirable for most hydrologic works and is essential for such projects as long-term disposal of radioactive and other hazardous waste. It offers a valuable tool in evaluating the role of climate change in existing flood series data. Paleoflood hydrology is an excellent example of interdisciplinary cooperation among practitioners of several specialized sciences. It represents a discipline that has not yet developed to its greatest potential, and will become more and more an integral part of water-resource investigations.

John E. Costa, U.S. Geological Survey

1. R. S. Sigafoos, USGS Prof. Paper **485-A**, (1964).
2. S. S. Harrison and J. R. Reid, Proc. N. D. Acad. Sci. **21**, 23 (1967).
3. C. W. Stockton and W. R. Boggess, Trans. Res. Rec. **922**, 10 (1983).
4. T. M. Yanosky, USGS Prof. Paper **1296**, (1983).
5. C. R. Hupp and W. R. Osterkamp, Ecology **66**, 670 (1985).
6. H. C. Riggs, *Streamflow Characteristics* (Elsevier, New York, 1985).
7. J. E. Costa, Geol. Soc. Am. Bull. **94**, 986 (1983).
8. V. R. Baker, G. Pickup, and H. A. Polach, Geology **13**, 344 (1985).
9. J. E. O'Connor, R. H. Webb, and V. R. Baker, Geol. Soc. Am. Bull. **97**, 410 (1986)
10. R. C. Kochel and V. R. Baker, Science **215**, 353 (1982).
11. J. R. Stedinger and T. A. Cohn, Water Resour. Res. **22**, 785 (1986).

Impact Cratering

A remarkable renaissance in the field of impact cratering has arisen over the past few years out of the appreciation for the profound consequences of these powerful geophysical events. For example, there is mounting evidence for a large-body impact at the end of the Cretaceous period that is almost certainly related to *some* aspects of the mass extinction at that time,[1,2] impacting cosmic objects may have accelerated coherent fragments of their planetary crust targets to escape velocity, thus bringing new lunar and probable martian samples to Earth;[3,4] and a physically (and chemically) plausible scenario for the creation of the Moon invokes a

titanic collision of a Mars-sized planetesimal with the proto-Earth sometime in the first 100 million years of solar system history.[5]

It is not my intention to discuss these fascinating topics, however, but to point out that in conjuction with ongoing work on them there has been much fundamental progress in the understanding of impact cratering physics. This includes computation, theory, and experiment. The application of this new and evolving understanding promises not only greater insight into the events mentioned above, but to the general problem of how the solar system was assembled.

Impact cratering, unlike nearly any other geophysical phenomenon, involves a very broad range of mass, length, and time scales, each with a rich physics. This makes any analytical theoretical description of the process approximate in one regard or another. The advent of economical, high-speed computation promises to transform our knowledge of cratering aspects that are inaccessible to experiment. These include large-scale impacts, the growth of craters to so-called late times, and cratering of complex and novel targets. Calculations have now been carried out from early to late times.[6,7] The modification stage of large cratering events, in particular the transition from transient cavity expansion to gravity-driven rebound of the crater floor, has been observed. Such rebounds have been inferred from field data and analytical models, but interpretation or even existence of crater rebound has remained controversial in the planetary geology community. This work illuminates the physics of the origin of flat crater floors (as opposed to simple bowl shapes), central peaks within them, and multiple-ring mountains seen around the largest craters on the Moon and other planetary bodies.

Code calculations also allow effects of complex target geometries to be explored. A water layer overlying a rock halfspace (for simulating impact into the Earth's ocean) is an obvious example.[6,7] Less obvious is "cratering" of the Earth's atmosphere. Here the vertical pressure and density structure and (in some cases) the Earth's sphericity render the "target" complex. The role of impact in accretion and ablation of the Earth's primordial atmosphere (and those of other solid planets and satellites) is just beginning to be modeled.

Our ability to interpret the results of large code calculations, high-explosive field trials, and laboratory-scale experiments has also greatly improved owing to greater comprehension of scaling.[8] Because many cratering phenomena occur at scales much larger than the impactor, it can be replaced by an equivalent point source of energy and momentum. Older energy-scaling rules are thus revised. While it is premature to declare this new scaling complete, it has proved remarkably successful. For instance, extrapolation from laboratory impact experiments in water is accurate for both 19th-century water-drop experiments and code calculations of multimegaton explosions in water.

Experimental support for the theories comes mainly through the use of centrifuges to simulate greater physical scales by means of elevated gravity.[8] Also novel experimental situations continue to pose theoretical challenges, among them cluster (or dispersed) impactors,[9] impact vaporization, and spallation and whole-target fragmentation.[10]

Much further progress and unexpected discoveries and applications are anticipated. One example is the issue of solar system bombardment history. Untangling the role of comets, asteroids, and circumplanetary debris in cratering the various satellites and planets may disentangle the collisional and dynamical evolution of these small-body populations and the relative/absolute chronologies of planetary surface processes. In turn, we may thus work, step by step, back through the history of accretion of the planets.[11–13]

William B. McKinnon, Washington University

1. *Geological Implications of Impacts of Large Asteroids and Comets on the Earth*, edited by L. T. Silver, and P. H. Schultz, Geol. Soc. Am. Spec. Paper **190** (1982).
2. L. W. Alvarez, Phys. Today **40**, 24 (July 1987).
3. D. Bogard, guest editor, Geophys. Res. Lett. **10**, 773 (1983).
4. H. J. Melosh, Geology **13**, 144 (1985).
5. *Origin of the Moon*, edited by W. K. Hartmann, R. J. Phillips, and G. J. Taylor (Lunar & Planetary Institute, Houston, 1986).
6. T. J. Ahrens and J. D. O'Keefe, Int. J. Impact Eng. **5**, 13 (1987).
7. D. J. Roddy, S. H. Schuster, M. Rosenblatt, L. B. Grant, P. J. Hassig, and K. N. Kreyenhagen, Int. J. Impact Eng. **5**, 525 (1987).
8. K. A. Holsapple and R. M. Schmidt, J. Geophys. Res. **97**, 6350 (1987).
9. P. H. Schultz and D. E. Gault, J. Geophys. Res. **90**, 3701 (1985).
10. D. R. Davis, P. Farinella, P. Paolicchi, and V. Zappala, Mem. S. A. It. **57**, 7 (1986).
11. C. R. Chapman and W. B. McKinnon, *Satellites*, edited by J. A. Burns and M. S. Matthews (University of Arizona Press, Tuscon, 1986), pp. 492–580.
12. R. G. Strom, Icarus **70**, 517 (1987).
13. EOS Trans., AGU **68**, 343 (1987).

Plate Tectonic Prediction Fulfilled

Why, according to a recent survey,[1] do 81% of Americans believe the Earth's surface to be covered by moving tectonic plates, when only 47% accept the notion that humans are descended from more primitive animals? Apparently many of those skeptical of the geologic record of life are convinced by the evidence for past production and consumption of the Earth's surface. Both plate tectonics and natural selection are theories of slow change that depend on a reading of the geologic record for their principal support. Evolution, however, has been subject to much longer public and scientific debate. Charles Darwin published *The Origin of Species* in 1859.[2] Fifty-six years later Alfred Wegener proposed, in *The Origin of Continents and Oceans,* that the continents drifted around the globe.[3]

The leap from Wegener's hypothesis to plate tectonics, in which the continents are envisioned as moving with the sea

floor rather than plowing through it, followed in 1965. Until now, neither species evolution nor continental motion could be observed during a human lifetime, but plate tectonics is no longer a matter of geologic conjecture: During the past four years the movement of the Earth's dozen plates has been measured, centimeter by centimeter, across four continents and three oceans.

Because of the stately pace of the plates, which slide at rates of 1 to 10 cm /yr on a substrate of partially melted rock, detection of plate motion awaited measurements of intercontinental baselines accurate to several centimeters. Currently three independent techniques yield comparable plate velocities and directions.[4]

To measure the relative movement of plate interiors, reflectors were launched into Earth orbit and several ground-mounted lasers were engaged in a three-dimensional positioning analogous to triangulation, called satellite laser ranging. During the past four years, observation of quasars—extragalactic radio sources emitting a random "universal bar code" that can be timed and cross-correlated between receivers—has given us the most precise method to gauge baselines spanning the girth of the Earth. This method, known as Very Long Baseline Interferometry (VLBI), has measured the relative motion of five of the Earth's plates to a precision of one part per billion.[5] Finally, a growing constellation of military NAVSTAR satellites that broadcast their position to small mobile receivers (the Global Positioning System) now provides the most versatile method to measure baselines shorter than 500 km.

The space and terrestrial observations yield a stunning result: the plate rates measured during the past few years are—within the measurement uncertainty—identical to those deduced for the past several million years from the geologic record. This discovery attests to the fidelity of the geologic record of our planet's past. More important, it means that the gravitational forces that drive the plates and the viscous forces that resist their motion must stay balanced over millions of years. The jerk of occasional great earthquakes at plate edges, and the perhaps million year cycle of transient convection—eddies of flowing rock beneath the plates—may thus leave the plates unperturbed.

Ten million years ago the Pacific plate began to take a western sliver of California with it on its northward march toward Alaska, the cut now known as the San Andreas fault system. The faults provide our best opportunity to measure plate movement and deformation on land. The stick-and-slip motion along the uppermost 10 km of the faults accounts for California's plentiful supply of earthquakes (see Fig. 1). During the past two million years, just under 5 cm/yr of relative plate motion has been accommodated by slip along the San Andreas fault system. Displacement of ancient tributaries across the fault reveals that during the past 15,000 years, the central San Andreas has slipped an average of 3–4 cm/yr. Recent resurvey of century-old triangulation monuments installed by the U.S. Coast and Geodetic Survey to

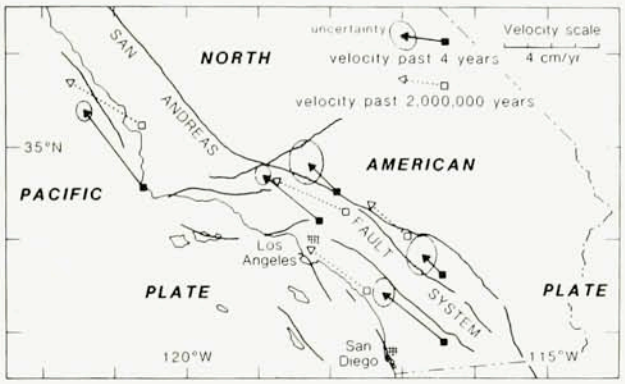

FIG. 1. Velocity vectors for the movement of the Pacific plate relative to the North American plate in southern California, deduced from four years of VLBI measurements (solid arrows) and from geologic rates of fault slip and sea-floor spreading (dotted arrows).

construct maps for the Gold Rush shipping traffic indicates a rate of at least 3.3 cm/yr during the past century.[4] The most recent VLBI measurements yield a rate across the San Andreas system of 3–4 cm/yr.[6] Thus a consistent picture of plate movement emerges on time scales sampled at 4, 100, 15,000 and 2,000,000 years.

The claim that we have finally measured the contemporary motion of continents oddly echoes one made prematurely by Alfred Wegener in 1929: "We begin the demonstration of our theory with the detection of present-day drift of the continents by repeated astronomical positioning, because only recently this method furnished the first real proof of the present-day displacement of Greenland—predicted by drift theory—and because it constitutes a quantitative corroboration."[7] From repeated longitude measurements Wegener inferred that Greenland had drifted 1610 ± 285 m from Europe between 1827 and 1907, a rate of 19 ± 3 m/yr. This result agreed with longtitude observations performed elsewhere on Greenland between 1860 and 1921. Wegener dismissed the possibility—now known to be true—that gradual improvement of the measurement precision, rather than drift of Greenland, accounted for the longitude changes: "This accumulation of similar results which do not stand in opposition to any others makes it highly improbable that it is all just a matter of unfortunate combination of extreme errors of observation."[7] Today, Wegener stands at once vindicated and discredited. Greenland is indeed drifting away from Europe, but at a velocity now measured to be 1.9 ± 1.0 cm/yr, one-thousandth Wegener's proffered rate.

It is ironic that plate tectonics enjoyed such widespread acceptance before this crucial confirmation, whereas evolution—read from the same geologic and fossil record—remains controversial. Our response to scientific advances appears to be bound more closely to how we view ourselves than it is to how we view the science. One cannot help but wonder whether confirmation of evolution, such as contemporary observation of speciation by natural selection, would encourage the reluctant 53% to acknowledge their simian

past. Or is a mobile planetary shell somehow less fantastic than the transmutation of life?

Ross S. Stein, U.S. Geological Survey

1. J. D. Miller, Am. Demographics **9** (6), 26 (1987).
2. C. Darwin, *The Origin of Species*, repr. of 1st ed. (Philosophical Library, 1951).
3. A. Wegener, *Die Enstehung der Kontinente und Ozeane* (Sammlung Vieweg, Braunschweig, 1915), Vol 23, p. 94.
4. R. S. Stein, Rev. Geophys. **25**, 855 (1987).
5. W. E. Carter and D. S. Robertson, Sci. Am. **255**, 46 (1986).
6. P. M. Kroger, G. A. Lyzenga, K. S. Wallace, J. M. Davidson, J.Geophys. Res. (in press, 1987).
7. A. Wegener, *The Origin of Continents and Oceans*, J. Biram translation of 4th (1929) ed. (Dover, New York, 1966), p. 23.

Dynamics of the Upper Ocean

The atmosphere presents an almost constantly changing heat flux and wind stress to the surface of the sea. Recent field and theoretical studies have given a greatly improved description of the upper ocean's response to this surface forcing, and here we note some advances in understanding the effects of heating by solar insolation.[1]

Much of the recent progress can be traced directly to new measurement techniques which have yielded field data sets with expanded duration and resolution. Notably, recent turbulence measurements from the equatorial Pacific Ocean show a pronounced diurnal cycle of upper ocean turbulence.[2–4] The immediate effect of solar heating is to produce a warm layer adjacent to the sea surface. The static stability of this layer inhibits the downward penetration of turbulent vertical mixing so that the surface flux of heat and momentum will be trapped near the sea surface during mid-day. After the sun sets, sea surface cooling by evaporation and infrared radiation produces an unstable heat flux, and the resulting free convection and turbulent mixing by the wind then penetrates to surprisingly large depths, up to about 100 m. This great penetration of nocturnal mixing may be connected with the presence along the equator of strong, highly sheared mean currents which at some depths flow against the prevailing wind, but other hypotheses involving internal wave generation and re-absorption at depth appear equally plausible.[5]

Field observations from mid-latitude sites show that this solar heating-induced variation in mixing depth imposes a diurnal pulse on the wind-driven velocity. During mid-day the momentum flux supplied by wind stress is absorbed within the warm surface layer which then accelerates downwind as a diurnal jet. The Coriolis acceleration due to the Earth's rotation turns the diurnal jet clockwise during the day (northern hemisphere) and by sunset the jet may be turned counter to the wind. During the remainder of the night the adverse wind stress together with the increased vertical mixing will often erase completely the diurnal jet generated during the preceding day. The long-term average of this diurnally pulsing current has a spiral shape.[6] These solar heating plays by modulating the penetration depth of vertical mixing.

Satellite-derived infrared views of the sea surface reveal the large scale patterns of diurnal warming. In many cases there is a remarkably clear signature of the overlying surface heat flux and wind stress. For example, large amplitude diurnal warming of up to 3 C occurs along the axis of marine high pressure systems where there is a coincidence of clear sky and light winds.[7] In the future it may be possible to exploit this new knowledge of the effects of solar heating to infer meteorological data in remote oceanic regions which are inaccessible to direct observations.

James F. Price, Woods Hole Oceanographic Institution

1. J. F. Price, E. A. Terray, and R. A. Weller, Rev. Geophys. Space Phys. **21**, 193 (1987)
2. M. C. Gregg, H. Peters, J. C. Wesson, M. S. Oakey, and T. J. Shay, Nature **318**, 140 (1985).
3. J. N. Moum and D. R. Caldwell, Science **230**, 315 (1985).
4. J. N. Moum, T. R. Osborn, and W. R. Crawford, J. Phys. Oceanogr. **16**, 1516 (1986).
5. C. C. Eriksen and E. J. Katz, Rev. Geophys. Space Phys. **21**, 217 (1987).
6. J. F. Price, R. A. Weller, and R. Pinkel, J. Geophys. Res. **91**, 8411 (1986).
7. L. Stramma, P. Cornillon, R. A. Weller, J. F. Price, and M. G. Briscoe, J. Phys. Oceanogr. **16**, 827 (1986).

High-Pressure Experiments and the Earth's Deep Interior

What is the nature of the Earth's core? How high is the temperature at the center of our planet? Advances in high-pressure experimental techniques are yielding new insights about the deep interior, revealing that the core is an unusual alloy of iron with a peak temperature exceeding that of the sun's surface.[1,2]

The experimental breakthroughs allow materials to be examined in detail at the extreme conditions of the core: pressures ranging from 136 GPa (billion Pascals) at the core-mantle boundary to 364 GPa at the center (1.36 to 3.64 million times atmospheric pressure) and temperatures above 3500 K. The most recent developments involve a laser-heated diamond cell, in which less than one microgram of sample is squeezed between the points of two gem-quality diamonds. Pressures in excess of 500 GPa have beeen achieved by this technique.[3,4] To simulate deep-Earth temperatures a laser beam is focused through the diamonds and into the sample area, thus producing temperatures of 1000–7000 K.[5,6] During the experiments the sample is directly observed through the diamond anvils (or more properly in this context, the diamond windows) by techniques ranging from x-ray diffraction to visible and infrared spectroscopy. In particular, temperature is determined by spectroradiometry. Complementing the diamond cell, in which high temperatures and pressures can be sustained for hour-long periods, are the well-established shock-wave experiments

involving hypervelocity impact of a projectile into a sample. Although lasting less than one microsecond, shock-wave measurements provide an important extension and cross-check of the newer diamond-cell techniques.

Using the approach of combining diamond-cell and shock-wave measurements, the melting point of iron has been recently determined to pressures in the 200–300 GPa range.[2] This is the highest-pressure melting curve so far determined for any material, and it represents the first time that melting has been continously monitored from zero pressure to pressures in excess of 100 GPa. As iron is the primary constituent of the Earth's core, the results provide the first direct constraint on the temperature at the boundary between the solid inner core and the liquid outer core. Accounting for the presence of impurities or alloying components in the iron of the core yields an estimate of 6900 ($\pm$ 1000) K for the temperature at the center of the planet, with a temperature profile as shown in Fig. 2. Compared with previous estimates that were hindered by the lack of any melting data above 7–20 GPa, the temperature of the core is found to be surprisingly high.

The major distinction between the core and the surrounding mantle and crust is compositional. Whereas the core is a metallic alloy consisting almost entirely of iron (over 90 to 95% by weight), the rocky or ceramic-like mantle and crust are composed mainly of oxygen in the form of silicate and oxide minerals. The distinction appears to be fundamental, both in physical properties and chemical bonding, between the metallic and insulating regions of the planet. Yet recent experiments show that oxygen changes dramatically in chemical behavior at the conditions of the deep mantle and core, as compared with ambient conditions. Specifically, oxygen is found to become a metallic alloying component at high pressures, combining readily with iron much as sulfur alloys with iron at low pressures.[1] Even iron oxide, which is a poor semiconductor at zero pressure, becomes metallic at pressures above 70 GPa and temperatures above 1000 K.[1,7] Also, in experiments with the laser-heated diamond cell liquid iron and iron alloys are observed to react vigorously with solid oxides and silicates at conditions simulating the core-mantle boundary.[1,2,8] Thus it appears inevitable that extensive chemical reaction has occurred between the core and mantle over geological time, with oxygen derived from the mantle perhaps now being the primary alloying component of the core. Indeed, the region near the base of the mantle is known from seismology to be extremely heterogeneous and complex, as might be expected for a chemical-reaction zone. Given the high temperatures expected at this depth, the core-mantle boundary is likely to be the most chemically active zone inside the Earth.

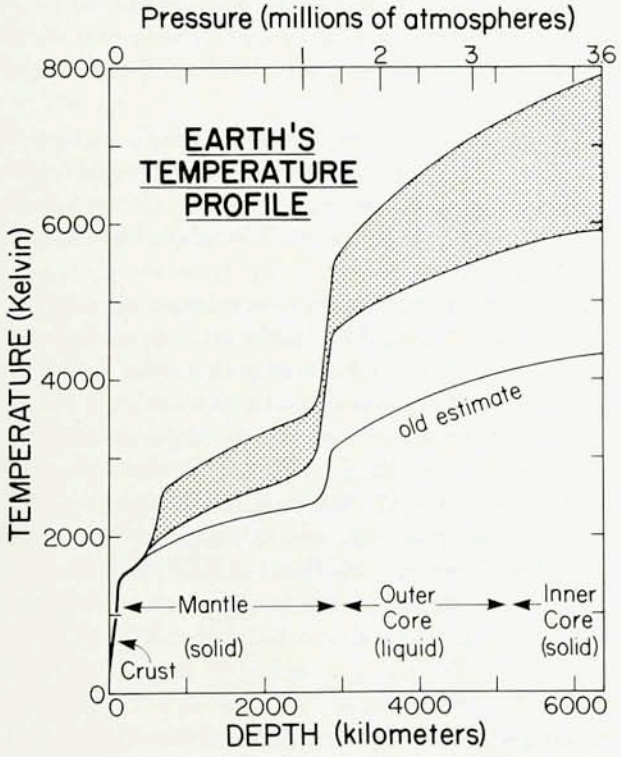

FIG. 2. New estimate of the average temperature as a function of depth in the Earth (shaded band: width reflects uncertainty) as compared with a typical earlier estimate.

The high temperatures inferred for the core have profound implications for quantitative models of the planet's internal evolution. In particular, these indicate that the core has remained as one of the primary sources of thermal energy driving solid-state creep and convection of the mantle. That is, the geological processes (and hazards) observed at the surface, including the volcanic and earthquake activity associated with plate tectonics, are largely powered by the heat lost out of the core throughout the 4.5 billion year history of our planet.

Raymond Jeanloz, University of California at Berkeley

1. E. Knittle and R. Jeanloz, Geophys. Res. Lett. **13**, 1541 (Dec. 1986).
2. Q. Williams, R. Jeanloz, J. Bass, B. Svendsen, and T. J. Ahrens, Science **236**, 181 (10 April 1987).
3. J. A. Xu, H. K. Mao, and P. M. Bell, Science **232**, 1401 (13 June 1986).
4. W. C. Moss, J. O. Halquist, R. Reichlin, K. A. Goettel, and S. Martin, Appl. Phys. Lett. **48**, 1258 (1986).
5. R. Jeanloz and D. L. Heinz, J. Phys. (Paris) **45**, 83 (November 1984).
6. D. L. Heinz and R. Jeanloz, in *High-Pressure Research in Mineral Physics*, edited by M. H. Manghnani and Y. Syono (Am. Union, Washington, DC, 1987), p. 39.
7. E. Knittle, R. Jeanloz, A.C. Mitchell, and W.J. Nellis, Solid State Commun. **59**, 513 (1986).
8. E. Knittle and R. Jeanloz, Lunar and Planetary Science **XVIII**, 495 (1987).

The Year of Perovskite

In 1987, perovskites attracted worldwide attention through the discovery of high-T_c superconducting oxides in this structural family. It was also in 1987 that perovskite-structured silicates were found to make up the bulk of our planet.[1] Unlike the superconducting, copper-based oxides, however, the silicates with compositions $(Mg,Fe)SiO_3$ and $CaSiO_3$

can only be made at high pressures: typically above 20 GPa or 200,000 atm.[2] Also the silicate perovskites appear to be highly insulating, even at pressures and temperatures as high as 90 GPa and 4000 K.[3] The lesson is that perovskite-type compounds exhibit an extremely rich diversity of electronic behavior and structural distortions. Yet the orthorhombically distorted, high-pressure perovskite phase of $(Mg,Fe)SiO_3$ is exceptionaly stable, existing to pressures in excess of 120 GPa.[1] Thus it is considered the most abundant mineral of the Earth, comprising over 55% of the entire mantle.

Raymond Jeanloz, University of California, Berkeley

1. E. Knittle and R. Jeanloz, Science **235**, 668 (6 Feb. 1987).
2. L. G. Liu and W. A. Bassett, *Elements, Oxides and Silicates* (Oxford Univ. Press, New York, 1986).
3. X. Li and R. Jeanloz, Geophys. Res. Lett. (in press).

True Polar Wander and Paleomagnetic Euler Poles

A fundamental problem in paleomagnetism is the kinematic interpretation of apparent polar wander (APW) paths, which are time sequences of paleomagnetic poles from a continent or tectonic plate. Paleomagnetic poles are thought to track the past locations of the Earth's spin axis because the time-average of the geomagnetic field approximates that of a geocentric dipole aligned with the spin axis. Pioneering paleomagnetic studies have established that the ancient paleomagnetic pole diverged with increasing age from the present north pole, suggesting true polar wander (TPW), the motion of the entire solid Earth relative to the spin axis. Later data showed that APW paths from different continents diverged, which reflected plate motion.

With the acceptance of plate tectonics, the concept of TPW is not needed to explain the paleomagnetic observations, but the question of whether TPW has an observable effect on APW paths has not been convincingly resolved. The paleomagnetic and plate motion data base has recently improved enough that TPW can be examined more rigorously. Recent research has taken two complementary approaches to exploring this problem.

The first approach focuses on the comparison of APW paths to plate motion relative to an independent deep mantle or absolute reference frame. The most popular reference frame assumes that long-lived vigorous volcanic sources, termed hotspots have moved relative to the paleomagnetic axis.[1,2] If the hotspots are a reliable reference frame, and if the paleomagnetic axis reliably tracks the spin axis, then this motion demonstrates TPW large enough to affect APW paths. No consensus on the fixity or mobility of hotspots has emerged, however, and attention has turned to alternative methods of determining absolute plate motions.

These alternatives include absolute motions determined by assuming that the lithosphere (the solid Earth's outermost layer of strength) exerts no net torque on the asthenosphere (the weak layer underlying the lithosphere). Recent work by R. Livermore, D. Jurdy, and R. Gordon suggests that the hotspot and no-net-torque reference frames agree well, and that the inferred motion of the paleomagnetic pole relative to the deep mantle depends only weakly on how absolute motions are estimated. The main conclusion is that TPW over the past 70 Ma (millions of years ago) was small, but a shift of 10–15° may have occurred between 100 and 70 Ma. Further paleomagnetic work is needed to narrow the timing and rate of this shift.

An alternative approach is to assume that TPW is negligible and to exploit the plate motion information available in APW paths, which consist of long, gently curved segments termed tracks, linked by short segments with sharp curvature, termed cusps or hairpins. A few years ago it was thought that paleomagnetic data provided information on only two of the three components of the rotation that describes plate motion. Once a plate is correctly oriented in paleolatitude and in paleo-declination, its paleolongitude is indeterminate because of the axial symmetry of the time-averaged geomagnetic field. Recently, however, it was realized that a time-sequence of paleomagnetic poles might yield all three components of plate motion if APW tracks correspond to intervals when the direction of plate motion was constant. APW tracks would thus tend to lie along small circles, the center of which is termed a paleomagnetic Euler pole (PEP).[3]

This new approach has yielded several useful results. Whereas plates with large continents are now moving slowly (less than 20 mm/yr), PEP analysis shows that North America and Eurasia moved rapidly (60–100 mm/yr) before 140 Ma.

This suggests that during intervals of rapid motion the continents were attached to oceanic lithosphere that was being subducted at some distance from the continent. Rapid motion stopped when the oceanic lithosphere had been consumed by subduction.[3]

PEP analysis introduces less smoothing than other approaches to determining APW paths and has yielded reference APW paths for North America that differ from prior paths. The new APW paths suggest that some crustal blocks may have moved much less relative to the stable interior of North America than thought before.[3,4] Current research is directed to paleomagnetic study of rocks from the critical ages spanned by APW cusps, and to testing geologic models of paleo-plate boundaries predicted by PEP analysis.

Richard G. Gordon, Northwestern University

1. R. G. Gordon, Ann. Rev. Earth Planet. Sci. **15**, 567 (1987).
2. W. W. Sager and U. Bleil, Nature **326**, 488 (1987).
3. R. G. Gordon, A. Cox, and S. O'Hare, Tectonics **3**, 499 (1984).
4. S. R. May and R. F. Butler, J. Geophys. Res. **91**, 11519 (1986).

Progress Towards Applications of High-Temperature Superconductivity

In January 1986 J. G. Bednorz and K. A. Müller, of the IBM Zürich Research Laboratory, discovered high-temperature superconductivity in a class of copper oxides containing rare earths and alkaline earth, a discovery which won them the 1987 Nobel Prize for physics. Only a year later superconducting transition temperatures in this class of materials had been pushed to almost 100 K, far beyond the previous record of 23 K that had remained unbroken since 1973 and well above the benchmark temperature 77 K of boiling liquid nitrogen. Many reports suggest the possibility of even higher temperatures. Here we will focus on the 90–100 K superconductors of the type YBaCuO with the highly anisotropic "123" structure.

Applications opportunities emerge from the special properties of the new superconductors. The high temperatures, of course, offer vastly simplified cryogenics. In addition critical fields are projected to reach above 100 T at low temperatures, and the superconducting large energy gap may reach 40 meV or more. These features suggest a variety of applications[1]: as wires in superconducting magnets and power transmission, as interconnects in hybrid superconducting semiconducting computing systems, as Josephson and other active superconducting devices, as instruments like SQUIDs and infrared sensors, as electromagnetic shields, and many others.

1987 has witnessed tremendous progress toward achieving the kind of materials parameters and processing needed to realize these applications opportunities, although much remains to be done. Flexible processing, high current densities, adequate mechanical properties, good chemical stability and (for certain applications) high-quality Josephson elements are also important.

The new superconductors have been prepared in the form of wires, ceramic green sheet, screen printing, plasma-sprayed coatings, ribbons, and thin films. While this variety of processing techniques demonstrates the considerable adaptability of the material, the measured current densities[2] in randomly oriented ceramics or in polycrystalline material have typically been at most 1000 A/cm^2 at 77 K, which is insufficient for most applications. Much larger current densities have been reported in epitaxial thin films on $SrTiO_3$ substrates[3,4] and in single crystals.[5] The observed[4] 10^6 A/cm^2 at 77 K would be satisfactory for many applications.[1] Present designs for the NbTi Superconducting Super Collider magnets, by comparison, call for a current density of 2.75×10^5 A/cm^2 to achieve fields in the range of 5 T. It must be emphasized, however, that the high current densities are not yet available in the polycrystalline or ceramic material needed for such applications. This is perhaps the key challenge to further progress.

Critical current densities are strongly affected by magnetic fields, an effect of special importance in magnetic design. Single crystals[6] with the field in the optimum direction give values of 2–3 T/K for the increase in upper critical field with temperature just below the transition. Thirty Tesla could be achieved even at 77 K if proper orientation of crystalline axes relative to field and current flow could be maintained. Unfortunately, in granular material, the slope is usually much less, at least when defined at the point of zero resistance. Grain boundaries or the random orientation of the anisotropic crystallites have been implicated in this problem.

Mechanical properties are vital to applications, and both ceramics and single crystals have been found to be brittle like typical oxides. Chemical stability and the role of oxygen diffusion are also an issue because the superconductivity is sensitively dependent on oxygen concentration. Considerable progress has been made in identifying the location of oxygen vacancies in the complex "123" structure, with its chains and planes of copper-oxygen bonds, and also in studying an orthorhombic-to-tetragonal structural phase transition in the 600–700 °C range, where a disordering of oxygen atoms occurs. Nevertheless, little is known about the structure of surfaces, grain boundary interfaces, or twin boundaries.

Optimization of superconducting properties typically involves annealing at about 900 °C, to establish the 123 phase, followed by 500 °C to order the oxygen vacancies. Lowering these temperatures will be important, particularly for electronics applications where previously deposited layers could interdiffuse and degrade at such temperatures. Recently the annealing temperature has been lowered to about 700 °C by an *in situ* thin film deposition in an oxide environment.[7]

YBaCuO thin film lines have been patterned by a variety of techniques, and 10 psec electrical pulses[8] have been propagated several millimeters down an YBaCuO coplanar transmission line without distortion. Pulses as short as 2 psec have been propagated down hybrid transmission lines consisting of aluminum lines with a superconducting ground plane.[8] These experiments confirm the absence of unusually large high-frequency losses in these superconductors and open the door to high-rate data transmission applications within computers.

There has also been progress in making superconducting devices based on Josephson effects, although there are as yet no published reports of tunnel junctions with YBaCuO as both electrode and counterelectrode. Tunnel junctions have been made with metal point contacts of Pb counterelectrodes

using insulating or semiconducting surface layers naturally occurring on YBaCuO. DC SQUIDs (Superconducting Quantum Interference Devices), which are ultrasensitive magnetic field detectors involving two Josephson elements forming a superconducting loop, have been made either by patterning thin films of weak links at grain boundaries[9] or by breaking a ceramic and putting it back together (breakjunction).[10] Microwave radiation on Josephson junctions has also revealed so-called Shapiro steps, which demonstrate the possibility of detecting microwave radiation.[11] The larger gap of these materials offers the possibility of infrared detectors with a wider frequency range than in earlier superconductors.

In summary, this heady progress, all within a half year since the discovery of YBaCuO, encourages the hope for near-term 77 K superconducting instruments involving SQUIDs and infrared detectors, as well as for the simpler (contactless and junctionless) magnetic shielding applications. Other magnet wire and electronics applications, probably longer term, are under active scrutiny throughout the world.

A. P. Malozemoff, IBM T.J. Watson Research Center

1. A. P. Malozemoff, W. J. Gallagher, and R. E. Schwall, Am. Chem. Soc. Symp. Ser., Sept. 1987 (to be published).
2. R. J. Cava *et al.*, Phys. Rev. Lett. **58**, 1676 (1987).
3. P. Chaudhari, R. H. Koch, R. B. Laibowitz, T. R. McGuire, and R. J. Gambino, Phys. Rev. Lett. **58**, 2684 (1987).
4. Y. Enomoto, T. Murakami, M. Suzuki, and K. Moriwaki, Jap. J. Appl. Phys. **26**, L1248 (1987).
5. T. R. Dinger, T. K. Worthington, W. J. Gallagher, and R. L. Sandstrom, Phys. Rev. Lett. **58**, 2687 (1987).
6. Y. Iye, T. Tamegai, H. Takeya, and H. Takei, Jap. J. Appl. Phys. **26**, L1057 (1987); T. K. Worthington, W. J. Gallagher, and T. R. Dinger, Phys. Rev. Lett. **59**, 1160 (1987).
7. D. K. Lathrop, S. E. Russek, and R. A. Buhrman, Appl. Phys. Lett. (to be published); H. Adachi, K. Setsune, and K. Wasa (to be published).
8. J. Chwalek *et al.* (submitted to Appl. Phys. Lett.); D. Grischkowsky (submitted to OSA Annual Meeting, Rochester, 1987).
9. R. H. Koch, C. P. Umbach, G. J. Clark, P. Chaudhari, and R. B. Laibowitz, Appl. Phys. Lett. **51**, 200 (1987).
10. I. Iguchi, A. Sugishita, and M. Yanagisawa, Jap. J. Appl. Phys. **26**, 70 (1987); J. E. Zimmerman, J. A. Beall, M. W. Croman, and R. H. Ono, Appl. Phys. Lett. **51**, 617 (1987).
11. D. Esteve *et al.*, Europhys. Lett. **3**, 1237 (1987).

New Approaches to X-Ray Computed Tomography

X-ray computed tomography (CT) has been a fixture in medicine for over a decade. The importance of the technology in this context resulted in Hounsfield and Cormack being awarded the Nobel Prize in 1979. Industrial applications, on the other hand, have been slow in coming, largely because of cost and the inapplicability of medical scanners to many problems. Special purpose systems have, however, been built for inspections of high-value or high-failure-consequence parts such as metal turbine blades and rocket motors. A recent application, quite different from the usual inspection task, is the use of CT for gauging of automotive castings.[1]

All the above applications have been based on conventional CT practice, which produces a sequence of two-dimensional slices of an object. Recently, interest has grown in pushing CT technology toward finer resolution than before and to obtain three-dimensional information more directly than by the repeated collection of slices. Efforts underway at Exxon and at Ford employ different approaches but both are aimed at achieving resolution in the range of a few microns. Both systems differ from medical scanners in that the sample, rather than the x-ray source and detector system, is rotated, and both systems generate three-dimensional reconstructions by employing two-dimensional detectors in place of the one-dimensional arrays used in conventional CT systems.

The Exxon effort uses an intense source of synchrotron radiation at Brookhaven National Laboratory.[2] The tunable wavelength of the radiation allows the variation in the attenuation cross section among the elements to be studied. Though few details have been made available, a new detector system based on an array of cellular phosphor plugs (spacing in the 2-μm range) whose output is imaged onto a charge-coupled device sensor is possible. The highly parallel nature of the x-ray beam enables reconstruction by direct Fourier inversion.[3] As implemented, the algorithm is much faster than the filtered backprojection technique almost universally used in medical scanners.

Work at Ford has sought to exploit the nature of the source geometry most likely to be available in the laboratory, namely a point source. Rather than use only a sheet, or fan, of radiation from the source, as in conventional systems, the full cone of radiation produced by the source is used. The resulting algorithm,[5] though approximate (no exact solution is known to exist), is both fast and accurate and has recently been applied to the analogous problem of single-photon emission tomography.[6]

The Ford system, wholly based on easily available components, is more a demonstration of the concept than a final implementation.[7] The detector is an x-ray image intensifier coupled to a Vidicon camera. Because of the point source, geometric magnification can be used to overcome resolution limitations of the detector. In fact, there is a strong analogy with the technique of microradiography, and much of what is known in that context will probably be applicable to this method of CT. Since the ultimate resolution depends greatly on how well the radiation source approximates a point, a microfocus source with a minimum spot size of less than 5 μm is used.

In many cases the system is used for samples in the range of 1 cm with resolution of about 70 μm. Reconstruction of cube-shaped regions 8 mm on a side on a three-dimensional mesh with 50 μm spacing is performed routinely. A convenient feature of the reconstruction algorithm is that it handles subvolumes in times that decrease nearly linearly with the number of points, so that for special purposes a region of

interest can be reconstructed in much less time than for the entire sample.

As the sample size decreases, greater magnification can be used and the resolution is improved. This technique is just beginning to be explored. For example, a 0.3-mm-diameter solder joint in a thick-film circuit package was inspected with a resolution of about 15 μm. By ignoring or correcting for the lack of complete information, high magnification can frequently be applied to fairly large objects with surprisingly good results. A case in point is the observation of cracks with separations estimated at 15–20 μm in a ceramic sample 2.2 cm in diameter.

Both the Exxon and Ford systems can be regarded as new laboratory instruments, applicable to a wide range of problems. Of particular interest to Exxon is the study of mineral samples, but remarkable images of biological specimens have also been produced. The Ford system was originally conceived for the inspection of structural ceramics, but has also been employed to inspect plastic parts, composites, elastomers, catalytic converter materials, and electronic components. The biomedical community has also responded with enthusiasm; an active program with The University of Michigan, funded by the National Institutes of Health, has produced previously inaccessible information on the internal architecture of bone. Recognizing the need for a facility dedicated to biomedical applications, the NIH has recently funded construction of a system based on the Ford design at the University of Michigan.

L.A. Feldkamp, Ford Motor Company

1. H. Ellinger, S. Suchele, and F. Hopkins (to be published); H. Ellinger, private communication.
2. H. W. Deckman, Bull. Am. Phys. Soc. **32**, 580 (1987); D. Thomsen, Science News **131**, 300 (1987).
3. H. Stark, J. W. Woods, I. Paul, and R. Hingorani, IEEE Trans. Biomed. Eng. **BME-28**, 496 (1981).
4. W. G. Roberge, Bull. Am. Phys. Soc. **32**, 580 (1987) and private communication.
5. L. A. Feldkamp, L. C. Davis, and J. W. Kress, J. Opt. Soc. Am. **A1**, 612 (1984).
6. R. J. Jaszczak, C. E. Floyd, S. H. Manglos, K. L. Greer, and R. E. Coleman, Med. Phys. **13**, 484 (1986).
7. L. A. Feldkamp and G. Jesion, in *Review of Progress in Quantitative NDE*, edited by D. O. Thompson and D. E. Chimenti (Plenum Press, New York, 1986), Vol. 5A, p. 555.
8. L. A. Feldkamp, D. J. Kubinski, and G. Jesion (to be published).

Surface Laser-Light Scattering

Convenient and accurate measurements of interfacial tension (IFT) and viscosity are often important in studies of fluid systems. In the petroleum industry, for example, values of these and other physical properties are essential input for oil reservoir modeling calculations. At the high temperatures and pressures which approximate oil field conditions, many of the classical measurement methods are difficult to use. In related studies, the understanding of surfactant behavior under such extreme conditions can be vital to the success of enhanced oil recovery schemes. In such systems, where species are adsorbed at the interface, the use of physical probes can disturb the equilibrium.

An interest has therefore developed in using optical methods to measure IFT and viscosity in situations where other techniques were not satisfactory. One promising method uses laser-light scattering[1] to measure the temporal behavior of microscopic ripples at the interface. This surface laser-light scattering (SLLS) technique was one of the many demonstrated during the early years of laser research;[2] but only recently is its potential being realized and its utility being fully exploited.[3]

The SLLS technique is based on the fact that fluid/fluid interfaces are constantly being deformed by the thermal fluctuations of the molecules at the interface. This deformation can be represented as a spatial Fourier series of thermally generated capillary waves, each with a characteristic wavelength (about 100 μm) and with an amplitude (a maximum of about 1 nm) which is a random function in time. The temporal behavior of the amplitude of these capillary waves, called *ripplons*, is governed by the properties of the fluids: the principal restoring force is the interfacial tension and the principal temporal damping mechanism is the bulk shear viscosity. Each ripplon acts as a diffraction grating and weakly scatters laser light at a small angle to the specular reflection.

SLLS uses optical heterodyning to measure the spectrum of the light scattered at selected angle. The scattering angle corresponds to a particular ripplon wavenumber q. The heterodyne local oscillator (LO) is generated from the incident laser by use of a transmission diffraction grating. Optical mixing occurs at the detector where the LO and a part of the scattered light spatially overlap. From the power spectrum of the scattered light intensity, the interfacial properties are calculated.

Our goal was to measure the IFT and viscosity of petroleum systems, which are strong optical absorbers. It was important, therefore, to minimize the incident laser power in order to avoid heating and subsequent distortion of the sample interface. This meant working at low ripplon wavenumbers (about 250 cm^{-1}), where scattering efficiency is higher. However, the SLLS spectrometer is an inherently low-resolution instrument. At low q, the power spectrum is broadened and frequency-shifted compared to that predicted for single-ripplon scattering. Accounting for this instrument effect has been a major problem in applying the technique to crude oil systems.

We recently completed a thorough analysis of the SLLS instrument design, particularly its measurement resolution.[4] We resolved a longstanding problem concerning the source of the extra broadening of the signal. We also showed how the precisely determined instrument resolution could be explicitly included in the spectral fitting calculations. To test the capabilities of the instrument, we used a series of model

systems (at 23 C) which spanned nearly four orders of magnitude in each of IFT, viscosity, and scattering intensity. One model system was glycerol, which has a surface tension of 63 dyn/cm and a viscosity of 1600 centipoise (cP). At the other extreme was a model three-phase microemulsion system which has an IFT of about 5×10^{-3} dyn/cm and a viscosity of 3 cP. An intermediate system was acetone, which has a surface tension of 23.5 dyn/cm and a viscosity of 0.3 cP. The SLLS measurements of IFT and viscosity for all these systems were in excellent agreement with the accepted values. All the measurements were made without major changes to the apparatus.

For what we believe to be the first time, the IFT and viscosity of a crude oil in equilibrium with a hydrocarbon gas mixture have been measured at temperatures and pressures commonly found in oil reservoirs. In the pressure range from 1.7–34.5 MPa, measurements at 37.8 C showed a monotonic decrease in both IFT (by a factor of 10) and viscosity (by a factor of 4). In the same pressure range, measurements at 93.3 C showed a similar decrease in IFT (by a factor of 7.2) and viscosity (by a factor of 4.2). As expected, the viscosity was lower at the higher temperature. However, at the higher temperature the IFT was higher, presumably because of the lower solubility of the hydrocarbon gas at the higher temperature.

We are continuing to use the SLLS technique to measure physical properties in fluid systems of interest to the petroleum industry. We know of no other technique that can provide these values over such a wide range of temperature and pressure.

R.B. Dorshow and Robert L. Swofford,
BP America Research & Development, Cleveland, OH

1. M. A. Bouchiat, J. Meunier, and J. Brossel C. R. Acad. Sci. Paris Ser. B **266**, 255 (1968); M. A. Bouchiat and J. Meunier, ibid. **266**, 255 (1968); J. Phys. (Paris) **32**, 561 (1971).
2. R. H. Katyl and K. U. Ingaard, Phys. Rev. Lett. **19**, 64 (1987); **20**, 248 (1968); and *In Honor of Philip M. Morse*, edited by H. Feshbach and K. U. Ingaard (MIT Press, Cambridge, MA, 1969).
3. S. Hård, Y. Hamnerius, and O. Nilsson, J. Appl. Phys. **47**, 2433 (1976); L. B. Shih, Rev. Sci. Instrum. **55**, 716 (1984); M. Sano *et al.*, Rev. Sci. Instrum. **57**, 1158 (1986); D. I. Jon, H. I. Rosano, and H. Z. Cummins, J. Colloid Interface Sci. **114**, 330 (1986); J. C. Earnshaw and R. C. McGivern, J. Phys. D 20, **82** (1987); S. Hård and R. D. Neuman, J. Colloid Interface Sci. **115**, 73 (1987).
4. R. B. Dorshow, A. Hajiloo, and R. L. Swofford (submitted to J. Appl. Phys).

Low-Temperature Silicon Device Processing

As the performance and density of modern microelectronic devices have increased, the tolerances required in their fabrication have become much tighter. The operation of such devices results from electronic interactions between narrow regions of the active semiconductor material, such as silicon, which have controllable chemical difference between each other. To prevent the atomic diffusion that accompanies normal high temperature processing in these regions and the concomitant degradation of electronic properties, it becomes increasingly important to pursue reduced processing temperatures as dimensions continue to be scaled downward. Recent developments at IBM have dramatically reduced the temperatures required for two of the most fundamental silicon device fabrication steps, the epitaxial growth of pure and doped silicon[1] and the growth of its native oxide, SiO_2.[2] Both techniques are based on Chemical Vapor Deposition (CVD) and have been used to fabricate functional test structures whose performances have shown the deposited layers to be of very high quality, comparable to those produced at much higher temperatures.[2,3]

The process of silicon epitaxy, in which single crystal silicon layers are deposited onto silicon substrates, is pervasive in device fabrication. Presently, commercial pyrolysis of a silicon halide to deposit silicon proceeds at temperatures of about 1000 °C. By allowing excessive diffusion, such temperatures hinder reduction of device dimensions and prevent needed density improvement. The new silicon growth technique,[1] known as Ultra-High Vacuum Chemical Vapor Deposition (UHVCVD) exploits a detailed knowledge of the equilibrium properties of the combined $Si/H_2/O_2/SiO_2$ system to achieve and maintain an atomically clean (oxide free) silicon surface before and during deposition. Epitaxy is achieved at 550 C by the pyrolysis of silane, SiH_4, in an isothermal hot-wall furnace operating at a pressure of about 10^{-8} Torr with excursions to the range 0.001–01 Torr during film growth. At such low total pressures, collisional energy transfer is inefficient, and thus the rate of undesireable silane gas pyrolysis away from the surface becomes limiting. Meyerson and Jasinski[4] applied the Rice, Ramsberger, Kassel, and Marcus (RRKM) theory to this low pressure regime of silane pyrolysis and predicted essentially no depletion by pyrolysis in the gas phase. This results in extremely uniform silicon deposition. The simple hot-wall furnace geometry had been avoided in the past and local substrate heating used instead because at normal CVD gas pressures rapid gas-phase pyrolysis produced excessive depletion and poor film uniformity. Epilayers grown by the UHVCVD technique are free of defects and have been doped *in situ*, producing atomically abrupt interfaces and arbitrary dopant profiles. At 550 C, a wide dynamic range of boron incorporation (10^{13}–10^{21} cm^{-3}) has been successfully demonstrated; highly nonequilibrium doping has been attained with carrier densities greater than 10^{20} cm^{-3}, thus exceeding the predicted boron equilibrium solubility by about two orders of magnitude. Also, because this new growth technique was developed primarily by control of the system chemistry without the need for external deposition enhancements, such as laser or plasma decomposition, a flexible, isotropic growth environment is provided.

The importance of silicon in microelectronics is due, in large measure, to the insulating properties of its native oxide, SiO_2, and to near perfection of the $Si:SiO_2$ interface. In

many respects SiO_2 is the ideal insulator; it has a large band-gap with very few defects and it retains these properties even in very thin films. As with Si itself, however, its growth by CVD or thermal oxidation has heretofore required high temperatures (900–1000 C) for achieving high quality. The new Plasma Enhanced CVD (PECVD) process[2] yields oxide films of very high quality, electronically and structurally, at temperatures as low as 350 C, opening up a multitude of potential new applications. This improvement has been achieved by using very low concentrations of reactive gases, for example, 0.03% SiH_4 and N_2O diluted in helium to suppress homogeneous (gas phase) reactions and to significantly reduce the deposition rate. The helium component of the plasma accomplishes more than simple dilution; it is important in minimizing impurity incorporation, for example.[5] Previous experience with PECVD in depositing SiO_2 had produced relatively low-quality films, porous and leaky with a high concentration of impurities and defects.

These two low-temperature processes open the door to a new level of miniaturization, and they illustrate the importance of rethinking fundamentals in seemingly well-tilled fields.

R. Rosenberg, IBM T.J. Watson Research Center

1. B. S. Meyerson, Appl. Phys. Lett. **48**, 797 (1986); B. S. Meyerson, E. Ganin, D. A. Smith, and T. N. Nguyen, J. Electrochem. Soc. **133**, 1232 (1986); B. S. Meyerson, F. K. LeGoues, T. N. Nguyen, and D. L. Harame, Appl. Phys. Lett. **50**, 113 (1987).
2. J. Batey and E. Tierney, J. Appl. Phys. **60**, 3136 (1986); J. Batey, E. Tierney, and T. N. Nguyen, IEEE Electron Dev. Lett. **EDL-08**, 148 (1987); J. Stasiak, J. Batey, E. Tierney, and J. Li, Device Research Conference, Santa Barbara, CA (1987).
3. T. N. Nguyen, D. L. Harame, J. M. C. Stork, F. K. LeGoues, and B. S. Meyerson, IEDM **86**, 304 (1986).
4. B. S. Meyerson and J. M. Jasinski, Appl. Phys. Lett. **61**, 785 (1987).
5. P. G. Pai, S. S. Chao, Y. Takagi, and G. Lucovsky, J. Vac. Sci. Technol. A **4**, 689 (1986).

Ultrashort Electrical Pulses and Their Applications

The generation of short electrical pulses via optical methods has for some time been performed by driving Auston switches (photoconductive gaps) with short laser pulses.[1] An IBM group has recently generated subpicosecond electrical pulses by photoconductively shorting a charged coplanar transmission line with 70 fsec laser pulses.[2] The resulting 0.5 psec (FWHM) electrical pulses are currently the shortest electrical pulses on electronic circuitry.

The pulses were measured by a fast photoconductive switch, driven by a time delayed beam of the same 70-fsec laser pulses, which connected the transmission line to an electrical probe. Typically, the 20-mm-long transmission line had a design impedance of 100 ohms and consisted of two parallel 5 μm wide, 0.5 μm thick, aluminum lines separated from each other by 10 μm. The transmission line was fabricated on a silicon on sapphire wafer which had been heavily implanted with O^+ ions to ensure the required short carrier lifetime.

Pulse propagation was studied on a superconducting transmission line fabricated out of 900-Å-thick niobium metal.[3] The optoelectronic sampling technique is well suited to operation inside a dewar since all fast electrical signals (0–1 THz) are confined to the sample and only slow signals must leave the dewar. At a temperature of 2.6 K a 1-psec input pulse broadened to only 1.4 psec after propagating a distance of 3 mm. The pulse energy was degraded by less than 5%. Also a strong ringing developed on the trailing edge, which constitutes the first observation of the effect of pair-breaking in a superconductor on pulse propagation (as predicted earlier by Kautz[4]).

This new technique has several advantages in comparison with traditional cw far-infrared spectroscopic techniques.[5] The effective available infrared power is significantly greater. Also, the optoelectronic technique detects the electric field and not the intensity. Thus the technique is sensitive, with an excellent signal-to-noise ratio, to changes in the phase and amplitude of the interfering spectral components. The spectral resolution of about 0.7 cm^{-1} can be increased simply by extending the delay time scan beyond 45 psec. An attractive feature is the possibility of time resolved spectroscopy on a picosecond timescale with the power increased to a level where the population of the relevant energy levels can be strongly influenced. For this case, possible applications are measurements of spin, electric dipole, and photon echoes from resonant excitations in the far infrared.

These electrical pulse techniques are also ideally suited for the characterization of high speed transistors and of wiring structures on integrated circuits. As the performance of these devices is entering the sub-20-psec regime, new techniques are required to evaluate their operation directly in the time domain. The photoconductive sampling gates provide ample time resolution together with very good calibration capabilities and well-defined impedances. For example, we have demonstrated that 3-psec pulses can be generated on a photoconductive chip and coupled with no broadening through wire bonds onto a device chip. In the case of wiring structures, the propagation of the pulses themselves yield the desired information[6]; for active devices the pulses induce switching of the device, and its response is characterized by a sampling gate connected to its output.

In addition, we have recently developed a fabrication technology which allows full integration of the generation and sampling sites on the same substrate as the devices. This will permit the highest speed available to be utilized for device characterization. Thus, these techniques, particularly for the large signal regime most relevant to real device application situations, should prove to be quite useful in the characterization of both devices and circuits.

D. Grischkowsky, M. B. Ketchen, J.-M. Halbout, and C.-C. Chi, IBM T. J. Watson Research Center

1. D. H. Auston, in *Picosecond Optoelectronic Devices*, edited by C. H. Lee (Academic, London, 1984), pp. 73–116.
2. M. B. Ketchen, D. Grischkowsky, T. C. Chen, C.-C. Chi, I. N. Duling III, N. J. Halas, J.-M. Halbout, J. A. Kash, and G. P. Li, Appl. Phys. Lett. **48**, 751 (1986).
3. W. J. Gallagher, C.-C. Chi, I. N. Duling III, D. Grischkowsky, N. J. Halas, M. B. Ketchen, and A. W. Keinsasser, Appl. Phys. Lett. **50**, 350 (1987).
4. R. L. Kautz, J. Appl. Phys. **49**, 308 (1978).
5. M. Tinkham, J. Appl. Phys. Suppl. **33**, 1248 (1962).
6. G. Arjavalingam, J.-M. Halbout, G. V. Kopscay, and M. B. Ketchen, Picosecond Electronics and Optoelectronics (to be published).
7. J.-M. Halbout *et al.*, in Picosecond Electronics Optoelectronics (to be published).

MEDICAL PHYSICS

Magnetic Signs of Neural Activity

Electrical currents flowing within active neurons in the human brain create an extremely weak, though detectable, magnetic field in the space surrounding the head. This "neuromagnetic" field is sensed with ultrasensitive superconducting devices, and mapping the field pattern across the scalp permits locating active neural tissue with a resolution of a few millimeters. The pattern of neural activity of the brain can be called a "neuromagnetic image," or NMI. This functional image, which reveals the spatial pattern of brain activity and how it varies over time, is complementary to x-ray CT images or magnetic resonance images (MRI) which provide largely structural information. At this stage the neuromagnetic image is quite patchy, since studies have been applied mostly to sensory and motor areas of the brain. Some deeper structures have also been explored, but it is only recently that deep-lying nuclei have been detected. These results are encouraging major advances in technology, and large arrays of sensors should be available in the near future. This will make it possible to measure the field over the entire head simultaneously, thus making NMI a versatile reality.

The raw data on which NMI is based is called the magnetoencephalogram (or MEG), which is rather similar in appearance to the conventional electroencephalogram (EEG) obtained by placing electrodes on the scalp. However, the brain and surrounding tissues are transparent to magnetic fields associated with the flow of ionic current within active neurons, and so they emerge from the head without distortion. By contrast, the volume electrical currents arising from the same neural sources spread throughout the intracranial space and must diffuse through the highly resistive skull before reaching the scalp, where they may be detected electrically. The pattern of scalp potentials is strongly influenced by varying conductivity within the head, including apertures in the skull and irregularities in its shape. This makes it more difficult to locate the sources of voltage changes recorded at the scalp.

Neuromagnetic fields are much weaker than fields that are normally present in the environment.[1] These include the Earth's field, which is about one billion times stronger than that of the brain, and fields produced by nearby electric motors, elevators, and metal doors, which are typically a million times stronger. The MEG is also weaker than magnetic fields produced by many other organs of the body, such as the heart.[2] This weakness makes their detection a technical challenge. Fortunately, the well-known low-temperature device commonly referred to as a "SQUID" (for superconducting quantum interference device) provides the necessary sensitivity.[3]

The MEG was first detected with a SQUID sensor in 1972 by Cohen,[4] who monitored the field associated with the well-known alpha rhythm. Subsequently, Brenner and his colleagues detected fields associated with neural activity responding to stimulation of the eyes by a changing visual display.[5] This group went on to find activity related to stimulation of the fingers of the hand, which demonstrated the localizing capability of magnetic measurements.[6] When the active area of the brain is small, the magnetic field encircles the source, emerging from the scalp at one region and entering at another. The source lies directly under the midpoint of the pattern, and its depth is determined by the distance between the positions of strongest inward and outward field perpendicular to the scalp.

Since this work, various investigators went on to explore the magnetic fields associated with activity in other sensory areas of the brain. These include the auditory cortex, the visual cortex, and motor cortex. In fact, the first description of the tonotopic organization of the auditory cortex in humans was achieved using neuromagnetic methods.[7] Also, a secondary sensory area responding to somatosensory stimulation was first observed in humans,[8] as was a deep source within the brain that is known to be related to some memory processes.[9] At present, more than two dozen laboratories are carrying out neuromagnetic studies with SQUID sensors,

and this interest has motivated the rapid development of improved magnetic sensing systems.

The principal challenge in field measurements is that presented by environmental magnetic noise. One method for overcoming this relies on a detection coil connected to the SQUID having a special geometry that discriminates against fields from distant sources. This coil, a "gradiometer," is composed of several coaxial loops with as many turns wound clockwise as counterclockwise. In very noisy environments, when the ultimate sensitivity is required, the gradiometer technique may be augmented by a magnetic shield. Innovative shielding techniques were introduced this year that provide a generous interior space of some 3 m by 4 m in floor dimensions.[10]

Traditionally, determining a field map was a laborious procedure, because it involved sequential measurements at a large number of positions, typically 30 or more for reasonable resolution of a single source. However, within the past two years systems with multiple sensors have been developed which greatly enhance speed and accuracy.[11] The largest system has 14 sensors, contained within two dewars (see Fig. 1) which hold the liquid helium needed to keep the sensors cold, and this is devoted to clinical and basic research at Bellevue Hospital of the New York University Medical Center.[10] Each dewar also has four sensors monitoring the magnetic noise, so that their outputs can be used to reduce the noise in the data of interest. This system therefore has a total of 22 SQUIDs! New devices for permitting the dewars to be moved easily about the head and a magnetic method for determining the positions of these sensors with an accuracy of about 2 mm have also been introduced. The present emphasis in technical development aims at increasing the number of sensors that can simultaneously measure the field at various positions over the scalp. It is reasonable to expect that within five years a system will be available for measurements at, say, 100 positions, so that an NMI can be obtained within a matter of minutes.

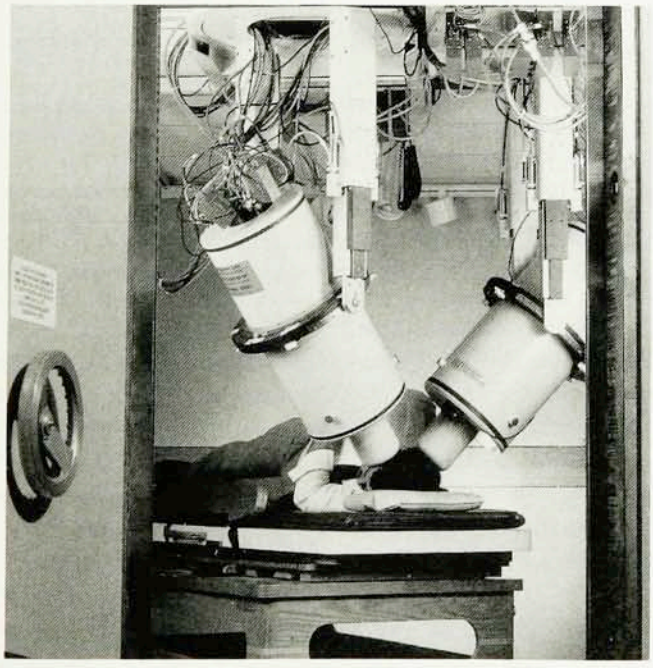

FIG. 1. A device used for making neuromagnetic images of the human brain. The system shown here uses 22 SQUID sensors, contained in two dewars.

Part of the motivation for these developments arises from ongoing clinical research at the University of California at Los Angeles[12] and at the University of Rome.[13] This demonstrates a significant application of neuromagnetism in pinpointing regions of the brain that are responsible for some epileptic seizures. In many patients anomalous signals can be seen at various moments between seizures. The MEG associated with this interictal activity is being measured to determine the location of its source, which may be a tumor or other diseased tissue. Sometimes surgical removal of this tissue improves the patient's condition. The application of magnetic techniques may well reduce the need to use electrodes placed deep within the brain to determine the epileptic source. This, however, is just the beginning of a potentially important role for neuromagnetism in basic and clinical research on the human brain. In the not too distant future, neuromagnetic images can become a useful adjunct to other imaging methods, and thus aid the physician in diagnosis and in monitoring efficacy of therapeutic procedures.

Samuel J. Williamson and Lloyd Kaufman,
New York University

1. *Biomagnetism: an Interdisciplinary Approach*, edited by S. J. Williamson, G. L. Romani, L. Kaufman, and I. Modena (Plenum, New York, 1983), 706 pp.
2. D. Cohen, Phys. Today **28**, 34 (August 1975).
3. J. Clarke, Phys. Today **39**, 36 (March 1986).
4. D. Cohen, Science **175**, 664 (1972).
5. D. Brenner, S. J. Williamson, and L. Kaufman, Science **190**, 480 (1975).
6. D. Brenner, J. Lipton, L. Kaufman, and S. J. Williamson, Science **199**, 81 (1978).
7. G. L. Romani, S. J. Williamson, and L. Kaufman, Science **216**, 1339 (1982).
8. R. Hari, K. Reinikaninen, E. Kaukoranta, M. Hämäläinen, R. Ilmoniemi, A. Penttinen, J. Salminen, and D. Teszner, Electroenceph. Clin. Neurophysiol. **57**, 254 (1984).
9. Y. Okada, L. Kaufman, and S. J. Williamson, Electroenceph. and Clinical Neurophysiol. **55**, 417 (1982).
10. D. S. Buchanan, D. Paulson, and S. J. Williamson, *Advances in Cryogenic Engineering*, edited by R. W. Fast (Plenum, New York, in press).
11. R. Ilmoniemi, R. Hari, and K. Reinikainen, Electroenceph. Clin. Neurophysiol. **58**, 473 (1984).
12. D. Barth, J. Sutherling, J. Engle, Jr., and J. Beatty, Science **223**, 293 (1984).
13. G. L. Romani and L. Narici, Med. Progr. Techn. **11**, 123 (1986).

Positron Emission Tomography

In the 1930s, during the development of the cyclotron for studying the structure of the nucleus, Ernest Lawrence produced small amounts of ^{18}F (with a half-life $t_{1/2}$ of 110 min)

for investigation of bone disorders. Researchers were able to measure the time course of the labeled fluoride in bone with Geiger counters. Today the technique[1] of positron emission tomography (PET) involves the detection of annihilation photons from short-lived positron-emitting nuclides of specific biological interest. Nuclides used include ^{18}F, ^{11}C ($t_{1/2} = 20$ min), ^{13}N ($t_{1/2} = 10$ min) and ^{15}O ($t_{1/2} = 2$ min). Radiotracers, or more appropriately, radiopharmaceuticals, are rapidly synthesized from labeled precursors and inhaled or injected into patients undergoing PET studies. PET scanners or tomographs rely on banks of scintillation detectors that surround the patient and are coupled to sophisticated computer acquisition systems. Images of the temporal and the spatial distributions of specific radiopharmaceuticals are made possible by utilizing similar mathematical image reconstruction techniques that were developed by Hounsfield[2] for use in CT (computerized tomography).

There are approximately 20 active PET Centers in the United States and Canada and about the same number in Europe and Japan. Nearly all installations utilize some type of particle accelerator, a radiochemistry laboratory, and at least one PET scanner. New centers are being constructed all over the world. Compact cyclotrons which accelerate protons and deuterons, or protons only, have become the norm for PET nuclide production. These units cost from $1,000,000 to $1,500,000 when target systems and automated control mechanisms are installed.

Research in tomograph design continues in the university and commercial environments with major efforts directed towards improving resolution in three dimensions. Scanners are available with coincidence resolving times between 5 and 10 nsec. Tomographs can also be purchased as time-of-flight (TOF) devices with temporal resolution of 600–900 psec. Commercially produced scanners yield a resolution of 5–6 mm and, depending on the sample volume desired, cost between $1,800,000 and $2,500,000.

New tomograph designs differ from earlier systems in that they detect photons with either a continuous position-sensitive or discrete position-sensitive configuration, rather than with a single crystal coupled to a single photomultiplier tube. A continuous two-dimensional position-sensitive PET tomograph with pulse clipping and digital position estimation has been developed at the University of Pennsylvania. Singles count rates in excess of 2×10^6 cps with coincidence count rates of 2×10^5 cps for the entire tomograph have been achieved.[3] The design incorporates six detectors, each of which has a useful area of 50×10 cm and is coupled to 30 photomultiplier tubes. The intrinsic resolution of this tomograph is 5.5 mm FWHM.

Four-millimeter resolution has been obtained without utilizing multiple sampling positions for the ring of detectors circumscribing the patient; that is, the detectors do not move with respect to the patients. For this system, eight scintillators are coupled to a dual photomultiplier tube. The tomograph consists of four rings in which each ring contains 96 photomultiplier tubes and 768 crystals.[4]

A more traditional design that couples single PMTs to individual 3-mm-wide crystals has been developed.[5] This is a single ring machine with the system composed of 600 detectors. Two-position "clamshell" detector sampling motion is employed which effectively doubles the number of detectors per ring up to 1200. The resolution of the scanner is 2.6 mm at the center. The resolution of this tomograph design thus begins to approach the finite range (1.5 to 0.5 mm average) of the particular positron emitters used in PET scanning. It now becomes extremely important that special care be taken to minimize patient motion artifact.

Advances in research that constantly improve image resolution, count-rate capability, and scanner sensivity are required to measure the significance of changes in human physiology and biochemistry. Positron emission tomography, when combined with morphological or anatomical information as obtained by magnetic resonance imaging or CT, offers medical researchers a unique and powerful tool for noninvasively investigating the cellular function of the intact working human body.

R.D. Hichwa, University of Michigan

1. *Positron Emission Tomography and Autoradiography—Principles and Applications of the Brain and Heart*, edited by M. E. Phelps, J. C. Mazziotta, and H. R. Schelbert (Raven, New York, 1987).
2. G. N. Hounsfield, A Method and Apparatus for Examination of a Body by Radiation such as X or Gamma Radiation, Patent Specification 1283915, The Patent Office (London, England, 1972).
3. G. Muehllener, J. S. Karp, D. A. Mankoff, and D. Beerbolm, J. Nucl. Med. **28A**, 641 (1987).
4. Y. Hirose *et al.*, J. Nucl. Med. **28A**, 607 (1987).
5. R. H. Huesman, S. E. Derenzo, T. F. Budinger, J. Cahoon, and T. Vuletich, J. Nucl. Med. **28A**, 608 (1987).

New Deformation Effects in Nuclei

Recent experiments are providing new information on nuclear deformation properties in two different regimes. Studies of the gamma decay of the giant dipole resonance (GDR) are affording the first clear view of the shape of highly excited "hot" nuclei. At the other extreme, very elongated "superdeformed" shapes have been discovered at high spin in cold nuclei. These experiments provide insights into nuclear behavior under unusual conditions.

In a hot nucleus, deformation effects due to shell structure are expected to disappear gradually with increasing temperature, leading to spherical shapes at low spin, and to oblate shapes at higher spin, owing to the effects of Coriolis and centrifugal forces. Because nuclei contain a small number of particles, shape fluctuations will also be important. The interplay between these effects leads to a variety of behavior expected in different nuclei as a function of spin and temperature.

Hot nuclei formed in heavy-ion fusion reactions emit high-energy gamma rays through a statistical radiation process involving the decay of the giant dipole resonance.[1] The sensitivity of the GDR to the nuclear deformation is well known from studies of cold, axially symmetric deformed nuclei in which the GDR is split into two components corresponding to vibrations along the long and short axes. The size of the splitting gives the deformation magnitude, and the relative strength of the two components gives the sense of the deformation—prolate or oblate.

Three different types of behavior in hot nuclei are currently being studied. First, in nuclei which are strongly deformed at low energies, such as some of the rare earths, the deformed nuclear shape remains essentially unchanged at temperatures of about 1 MeV and low spins, as evidenced by the observation of a split GDR in the decays of the hot nuclei.[2] This is consistent with the expected persistence of shell effects at such temperatures. Second, at temperatures of about 1–2 MeV, nuclei which are spherical at low energies show a strongly broadened GDR shape compared to the GDR excited in the cold nucleus.[3] This broadening is believed to be due primarily to thermally induced shape fluctuations.[4] Apparently the shape fluctuations in spherical nuclei at these temperatures are comparable in magnitude to the static deformation of the strongly deformed, cold rare earth nuclei.

The third type of behavior involves possible shape changes at nonzero spin. The oblate shape discussed above is expected to occur at lower spin in hot nuclei than in cold nuclei owing to the thermal softening of the nuclear surface. The expected features of such shape transitions can be derived from microscopic calculations, or from the macroscopic Landau theory of phase transitions with deformation as the order parameter.[5] So far there are some experimental suggestions, but no definitive results, of prolate–oblate shape changes.[6]

Nuclei with superdeformed shapes occur, in large part, because of stabilizing shell effects (gaps in the spacing of single particle levels). Large shell effects are expected when the lengths of the axes are in the ratio of small integers, with the largest occurring for spherical shapes (ratio 1:1:1). Superdeformed shapes with an axes ratio of 2:1:1 (or "2:1") were first observed in the fission isomers occurring in the uranium region,[7] where the strong Coulomb repulsion tends to cancel the nuclear surface tension, thus helping to stabilize elongated shapes. At high spins the centrifugal force can provide a similar stabilizing effect.

The first clearly superdeformed band with high spins was discovered[8] as a series of 19 regularly spaced gamma rays in the nucleus ^{152}Dy formed in a heavy-ion fusion reaction. The observed gamma-ray energies vary from about 0.6–1.4 MeV, corresponding to probable spins ranging from 24 to 60. Both the moment of inertia (estimated from the 47-keV separation between gamma-ray energies) and the electric quadrupole moment (estimated from the emission time of the rotational gamma rays) are consistent with the 2:1 axis ratio. This band is the most regular known in any nucleus; however, the significance of this is not clear, since a second superdeformed band has just been found[9] in this mass region (^{149}Gd) and is much less regular.

Several "superdeformed" bands found in the mass-134 region[10] have a prolate deformation considerably larger than the coexisting "normal" bands, but an axis ratio that is less than 2:1. It will be interesting to find out whether it is the same general shell effect that produces both regions.

At the highest spins, these cold superdeformed states are populated much more strongly than expected; this may be related to the giant dipole resonances discussed earlier. In a superdeformed nucleus the large splitting of the GDR would bring the lower component down to 8–9 MeV. This would increase the probability of the E1 statistical transitions that cool the nucleus, and thus may explain the more rapid cooling observed.

K.A. Snover, University of Washington,
F.S. Stephens, Lawrence Berkeley Laboratory,
and Y. Alhassid, Yale University

1. J. O. Newton *et al.*, Phys. Rev. Lett. **46**, 1383 (1981); K. A. Snover, Ann. Rev. Nucl. Part. Sci. **36**, 545 (1986).
2. C. A. Gossett *et al.*, Phys. Rev. Lett. **54**, 1486 (1985).
3. J. J. Gaardhoje *et al.*, Phys. Rev. Lett. **56**, 1783 (1986).

4. M. Gallardo *et al.*, Nucl. Phys. **A443**, 415 (1985).
5. A. V. Ignatyuk *et al.*, Nucl. Phys. **A346**, 191 (1980); Y. Alhassid *et al.*, Phys. Rev. Lett. **57**, 539 (1986); A. L. Goodman, Phys. Rev. **C35**, 2338, (1987).
6. J. J. Gaardhoje, *Nuclear Structure 1985*, edited by R. Broglia *et al.*, (North Holland, Amsterdam, 1985), p. 519.
7. S. M. Polikanov *et al.*, Soviet Phys. JETP **15**, 1016 (1962).
8. P. J. Twin *et al.*, Phys. Rev. Lett. **57**, 118 (1986).
9. Private Communication, 8pi-Spectrometer Group, Chalk River Nuclear Laboratory.
10. P. J. Nolan *et al.*, J. Phys. **G11**, L17 (1985); E. M. Beck *et al.*, Phys. Rev. Lett. **58**, 2182 (1987).

High-Energy Nucleus–Nucleus Collisions at BNL and CERN

In late 1986 and early 1987, major new research efforts to study high-energy nucleus–nucleus collisions were initiated almost simultaneously at the Brookhaven Alternating Gradient Synchrotron (AGS) and CERN Super Proton Synchrotron (SPS) with the acceleration of light ions. These high-energy studies, previously the exclusive research province of cosmic-ray experiments, were carried out with 14.5-GeV/nucleon ^{16}O and ^{28}Si projectiles at the AGS and with 60- and 200-GeV/nucleon ^{16}O projectiles at the SPS.

The central theme of this rapidly evolving area of nuclear physics research is the continuing exploration of extreme conditions of temperature and baryon density produced in violent central collisions between nuclei.[1] In particular, QCD lattice gauge calculations indicate that at sufficiently high energy densities (1–2 GeV/fm^3), hadronic matter should evolve into a new phase of matter containing "deconfined" quarks and gluons, called the quark–gluon plasma (QGP). Such a state of matter is thought to have briefly existed in the period of about 1 μsec after the Big Bang. Earlier work at the Berkeley Bevalac had provided evidence for "hot" nuclear matter at an equivalent temperature of 50–100 MeV and densities of 2–4 times nuclear matter density; but these conditions were not sufficient for plasma formation. By going to yet higher energies, experimentalists hope to increase the energy density sufficiently to induce formation of the QGP. Although no unique signature for the QGP has emerged as yet, several promising probes or observables have been suggested. These include: (1) enhanced strange particle production, (2) ψ suppression owing to Debye screening of the charm–anticharm quark potential, (3) increasing transverse momentum per particle as a function of the rapidity density with a break in the slope near the phase transition, (4) enhanced fluctuations in the rapidity density, and (5) detailed spectral states of direct photons or dileptons as a probe of the hot, dense phase of the collision. All of these quantities are experimentally accessible and were sought in these first-run experiments.

The first nuclear collisions at both accelerators were measured by teams of nuclear and particle physicists utilizing an arsenal of detectors including a streamer chamber highly segmented electromagnetic and hadronic calorimeters, magnetic spectrometers, and a variety of multiplicity counters. A second category of survey experiments involved smaller setups, including nuclear emulsions and plastic track detectors to search for anomalous fragments including quark searches. An international community representing research institutions from Eastern and Western Europe, the Middle East, India, Japan, and the United States is taking part in these programs with the participation of over 200 researchers at the AGS and over 300 at CERN.

The new data and possible implications were recently discussed at the Quark Matter '87 meeting, held in Nordkirchen, West Germany, in August 1987.[2] The meeting demonstrated that the first experiments at both accelerators had performed well in the novel environment where several hundred charged particles are produced per central collision (see Fig. 1). A sampling of results includes: (1) completed reconstruction of streamer chamber events with over 300 tracks, allowing for the first time the use of the like-pion interferometry technique for determining the space-time development of the source to be applied to an individual event; (2) reconstruction of high-transverse-momentum π^0's in Pb-glass detectors; (3) first measurements of strange particle yields; (4) observation of large-transverse-energy flow at both AGS and SPS energies, suggestive of a large amount of

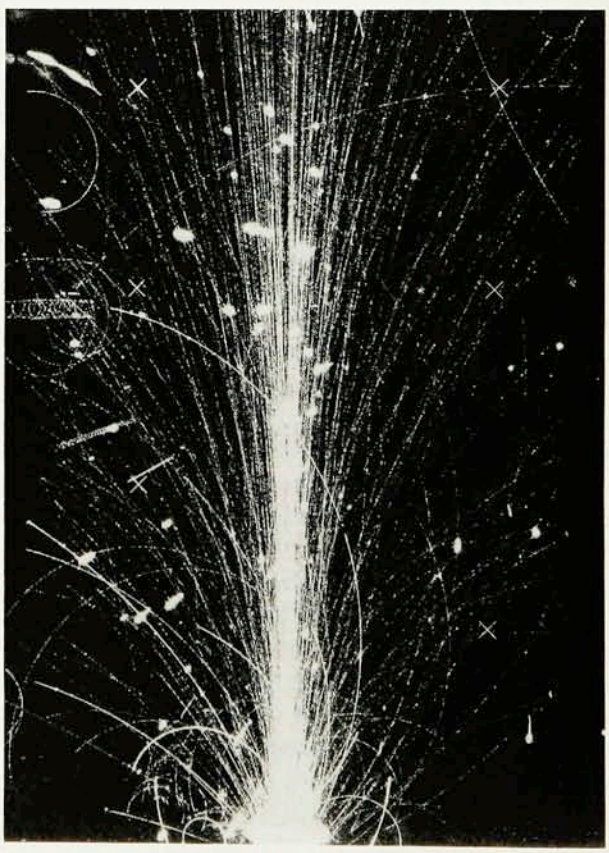

FIG. 1. Oxygen–lead collisions produced showers of some 250–300 charged particles in the streamer chamber at CERN. Experiments were run at both 60 GeV and 200 GeV/nucleon (a total beam energy of 3200 GeV).

the incident energy being "stopped" in the projectile-effective target center-of-mass, and thus available for exciting additional degrees-of-freedom; and (5) the observation of very clean ψ spectra in a dimuon experiment. The most provocative preliminary data were those suggesting a large K^+/π^+ ratio at the AGS and a reduction of ψ's at the SPS for central collisions.

Although it is too early to determine whether the QGP has been observed in nuclear collisions at these energies, the trends in the data are very encouraging and provide confirmation of the large nuclear stopping power and inelasticities in such collisions. Analysis and further experimentation continues on these experiments, including a ^{32}S run in late 1987 at CERN and continued dedicated running at the AGS in 1987 and 1988. The AGS Booster project will provide Au beams in 1990 and there is discussion underway at CERN for a Pb-injector, again for the early 1990s. Finally, at AGS/SPS energies one expects a baryon-rich environment for plasma production. A baryon-free plasma, more closely approximating the conditions of the early universe, awaits yet higher energies, such as those being discussed for the proposed RHIC ("Relativistic Heavy Ion Collider") facility at Brookhaven.

Lee Schroeder and M. Gyulassy, Lawrence Berkeley Lab

1. Quark Matter '86, Nucl. Phys. A **461**, 1C (1987), edited by L. Schroeder and M. Gyulassy.

2. Quark Matter '87, Z. Phys. C (to be published).

The Beta Decay of Tritium and the Search for Neutrino Mass

Although the neutrino plays an important role in both elementary particle physics and cosmology, little is known about its properties after more than 50 years. In particular, the question of whether the neutrino has a finite rest mass is still unresolved. If the rest mass is shown to be nonzero, as predicted by essentially all Grand Unified Field Theories (GUTs), the impact on field theory would be tremendous since it would provide the first indication of new physics predicted by GUTs and serve to constrain the many different GUT models. In addition, if the rest mass were on the order of a few tens of electron volts, neutrinos would account for all the dark matter in the universe; they could in fact close the universe if the rest mass were greater than about 25 eV. Thus reports in 1980 of evidence for a 35-eV mass for the electron antineutrino stirred great interest. This claim was made by a group studying the beta decay of tritium at the Institute of Theoretical and Experimental Physics (ITEP) in Moscow.

Searches for a finite neutrino mass in nuclear beta decay involve accurately measuring the electron spectrum close to the endpoint (the maximum energy of the decay) of the spectrum, where the effect of a finite neutrino mass would appear, owing to the fact that some of the decay energy must go into the rest mass of the neutrino. The difficulty is that the count rate near the endpoint is small, and effects of spectrometer resolution, energy loss and final-state distributions are maximal. These effects distort the spectrum in a way that strongly influences the neutrino mass extracted, and must, therefore, be very carefully determined by independent means. Tritium, having a simple atomic structure and an allowed decay with a low endpoint energy, provides the only case with sufficient sensitivity to resolve the question of whether the electron antineutrino has enough rest mass to close the universe.

The ITEP group used a source consisting of tritium-substituted valine (an amino acid) and a toroidal magnetic spectrometer.[1] Although this experiment has been carefully studied and no single problem identified as cause for a possibly spurious result, there are several concerns about the experiment, mostly revolving around the source used. Following the beta decay of an isolated tritium atom, the helium daughter atom is left in an excited state about 40% of the time, with an average excitation energy of about 30 eV (comparable to the neutrino mass being claimed). Since it is essentially impossible to demonstrate that these final-state excitations in valine (with 64 electrons in the molecule) can be calculated to sufficient accuracy, 17 other groups around the world have initiated tritium beta decay experiments using simpler sources to check the Russian claim. Three groups (University of Zürich,[2] Institute for Nuclear Studies, Tokyo,[3] and Los Alamos National Laboratory[4]) have published initial results using different approaches to minimizing systematic problems.

Like ITEP, the groups at Zürich and Tokyo are using solid sources (tritium implanted in carbon and a tritiated organic acid, respectively) while the Los Alamos group is using a differentially pumped gaseous molecular tritium source. All three groups use magnetic spectrometers to analyze the betas, but the Zürich group first decelerates the electrons from the source before analysis in order to improve the energy resolution while the Tokyo and Los Alamos groups first accelerate the electrons from the source in order to reduce backgrounds. The results from all three groups are consistent with a zero neutrino mass; the Zürich, Tokyo, and Los Alamos groups set limits, respectively, of 18, 32, and 27 eV. It is presumably no more than a curious coincidence that the limits on electron neutrino mass derived[5] from the recent supernova in the Large Magellanic Cloud are so similar to the laboratory ones. While these results are in conflict with the current central value of 30 eV claimed by the ITEP group, the lower part of the 17–40 eV range allowed by the ITEP data cannot be ruled out. Further efforts underway by these and other groups are expected to provide ultimate sensitivities of less than 10 eV.

It does seem clear at this point from laboratory measurements that the mass of the electron antineutrino is unlikely to be the sole source of the dark matter in the universe. Of

course, the mu and tau neutrinos are still candidates for dark matter and are likely to remain so for the foreseeable future.

T.J. Bowles and R.G.H. Robertson,
Los Alamos National Laboratory

1. S. Boris *et al.*, Phys. Rev. Lett. **58**, 2019 (1987).
2. M. Fritschi *et al.*, Phys. Lett. **173b**, 485 (1986).
3. H. Kawakami *et al.*, Phys. Lett. **187b**, 198 (1987).
4. J. F. Wilkerson *et al.*, Phys. Rev. Lett. **58**, 2023 (1987).
5. E. W. Kolb *et al.*, Phys Rev. D **35**, 3598 (1987).

Y-Scaling in Nuclei

"Knocking out" constituents is a common method for probing the structure of quantum many-body systems. Recent experiments that use high-energy electrons to knock nucleons out of nuclei (quasi-elastic scattering) are offering new insights into the properties of nuclear matter.

The cross section for scattering from a many-body system can be expressed in terms of a response function describing the many-body structure. This response function, related to the motion of the constituents and their interactions, generally depends upon both the energy and momentum transferred in the scattering process. However, if the reaction mechanism is a "clean" knockout, only one function of a single variable is important: the distribution of constituent momenta. Thus if the energy and momentum transfers are transformed into a "proper" pair of kinematic variables, the response function will be independent of one of them ("scaling") and its dependence upon the other will reveal the momentum distribution. Various higher order processes that might contribute lead to "scaling violations," which must be understood for quantitative analysis of the response function.

Neutron scattering from liquid ^{4}He has been used to study the Bose condensate in that system.[1] Similarly, high-energy lepton scattering has been used to demonstrate the quark substructure of nucleons.[2] In nuclear physics, the momentum distribution of nucleons can be probed by quasi-elastic electron scattering where the rough features of nuclear systems were extracted from low-momentum transfer.[4,5]

A recent experiment performed at the Stanford Linear Accelerator Center extended measurements of quasi-elastic electron scattering in the regime where scaling is expected to occur for heavy nuclei.[6] This was the first experiment to use the Nuclear Physics Injector at SLAC, which provides high-intensity electron beams up to 4 GeV in energy.

The scaling analysis was performed in terms of the kinematic variables Q^2 and y, the square of the four-momentum transferred by the scattered electron and the momentum of the struck nucleon along the direction of the three-momentum transferred, respectively. When y is less than zero the response functions of various nuclei show an approach to scaling behavior at high Q^2, but show a definite violation of scaling as Q^2 decreases. The region for which y is larger than zero contains cross-sections from nucleon resonance excitation and deep-inelastic scattering from quarks and therefore does not exhibit the scaling property expected from quasi-elastic scattering from nucleons.

The scaling of the data for y less than zero has a number of implications. At low momenta, the scaling function varies from nucleus to nucleus. These nucleons within the fermi sea are sensitive to the nucleus as a whole. However, at higher momenta (as large as 800 MeV/c) the scaling function becomes independent of the choice of target because these high momenta arise from the repulsive interaction of two nucleons at short distances, which is largely unaffected by the global nuclear environment. The observed approach to scaling at high momenta is consistent with theory.[7] However, the magnitude of the scaling function is calculated to be about a factor of 3 to 5 times higher than the experimental data. Since the momentum distribution in this region is dominated by the potential at short distances, this disagreement may be evidence for deficiencies in the interaction used.

Several conclusions can be drawn from this work. First, the scattering of high-energy electrons from nuclei in the quasi-elastic region scales in the way expected of a knock-out mechanism, provided the momentum transfer are large enough. Second, the scaling function that results measures the momentum distribution of nucleons within the nucleus, and this becomes independent of target at momenta greater than the fermi momentum. Third, the Q^2 dependence at these momentum transfers can be reliably used to test for modification of the nucleon structure in the nuclear medium. Further work is presently in progress to analyze these data and to explore experimentally the transverse/longitudinal aspects of the nuclear response at these high-momentum transfers.

R.D. McKeown and S.E. Koonin,
California Institute of Technology

1. A. L. Bennani *et al.*, Phys. Lett. **41**, 470 (1976); L. J. Rodriguez, H. A. Gersch, and H. A. Mook, Phys. Rev. A **9**, 2085 (1974).
2. A. Bodek *et al.*, Phys. Rev. D **20**, 1471 (1979).
3. E. J. Moniz *et al*, Phys. Rev. Lett. **25**, 445 (1971).
4. G. B. West, Phys. Rep. **18C**, 264 (1975).
5. I. Sick, D. Day, and J. S. McCarthy, Phys. Rev. Lett. **45**, 87 (1980).
6. D. B. Day *et al.*, Phys. Rev. Lett. **59**, 427 (1987).
7. M. N. Butler and S. E. Koonin (to be published).

The M1 Scissors Mode in Nuclei

A new mode of nuclear collective motion, a "scissors" mode, has been discovered and elucidated in permanently deformed nuclei in the past few years.[1] Macroscopically,[2] this mode can be pictured as a scissors-like vibration of the deformed bodies of protons against neutrons in a nucleus. The restoring force tending to align the symmetry axes of the

ellipsoidally-shaped proton and neutron bodies is connected to the nuclear symmetry energy which resists a separating of protons from neutrons.[3]

This new mode is manifest in the existence of a $J^{\pi} = 1^{+}$ state found in heavy deformed even–even nuclei at an excitation energy as low as about 3 MeV. Since the magnetic dipole (M1) transition leading to this state is caused predominantly by an orbital motion of the protons with respect to the neutrons, it is seen best in electron or photoexcitation processes and hence had been missed in all previous studies with hadronic probes. The scissors mode is not to be confused with the spin magnetic dipole motion at much higher excitation energy (around 10 MeV), which can be studied conveniently with either electromagnetic or hadronic probes. There is, of course, interference between the orbital and spin M1 modes, as will be remarked upon below.

At the microscopic level, the out-of-phase motion of the protons with respect to the neutrons and the nature of the neutron–proton force responsible for this motion has been studied in a large number of deformed-shell model, quasiparticle random phase approximation, projected Hartree–Fock, and particularly interacting boson model (IBM) calculations.[4] In the treatment of deformed nuclei in the IBM, in which the nuclear structure results from interactions among the valence particles outside closed shells, the "important" interactions are amongst pairs of nucleons coupled to bosons and only those pairs in the valence shells are taken into account; the excitation strength of the scissors mode can be related directly to the number of nucleons participating in the motion. A further attractive feature of this model is that by taking linear combinations of proton and neutron bosons, basis states with a definite symmetry character under neutron–proton exchange (i.e., symmetric and mixed-symmetry) can be constructed. The M1 scissors mode involves those states of mixed symmetry.

Since the discovery, electro- and photonuclear experiments have revealed the scissors mode in nuclei ranging from the medium–heavy fp-shell nuclei to a number of deformed rare-earth nuclei to the actinides thorium and uranium. Its excitation energy scales roughly as 66 MeV $\delta A^{-1/3}$, where δ is the dimensionless mass deformation parameter and A the mass number. The transition strength is often concentrated into one (or a very few) collective states (i.e., there is little spreading). The largest transition strength (about five nuclear magnetons squared) is observed in ^{164}Dy, while the strength in other nuclei is about half as large. Since the strength of the mode relates directly to the number of nucleons participating in the motion, the average proton–neutron interaction and its role in causing nuclear deformation can be determined.[5]

Of particular interest is the appearance of the scissors mode in the even–even nuclei of the fp-shell, where the existence of mixed symmetry neutron–proton states has long been known.[6] However, since the valance neutrons and protons here occupy the same shell, both orbital and spin magnetism are present. These contribute equally to the transition strength, as has been derived from a comparison of high resolution inelastic electron and proton scattering experiments. Unlike the heavy deformed nuclei, where it can be experimentally demonstrated that the orbital magnetism dominates the spin magnetism, the lighter nuclei do not show a pure scissors vibration.

Because of its collectivity and its low excitation energy the scissors mode is a major contributor to the magnetic dipole polarizability of nuclei. This elementary mode of excitation can also be regarded as a $o\hbar\omega$ isovector orbital magnetic dipole giant resonance. Its properties are also very helpful in distinguishing between various commonly used effective nuclear interactions.

Achim Richter, Technische Hochschule
Darmstadt, West Germany

1. D. Bohle, A. Richter, W. Steffen, A. E. L. Dieperink, N. Lo Iudice, F. Palumbo, and O. Scholten, Phys. Lett. **137B**, 27 (1984).
2. N. Lo Iudice and F. Palumbo, Phys. Rev. Lett. **41**, 1532 (1978).
3. R. Nojarov, Z. Bochnacki, and A. Faessler, Z. Phys. A **324**, 289 (1986).
4. See, for example, P. van Isacker, K. Heyde, J. Jolie, and A. Sevrin, Ann. Phys. **171**, 253 (1986).
5. R. F. Casten, D. S. Brenner, and P. E. Haustein, Phys. Rev. Lett. **58**, 658 (1987).
6. L. Zamick, Phys. Rev. C **31**, 1955 (1985).

Spectral Changes and Frequency Shifts Produced by Source Correlations

Spectroscopy is based on the implicit assumption that, apart from trivial geometrical scaling factors, the spectrum of light emitted by a source that is at rest relative to an observer is independent of the location of the observer. Recent research, both theoretical and experimental, carried out at the University of Rochester has shown that this is not always so and that "spectral invariance" on propagation, observed with light generated by traditional sources, is somewhat of an exception. This discovery is related to some theoretical considerations of L. Mandel,[1] published more than 25 years ago, when he showed that if two beams of light which have the same normalized spectrum are superimposed, the resulting beam will have a different normalized spectrum unless the correlation between the two beams satisfies a certain relationship (known as the reduction formula for cross-spectrally pure beams).

Recently Wolf [2] showed that the spectrum of light generated by a planar secondary source of a wide class depends, in general, on the location of the point of observation, unless the degree of spectral coherence of the light across the source plane satisfies a certain functional relationship, called the scaling law. He showed that the usual thermal sources obey this law. It is undoubtedly for this reason that the noninvariance of the spectrum of light on propagation has not been observed before.

The degree of spectral coherence is a measure of correlation between fluctuations of the source distribution at different points in the source. Very recent work has shown that the spectrum of emitted light depends, in general, not only on the spectrum of the source distribution, but also on its degree of spectral coherence.[2-5] This conclusion holds whether the source is a primary one, such as a set of radiating atoms, or a secondary source, such as the opening in the walls of a cavity containing blackbody radiation or a scattering medium illuminated by a light wave. The modification of the spectrum of emitted light due to source correlations was observed not long ago.[6]

The spectral changes due to source correlations can be quite drastic. Source correlations may, for example, produce shifts of an emitted spectral line either towards the longer wavelengths (thus generating a red shift) or towards the shorter wavelengths (generating a blue shift). These theoretical predictions have been verified by recent experiments with acoustical waves.[7] This new mechanism for generating line shifts is obviously of special interest for astrophysics, since it bears on the nature of the redshifts of quasars and other celestial objects.

M.F. Bocko, G.M. Morris, and E. Wolf,
University of Rochester

1. L. Mandel, J. Opt. Soc. Am. **51**, 1342 (1961); L. Mandel and E. Wolf, *ibid.* **66**, 529 (1976).
2. E. Wolf, Phys. Rev. Lett. **56**, 1370 (1986).
3. E. Wolf, Nature **326**, 363 (1987).
4. E. Wolf, Opt. Commun. **62**, 12 (1987).
5. E. Wolf, Phys. Rev. Lett. **58**, 2646 (1987).
6. G. M. Morris and D. Faklis, Opt. Commun. **62**, 5 (1987).
7. M. F. Bocko, D. H. Douglass, and R. S. Knox, Phys. Rev. Lett. **58**, 2649 (1987).

External Electro-Optical Probing for High-Speed Devices and Integrated Circuits

Scientists at Bell Laboratories have developed and demonstrated a new, noncontact, picosecond, electro-optic technique for obtaining signal waveforms at internal nodes of high-speed integrated circuits or from discrete devices fabricated on any substrate material.[1] This technique, referred to as *external* electro-optic sampling, achieves subpicosecond temporal resolution with a spatial resolution of a few microns. It is designed to operate at the wafer level on conventional wafer-probing equipment without any special circuit preparation. Initial experiments have characterized GaAs selectively doped heterojunction transistor (SDHT) prescaler circuits,[1] and also addressed the inherent speed and loading limits of the technique. Temporal resolution of less than 300 fsec has been shown.[2]

Electro-optical sampling has been used extensively for the characterization of discrete picosecond electronic devices such as photodetectors, transistors, and diodes.[3] However, there is great interest in being able to probe internal points of integrated circuits in order to characterize device and circuit operation *in situ.* Recently, a specialized embodiment of electro-optic sampling was developed to perform sampling directly in the electro-optic substrate of GaAs integrated circuits.[4] However, GaAs is the only commonly used semiconducting material that is also electro-optic. Ideally one would like a nonperturbative means of probing integrated circuits with high temporal and spatial resolution that is generally applicable to circuits fabricated on any type of substrate.

External electro-optic probing is based on the use of an extremely small electro-optic crystal as a proximity electric

field sensor near the surface of an integrated circuit. This technique exploits the open electrode structure of two-dimensional circuits where there exists a fringing field above the surface of the circuit between metallization lines at different potentials. "Dipping" an electro-optic tip into a region of fringing field induces a birefringence change in the tip that can be measured from above by an optical beam directed through the tip. In this way, the electro-optic tip is employed as the modulator in a conventional electro-optic sampling system. By using an external electro-optic medium, the sampling system does not require the circuit to become an element of the optical system. This relaxes the material and fabrication requirements making external probing applicable to a wide variety of circuit embodiments.

The temporal resolution of this probing technique enables one to accurately characterize signals that previously could only be measured by autocorrelation techniques, if at all. In this way it is possible to obtain true information about the shape of picosecond electrical signals and hence more accurately characterize device performance and, in particular, charge carrier dynamics. Subpicosecond temporal resolution is essential if one is interested in directly observing hot electron effects such as, for example, velocity overshoot. Bell Laboratories scientists Janis Valdmanis, Martin Muss, and Peter Smith recently also investigated the carrier recombination dynamics in amorphous silicon, by measuring the impulse response of an ion-bombarded silicon-on-sapphire photoconductor when excited by 100-fsec optical pulses. The sample was fabricated in a 5 micron transmission line geometry on a sapphire substrate and generated electrical pulses of 760-fsec duration. This is the shortest electrical pulse ever directly resolved on a transmission line.

Federico Capasso, AT&T Bell Laboratories

1. J. A. Valdmanis and S. S. Pei, Proceedings of the Picosecond Electronics and Opto-Electronics Conference, Lake Tahoe, 1987 (to be published).
2. J. A. Valdmanis and S. S. Pei, Conference on Lasers and Electro-Optics (Baltimore, April 1987).
3. J. A. Valdmanis, G. A. Mourou, and C. W. Gabel, IEEE J. Quantum Electron. **QE-19-4**, 664 (1983).
4. K. J. Weingarten, M. J. W. Rodwell, H. K. Heinrich, B. H. Kolner, and D. M. Bloom, Electron. Lett. **21**, 765 (1985).

Quantum Nondemolition Detection and Four-Mode Squeezing

Typically, when a laser beam is measured with a photodetector, the light is absorbed. Thus information about the amplitude of the beam is obtained at the cost of its destruction. A portion of the beam can be diverted with a beam splitter and measured, leaving the remainder of the beam available for further measurements. At the quantum level, this also destroys any correlation between the amplitude of the detected beam and the transmitted beam. Both of these measurements are termed "quantum demolition" measurements because they do not provide information about the quantum state of the light subsequent to the measurement event. A method of measuring light amplitude which does not alter that amplitude would be valuable to experimentalists. Such a method has now been realized using nonlinear optics.

When a quantum-mechanical observable of some physical system is measured, the measuring apparatus unavoidably perturbs the system, introducing uncertainty in subsequent measurements of the same system. However, this uncertainty need not appear in the observable quantity that was measured (in this case the optical amplitude). Back-action-evading or "quantum nondemolition" (QND) measurement schemes[1] cause the perturbation of the system (the back action) to appear in observables conjugate to the one being measured, thus leaving the latter unchanged by the measurement process. The observable of interest (the QND observable) is coupled to a second system (the QND readout) in such a way that a measurement of the readout allows one to infer the value of the QND observable. In this way, repeated QND measurements of an observable can determine its evolution without disturbing it.

The nonlinear coupling between two light beams in a medium exhibiting the optical Kerr effect has the form suitable for a quantum nondemolition measurement of the amplitude of one of the light beams.[2] Such a QND measurement scheme has been demonstrated experimentally for the first time at the IBM Almaden Research Center in San Jose, California.[3]

In this experiment, the observable of interest was the amplitude modulation of one light wave (the signal beam), and the QND readout was the phase modulation of a second wave of different wavelength (the readout beam). The conjugate observable perturbed by the measurement was the phase of the signal beam, a quantity which cannot be measured directly. The two beams copropagated in a single-mode optical fiber. The nonlinear index of refraction of the fiber coupled the phases and amplitudes of the two beams.

The IBM experiment has demonstrated the quantum correlations between the QND readout signal and the amplitude fluctuations of the signal beam (the QND observable). Back-action evasion was not unequivocally confirmed, but was strongly suggested by the fact that the signal-beam amplitude fluctuations at both the input and output of the fiber were at the vacuum noise level to within the 2% experimental uncertainty. In other words, the interactions in the fiber added essentially no noise to the QND observable beyond that present at the input.

At the output of the fiber, the signal and readout beams were separated by a prism. The readout beam was reflected from an optical cavity that shifted the phase of its carrier wave with respect to the sidebands which carried the modulation information. This phase shift converts the phase fluctuation of the readout beam into amplitude fluctuations which can then be detected with a photodiode, and the fluctuations in this photocurrent constituted the QND readout signal. These fluctuations were shown to be strongly corre-

lated with the vacuum-level quantum fluctuations of the signal beam, by directly detecting the signal beam with a second photodiode, and electronically adding this "quantum demolition" signal to the QND readout signal. The resulting noise level was 5% below the vacuum level ("shot noise limit") as calculated for the signal-beam photodetector and 20% below the vacuum noise if both photodetectors are taken into account. Thus the correlations between the QND readout signal and the direct detection signal cannot be explained classically.

The quantum correlations observed among the four sideband modes (two for each beam) are the manifestation of the existence of a new kind of squeezed state, a "four-mode squeezed state."[4] This is in contrast to the usual two-mode squeezing which arises from quantum correlations between two modes, symmetrically placed about a single carrier frequency. Observation of four-mode squeezing can be accomplished by phase-sensitive homodyne detection with two local-oscillator waves, provided in the IBM experiment by the signal-beam and readout-beam carrier waves. As noted above, the overall noise level was 20% below the vacuum level, even though both detector signals taken individually exhibited noise levels above the vacuum level. This experiment is thus the first observation of a four-mode squeezed state.

The source of the non-negligible uncorrelated background noise level in these experiments is light scattering in the fiber owing to localized relaxational modes of the glass. This adds noise to the QND readout that is a factor of five larger in power than the noise that is correlated to the vacuum noise of the signal beam. Thus as a QND detector, this noise level is 7 dB above the standard quantum limit. An improved system, using optical fiber with a more favorable magnitude of optical nonlinearity compared to the light scattering cross section, would be useful for sensitive optical measurements where the standard quantum limit does not allow sufficient precision.

R.M. Shelby, IBM Almaden Research Center

1. C. M. Caves, K. S. Thorne, R. W. P. Drever, V. D. Sandberg, and M. Zimmerman, Rev. Mod. Phys. **57**, 341 (1980).
2. G. J. Milburn and D. F. Walls, Phys. Rev. A **28**, 2065 (1983); N. Imoto, H. A. Haus, and Y. Yamamoto, Phys. Rev. A **32**, 2287 (1987).
3. M. D. Levenson, R. M. Shelby, M. D. Reid, and D. F. Walls, Phys. Rev. Lett. **57**, 2473 (1986).
4. B. L. Schumaker, J. Opt. Soc. Am. **A2**, 92 (1985); B. L. Schumaker, S. H. Perlmutter, R. M. Shelby, and M. D. Levenson, Phys. Rev. Lett. **58**, 357 (1987) *Physics News in 1986*, p. S15.

Optical Associative Memories: First Step Toward Neuromorphic Optical Data Processing

Since the first optical associative memory was described and demonstrated in 1985,[1,2] work and interest in neuromorphic optical signal processing have been growing steadily, owing to improved techniques in neural net modeling and to the inherent capabilities of optics (parallelism and massive interconnectivity). Work in this area is evolving rapidly enough as to make it difficult to be aware of all relevant developments and to assess their implications for the purposes of this report. Some noteworthy work may therefore have been left out.

Work in optical associative memories is currently being conducted at several academic institutions (e.g., California Institute of Technology, University of Colorado, University of California at San Diego, Stanford University, University of Rochester, and the University of Pennsylvania) and at several industrial and governmental laboratories (e.g., Hughes Research Laboratories at Malibu and the Naval Research Laboratory, and more recently the Jet Propulsion Laboratory and the BDM Corporation). In these efforts, in addition to the vector matrix multiplication with thresholding and feedback scheme utilized in early implementations, an arsenal of sophisticated optical tools such as holographic storage, phase conjugate optics, and wavefront modulation and mixing are being drawn upon to realize associative memory functions. Such functions include auto-associative, hetero-associative, and sequential or cyclic storage and recall[3-8] with signal recovery from partial information receiving much attention as a potential application.[5,9,10]

It is gradually becoming clear, however, that associative memory is only one apparent function of biological neural nets that lends itself to optical implementation. Optics can play a useful role in the implementation of artificial neural nets capable of self-organization and learning (that is, self-programming nets). One can safely state that self-organization and learning is the most distinctive single feature that sets neuromorphic processing apart from other approaches to information processing. Learning in these nets is by adaptive modification of the weights of interconnections between neurons (plasticity). It can be supervised or unsupervised, deterministic or stochastic. To the author's knowledge, work on optical learning networks is currently being pursued by two of the groups mentioned earlier, the one at the University of Pennsylvania (Penn) and the one at the California Institute of Technology (Caltech).

Important progress in multilayered optical learning networks based on holographically interconnected nonlinear Fabry–Perot etalons has been achieved by the Caltech group.[11] Making use of a deterministic error back-propagation algorithm these nets can learn the connectivity weights that represent associations they are presented with. The focus in this work is on the use of volume holograms formed in photorefractive media, as opposed to planar holograms, for defining and storing the interconnectivity patterns between neurons. A clever fractal-based method for the implementation of arbitrary interconnects between input and output planes defined within the net's architecture with minimal cross-talk has also been devised and verified.

The effort at Penn focuses, on the other hand, on architectures and methodologies for opto-electronic implementation

of stochastic learning in self-organizing multilayered nets. This work derives from simulated annealing within the framework of a Boltzmann machine. Stochastic rather than deterministic learning is of primary interest because of its physical plausibility and because it can shed light on the way nature has turned noise present in biological neural nets to work to its advantage.

The primary result of this work so far is a scheme that combines optical random array generators with the parallelism of optics to accelerate stochastic learning by an estimated factor of 10^5 as compared to serial machine executions of the same learning algorithm. The scheme basically imparts to the neurons a random threshold component that produces controlled shaking of the "energy landscape" of the net which can, so to speak, shake the net loose whenever it tends to get stuck in a state of local energy minimum accelerating thereby search for the state of global energy minimum which is a required for the learning algorithm.[1,2]

The above work on optical learning nets is helping bring into focus the acute need for suitable materials and devices for the implementations of programmable interconnects and plasticity. Examples are modifiable nonvolatile volume holographic materials, spatial light modulators, and dense arrays of nonlinear light amplifiers or optically bistable elements.

Finally we close with a few remarks that might help indicate where the field of neuromorphic signal processing is headed. Biological neural nets were evolved in nature for one ultimate purpose: that of maintaining and enhancing survivability of the organism in which they reside. Embedding artificial neural nets in man-made systems and, in particular autonomous systems, can serve to enhance their survivability and therefore reliability. Survivability is also a central issue in a variety of systems with complex behavior encountered in biology, economics, societal models, and military science. One can therefore expect neuromorphic processing to play an increasing role in the modeling and study of such complex systems, especially if optical techniques can be made to furnish speed and flexibility. Finally, one should expect also that software development for emulating neural functions on serial and parallel digital machines will not continue to be confined to the realm of straightforward simulation, but, spurred by the mounting interest in neural processing, will move into the algorithmic domain where fast efficient algorithms may become to neural processing what the FFT was to the discrete Fourier transform. Thus we expect that advances in optical and digital neuromorphic signal processing will proceed in parallel.

Nabil H. Farhat, University of Pennsylvania

1. D. Psaltis and N. Farhat, Opt. Lett. **10**, 4 (1985).
2. N. H. Farhat, D. Psaltis, A. Prate, and E. Paek, Appl. Opt. **24**, 1469 (1985).
3. A. D. Fischer, C. Giles, and J. Lee, J.Opt. Soc. Am. **A1**, 1337 (1984).
4. D. Z. Andersen, Opt. Lett. **11**, 56 (1986).
5. B. Soffer, G. Dunnign, Y. Owechko, and E. Maron, Opt. Lett. **11**, 118 (1986).
6. A. Yariv and S. K. Kwong, Opt. Lett. **11**, 186 (1986).
7. B. Kosko and C. Guest, Proc. SPIE, 758 (in press).
8. M. Takeda and J. W. Goodman, Appl. Optics **25**, 3033 (1986)
9. N. Farhat, S. Miyahara, and K. S. Lee, in *Neural Networks for Computing*, edited by J. S. Denker (American Institute of Physics, New York, 1986), p. 146.
10. Y. S. Abu-Mustata and D. Psaltis, Sci. Am. **256**, 88 (March 1987).
11. K. Wagner and D. Psaltis, Proc. SPIE, 756 (in press).
12. N. Farhat, Opt. Lett. **12**, 448 (1987); also see N. Farhat and Z. Y. Shae, Proc. ICNN, San Diego, CA, 1987 (in press).

PLASMA AND FUSION PHYSICS

Advanced Tokamaks and a Path to Ignition

It has long been recognized that tokamak magnetic confinement experiments can be conducted with a standard circular plasma cross section or a plasma cross section extended along the axis of revolution and deformed into a modest crescent shape. Until the last several years, the circular tokamak was the most prevalent confinement configuration. Experiments in standard tokamaks contributed much to the understanding of plasma transport and resulted in the attainment of significant parameters such as surpassing the Lawson criteria[1]: that is, the product of central density and global confinement time exceeded 6×10^{19} sec/m^3. In addition the attainment of ion temperatures greater than 20 keV exceeded the minimum of 4.6 keV necessary for ignition.[2]

However, the conventional circular tokamak is now giving way to advanced tokamaks that have significantly elongated and highly shaped plasma cross sections, and "divertors" which define the plasma boundary magnetically. Elongated and shaped plasmas allow higher plasma current operation, which results in improved beta (the ratio of the plasma pressure to the magnetic pressure) values and energy confinement. Magnetic divertors also provide improved

confinement and unique control of the plasma edge. Radio-frequency heating allows one to elegantly control the heating profile is used in the advanced tokamak and is directly applicable to reactor requirements. All of these features are incorporated into the three advanced tokamaks presently operating in the world; JET (Joint European Torus, a joint undertaking of the European Atomic Energy Community), the DIII–D (at GA Technologies in San Diego), and PBX-U (the Princeton Beta Experiment-Upgrade at the Princeton Plasma Physics Laboratory). These features are also fundamental to the design of the CIT (Compact Ignition Tokamak), a device planned for operation in mid-1990 to investigate and understand the physics of heating via alpha particles arising from fusion reactions in an ignited plasma.

Experimental tests and magnetohydrodynamic (MHD) theoretical studies indicated that the advanced-tokamak approach would improve stability and confinement of high-temperature plasmas. Analysis of conventional tokamaks led to pessimistic conclusions regarding their ability to adequately confine the plasma pressure required to reach ignition and, ultimately, reactor conditions. The stability limit is referred to as the beta limit. High plasma pressure, thus high beta, is important since the fusion output power is proportional to plasma pressure squared.

The beta limit is theoretically predicted to manifest itself through localized helical distortions of the internal magnetic flux surfaces. These distortions tend to be larger or bulge in the weak toroidal field region of the plasma and are therefore called ballooning modes. In addition, helical distortions of the outer flux surfaces (called kink modes) are also expected to occur. Greatly enhanced energy transport is predicted as a consequence of ballooning modes. The simultaneous onset of ballooning and kink modes can lead to an instantaneous and uncontrolled termination of the discharge. Theory also predicts that the beta limit for both the kink and ballooning modes could be significantly increased by shaping the plasma into an elongated Dee shape and increasing the plasma current I. A series of experiments first performed on the Doublet III at GA Technologies, the predecessor of the DIII–D, and repeated on the PBX device at Princeton confirmed the theoretical prediction that the limit for beta is approximately equal to I/aB, where a is the minor radius of the plasma cross section and B is the magnetic field strength.

In these experiments both ballooning and kink type instabilities or modes were observed as one approached the limit, typically leading to a plasma termination within 10% of the theoretically predicted limiting beta value. This increase of beta with increasing I/aB has continued. The DIII–D recently achieved a record beta for a tokamak, 6.2%, in a stable, Dee-shaped, diverted plasma with an elongation 2:1 and an I/aB value of 2.5, 50% greater than previous experiments. This beta value, more than twice the maximum beta ever achieved in a conventional cylindrical tokamak, was approximately two-thirds of the predicted beta limit for the operating conditions. The plasma was stable, well confined, and exhibited no ballooning or kink type instabilities. In future experiments the DIII–D scientists will attempt to attain I/aB values up to 4.5 and beta values of up to 15%. This experiment will provide a significant test of present theoretical models for MHD stability.

A second benefit of the advanced tokamak is improved energy confinement. Earlier experiments in the shaped T-8 tokamak[3] in the USSR and the Doublet III[4] in the U.S. indicated that confinement improved with plasma elongation. With the application of auxiliary heating, both circular and noncircular tokamaks have demonstrated that confinement also improves with increasing plasma current. Since elongated advanced tokamaks can operate with significantly higher plasma currents they should realize greater energy confinement than comparable circular tokamaks. In addition, there may be further confinement benefits owing directly to the plasma elongation. Clarification of this issue is one of the elements of the present DIII–D research program.

A simplified magnetic divertor, first used by GA Technologies on the Doublet III and designed into the DIII–D and the CIT, offers benefits for impurity control and particle recycling, as well as confinement improvement. Experiments on the ASDEX tokamak in Germany were the first to demonstrate high confinement, referred to as the H-mode,[5] with high-power, neutral-beam heating and a magnetic divertor configuration. However, the ASDEX divertor configuration is rather complicated for use in an ignition device or a reactor. Recent neutral-beam heating experiments in the DIII–D, equipped with a simplified poloidal divertor, now demonstrates the H-mode for heating powers up to 6 MW[6] and for the first time ever with 0.9 MW of electron cyclotron heating (ECH) alone.[7] These divertor configurations with ECH heating are directly applicable to the CIT and future reactor compatible divertors. Density profiles of H-mode plasmas differ appreciably from standard discharges, indicating that magnetic divertor configurations affect plasma transport in a manner that was unanticipated theoretically and still remains largely unexplained.

The final element of the advanced tokamak is the utilization of radio-frequency (rf), or wave, heating. Since wave heating is typically a resonant phenomenon, it results in localized heating which allows unique control over the pressure profile which could result in even higher beta values than anticipated to date when combined with highly shaped plasma operation. In addition, it is thought that wave heating may provide more flexibility in attaining H-mode confinement. The investigation of ion cyclotron heating physics is being carried out in a number of tokamaks in the U.S. and abroad; however, only the circular T-10 device in the USSR, and the advanced DIII–D are addressing the physics of high-power electron cyclotron at the 90 GHz/4 MW and 60 GHz/2 MW levels, respectively. The ability to simultaneously generate significant plasma current and change the current profile in a way that enhances the beta limit and improve energy confinement may be corollary benefits from successful rf heating techniques.

All of the above elements of advanced tokamak physics—enhanced beta limits and confinement improvement through elongated shaped plasmas at high current, simplified magnetic divertors, and rf heating and current drive—are elements of the present DIII–D research program, and represent a significant evolutionary improvement in the magnetic confinement concept. These advances are all fundamental elements in the design of the CIT, which is expected to be the first device ever to attain and control an ignited plasma and will provide physicists the opportunity to study the physics of alpha heating. The present design for the CIT is very similar to the DIII–D device: slightly larger in major radius, and slightly smaller in minor radius as compared to the DIII–D, but with a similar elongation of 2:1 and a similar simplified magnetic divertor, ion and electron cyclotron heating capability. The CIT differs from DIII–D in that the CIT toroidal field of ten Tesla and plasma current of 9 MA are five and three times larger than the DIII–D capabilities, respectively. These magnetic fields will achieve the required conditions for ignition assuming that the energy confinement continues to scale linearly with plasma current. The MHD operational regime and the required beta values for ignition have already been successfully demonstrated in experiments on the DIII–D tokamak.

Advanced tokamak concepts, which presently are being tested in the DIII–D, JET, and PBX experiments, will provide the basis for success of the CIT program. With the attainment of ignition plasmas in the CIT, we will have realized a long sought-after goal and a new physics regime as yet unexplored. The outcome of this experiment will likely further improve the tokamak concept and contribute to the goal of controlled magnetic fusion as a potential energy resource.

David Overskei, GA Technologies, Inc., San Diego, CA

1. Phys. Today **37**, 20 (February 1984).
2. R. J. Goldston, *Physics News in 1986*, p. S-59.
3. E. I. Dobrokhotov *et al.*, *Plasma Physics and Controlled Nuclear Fusion Research* (Proc. 8th Int. Conf., Brussels, 1980), Vol. I; (IAEA, Vienna, 1981), p. 713.
4. M. Nagami *et al.*, Nucl. Fusion **22**, 3 (1982).
5. F. Wagner *et al.*, Phys. Rev. Lett. **49**, 1408 (1982).
6. K. Burrell *et al.*, Phys. Rev. Lett. (to be published).
7. R. Prater, Report GA–A19009, Sept. 1987, GA Technologies Inc.

Recent Progress in Laser Fusion

Inertial fusion is an inherently simple approach to producing fusion energy: the fuel would consist of small pellets injected into the center of a large chamber. The outside of the pellets would be heated either directly or indirectly by laser light or ion beams, with the hot blowoff driving the rest of the fuel inward to high density by a spherical rocket effect. An inertial fusion chamber would require no magnetic coils, and perhaps no high vacuum. The high-technology components, the laser or ion accelerator plus a pellet factory, could be located far from the chamber for easy access and maintenance.

Although the inertial fusion concept is simple in principle, it becomes somewhat more complex when examined closely. The fuel is accelerated by tens of megabars of pressure from the plasma corona and then compressed to several thousand times solid density. In the center of the cold, compressed fuel there is a hot central ignitor whose radius is 1–2% of the initial pellet shell radius. These inertial fusion pellets therefore require excellent symmetry of illumination, control of hydrodynamic instabilities, minimal preheat of the cold fuel by suprathermal electrons, and high rocket implosion efficiency.

There are two approaches to inertial fusion: direct and indirect drive. With direct drive, the laser or ion energy is focused directly on the fuel pellet. With indirect drive, the energy is first converted to soft x rays in a cavity hohlraum, and these x rays in turn drive the pellet. If direct drive works, it could potentially have higher energy gain because of one less energy conversion step. Theoretical estimates indicate that direct drive could achieve ignition at about 100 kJ and achieve pellet gains of a few hundred with a multi-megajoule laser.

This review will concentrate on inertial fusion using lasers, and on the U.S. program. Two facilities in the U.S. can implode pellets: the Nova laser at Lawrence Livermore National Laboratory and the Omega laser at the University of Rochester. Recently, Livermore scientists have shown x-ray pinhole photographs of an implosion in an optimized hohlraum. This indirectly driven implosion achieved a convergence ratio in excess of 30, in agreement with their spherical one-dimensional calculations. Also recently, University of Rochester scientists have obtained 50 times liquid density with direct drive implosions, slightly less than the 100–120 times liquid density reported earlier for indirect drive using the Shiva and Nova lasers.

The direct drive laser fusion approach has had to face the fundamental problem that large, high-power lasers have inevitable optical imperfections, and can only produce uniform illumination on target if special beam smoothing techniques are used. These techniques generally use an optical array at the laser output to split the beam into hundreds or thousands of independent randomly phased beamlets that are then overlapped on the target. Last year NRL proposed a simplified version that introduces the incoherence back at the oscillator rather than at the end of laser chain; this provides greater simplification and flexibility, and is suited for use with gas lasers such as KrF.

Historically, both direct drive and indirect drive were plagued by suprathermal electrons produced from laser–plasma instabilities. This problem was essentially solved by the switch to shorter laser wavelengths; it remains to be verified that these plasma instabilities are not harmful with the larger plasmas associated with a high-gain pellet. We also need to understand the impact of the spatial and temporal incoherence that is introduced by the optical smoothing techniques. A recent series of experiments at NRL has found that the combination of spatial and temporal incoherence

used with induced spatial incoherence (ISI) substantially ameliorates laser–plasma instabilities when compared with an ordinary laser beam, while the use of just spatial incoherence can actually enhance some of the plasma instabilities. There is a suspicion that many previous laser–plasma instability experiments may have been dominated by hot spots in the ordinary laser beams.

Last year it was discovered at Livermore that the x-ray conversion efficiency was not as high as previously thought. Scaling to a high-gain facility, the conversion is now predicted to be in the range of 50 to 70% instead of the earlier prediction of 90%. This is a substantial enhancement (a factor of 3 to 5) in energy that does not go into x rays, and will necessitate a redesign of indirect-drive targets. Recently, a joint experiment between Livermore and NRL found that the x-ray conversion efficiency was relatively 30% higher with ISI optics than with an ordinary laser beam. A joint experiment between Los Alamos National Laboratory and Rochester found a conversion efficiency of 60–70%, using the Rochester laser without any additional optical smoothing. These two results indicate that x-ray conversion efficiency is limited, in part, by laser beam nonuniformities.

Because of the many recent advances in laser fusion, and its potential for both civilian and military applications, there is renewed interest in driver development. The optimum laser for either direct or indirect drive would have both a short wavelength and a broad bandwidth (for ISI). The only such contender, the KrF laser, is under development at several laboratories, with the largest efforts in Japan and the U.S. Los Alamos is now completing a few-kilojoule KrF laser, and NRL has started a KrF development program. In Japan, 500- and 1000-J lasers are near completion, and 10- and 500-kJ lasers are being proposed.

S. E. Bodner, Naval Research Laboratory

1. S. E. Bodner, "Inertial Confinement Fusion," Nucl. Fusion **27**, 505 (1987).

High-Latitude Ionospheric Structure Simulation Studies

The high-latitude ionosphere (poleward of 70° latitude) is a region which exhibits a collection of rich and highly dynamic plasma phenomena. These phenomena primarily exist because of the direct electromagnetic connection to the magnetosphere, the plasma which is strongly influenced by the Earth's magnetic field. This field at high latitudes is effectively vertical, and allows the entry of energetic plasma and electromagnetic stresses into the ionosphere along magnetic field lines, causing polar ionospheric dynamics to reflect the dynamics of the outer magnetosphere. In addition, the boundary between the polar and mid-latitude ionosphere is itself a source of instability and structure since it is both the location of the auroral plasma and the boundary between trapped and untrapped plasmas in the Earth's magnetic field.

Computer simulation is an increasingly important tool used in an attempt to understand the growing body of complex observational plasma data from this region obtained with ground-based radar, rocket, and satellite observations. Initial simulation efforts focusing on the growth and evolution of ionospheric structure assumed that the dynamics of the structure were primarily local, that is, that there was no "feedback" to the evolution of such structures from the other plasma regions in the magnetosphere.[1] However, theory indicates that kilometer-size plasma irregularities in the high-latitude ionosphere result in electric fields which can propagate several Earth radii upwards along the Earth's magnetic field in the tens of seconds during which the ionospheric irregularities grow. The electric field dynamically couples all of the plasma throughout that magnetic field region to the development of the irregularities.

Recent two-dimensional simulations performed at the Naval Research Laboratory (NRL) have modeled the effect of this ionosphere–magnetosphere plasma coupling on the development of two major structure mechanisms in the polar regions: gradient-drift and velocity-shear instabilities.[2] For the gradient-drift instability, a plasma density gradient moving relative to the background neutral atmosphere in the ionosphere is unstable and causes rapid growth of structure in the plasma density if the effective neutral velocity is directed opposite to the density gradient. In the absence of coupling to the magnetospheric plasma, the instability produces "filaments" which are greatly elongated in the direction of the gradient and have a small width perpendicular to the gradient. Electrostatic coupling to the magnetospheric plasma increases the amount of plasma which is set in motion by the instability electric fields. This effective increase in the inertia of the ionospheric plasma slows the growth of the instability and interferes with the filament formation by coupling the structure growth in the two directions perpendicular to the magnetic field. The resulting structure is more isotropic and exhibits less elongation parallel to the density gradient than in the noncoupling case.

The theory and physical parameters of the high-latitude ionosphere–magnetosphere region suggest that coupling should play a role in the development of ionospheric structure, and, indeed, wave spectra taken from these simulations show a shallower spectrum than in the absence of coupling. This result is consistent with recent satellite data from the Dynamics Explorer of the plasma density and electric field spectra in the northern and southern polar regions. Three-dimensional simulation models of this coupling region are currently in development and should begin to clarify physical phenomena not addressed by the two-dimensional model, such as the electric structure parallel to the magnetic field.

Horace Mitchell, Science Applications International Corporation

1. See M. J. Keskinen and S. L. Ossakow, Radio Sci. **18**, 1077 (1983) and references therein.
2. See J. D. Huba *et al.* in "The Effect of the Ionosphere on Communications, Navigation, and Surveillance Systems," edited by John M. Goodman, Government Printing Office, 1987, and references therein.

POLYMER PHYSICS

The field of polymer physics continues to expand and overlap many areas of traditional physics. This has led to an increased commonality in the critical issues being addressed by the various physics disciplines. In fact, areas such as the glassy state and liquid crystalline polymers continue to attract considerable theoretical and experimental interest within the scientific community, serving as a focal point for those working on both small molecules and polymers. To an even greater extent the area of nonlinear optical materials has emerged as one in which polymer physics promises to make a significant impact. The momentum has clearly shifted from inorganic nonlinear optical materials to their organic counterparts, which include polymers. Activity in this area is expected to increase in the coming year.

Perhaps typical of the interdisciplinary nature of polymer physics in the 1980s is the selection of the following topics chosen for more explicit discussion. They represent illustrative examples of the role that polymer scientists have in helping unravel the physics of novel macromolecular structures.

John F. Rabolt, IBM Almaden Research Center

Thermochromism in Long Chain Polymers

Reversible thermochromism in long chain polymers is rare and, when it does occur, generally involves small shifts in the UV–visible absorption bands due to temperature induced changes in intermolecular interactions.

Although the first organosilane polymers (those having only silicon atoms in the backbone) were reported in 1924,[1] they evoked little scientific interest owing to their insolubility and intractability. Recently, however, soluble substituted polysilane derivatives have been synthesized that have both a Si backbone and alkyl side chains of various lengths.[2] These exhibit intriguing electronic properties. An intense UV–visible absorption, normally observed at wavelengths of 305–320 nm in all previously studied poly(di-*n*-alkylsilanes), is found at 370 nm in the spectra of crystalline poly(di-*n*-hexylsilane), poly(di-*n*-heptylsilane), and poly(di-*n*-octylsilane).[3,4] Furthermore, upon heating above 45 °C, this absorption was observed to shift to the 320-nm region, returning to 370 nm upon cooling. Thermal analysis of these poly(di-*n*-alkylsilanes) revealed a strong endothermic transition in the 40–45 °C range that was shown to correspond to a conformational change in both the polymer backbone and its side chains. Early spectroscopic results[3] suggested that the backbone existed in a planar zigzag conformation in the solid state at room temperature, giving rise to regions of extended trans conformation maximizing the overlap of electronic wave functions causing the absorption to occur at 370 nm. X-ray diffraction measurements[5–7] later confirmed that this was the case.

Detailed studies of the ambient and high-temperature phase were soon carried out using a number of characterization techniques[4–9] with the results indicating that: (1) the observed transition is reversible; (2) the transition involves the disordering of the alkyl side chains from the trans conformation to one which is more characteristic of a melt; (3) partial disordering of the backbone occurs, although many trans sequences remain; and (4) above the transition, the polysilane chains are packed effectively as cylinders on a hexagonal lattice with the orientation of the Si backbones unchanged. To further verify the latter result, conformational energy calculations were undertaken[10] so as to gain some insight into the most probable conformation adopted by the polysilane backbone above the transition. It was found that the lowest energy conformation for a poly(di-*n*-hexylsilane) chain is a 7/3 helix (every Si-Si bond rotated 30° and every Si-C bond rotated from trans). These results also indicated that it is intermolecular interactions in the crystal which lead to the planar zigzag structure at room temperature. Above 42 °C these intermolecular constraints are reduced owing to the disordering of the side chain, and the backbone adopts a disordered conformation perhaps having some similarity to the 7/3 helix suggested by the calculations[10] and recently verified[11] experimentally for poly(di-*n*-pentylsilane) in the solid state at room temperature.

To put this observation of reversible thermochromism in poly(di-*n*-alkylsilanes) in perspective, it is somewhat instructive to briefly explore some of the applications of these unique polymers. Perhaps the most obvious are those applications in the lithography[12] field, owing to the strong absorption of poly(di-*n*-alkylsilanes) in the UV. At these short wavelengths, submicron lithography becomes feasible. More recent reports of photoconductivity and nonlinear optical properties in related structures only foreshadow the exciting potential of these polymers in future optical and microelectronic applications.

John F. Rabolt

1. F. S. Kipping, J. Chem. Soc. **125**, 2291 (1924).
2. R. West, J. Organomet. Chem. **300**, 327 (1986).
3. R. D. Miller, D. Hofer, J. Rabolt, and G.N. Fickes, J. Am. Chem. Soc. **107**, 2172 (1985).
4. J. F. Rabolt, D. Hofer, R. D. Miller, and G. N. Fickes, Macromolecules **19**, 611 (1986).
5. B. L. Farmer, H. Kuzmany, J. F. Rabolt, and R. D. Miller, Bull. Am. Phys. Soc. **31**, 519 (1986).
6. A. J. Lovinger, F. C. Schilling, F. A. Bovey, and J. M. Ziegler, Macromolecules **19**, 2657 (1986).

7. H. Kuzmany, J. F. Rabolt, B. L. Farmer, and R. D. Miller, J. Chem. Phys. **85**, 7413 (1986).
8. F. C. Schilling, F. A. Bovey, A. J. Lovinger, and J. M. Ziegler, Macromolecules **19**, 2663 (1986).
9. W. W. Fleming, G. C. Gobbi, R. Sooriyakumaran, and R. D. Miller, J. Am. Chem. Soc. **108**, 5624 (1986).
10. B. L. Farmer, J. F. Rabolt, and R. D. Miller, Macromolecules **20**, 1167 (1987).
11. R. D. Miller, B. L. Farmer, W. Fleming, R. Sooryakumaran, and J. Rabolt, J. Am. Chem. Soc. **109**, 2509 (1987).
12. P. Trefonas III, R. West, and R. D. Miller, J. Am. Chem. Soc. **107**, 2737 (1985).

New Results on the Dynamics of Entangled Liquids

Recently, important advances have been made in understanding the dynamics of entangled polymer liquids. The most promising approaches have started from the work of de Gennes[1] and Doi and Edwards.[2] In their model, topological constraints between molecules confine each polymer to a tubelike region. The slithering motion, by which the polymer disengages from its old tube and forms a new one around itself, is called *reptation*. This article discusses current theoretical and experimental work directed at determining the importance of other processes that should compete with the basic reptation mechanism.

When the chain end of one polymer diffuses past the contour of another, it releases a constraint on the latter allowing some movement transverse to the tube. This process is called *tube renewal*, and it has a large effect on the relaxation of systems with a broad molecular weight distribution. Experiments in which a labelled diffusant penetrates into a matrix of a different molecular weight have demonstrated that tube renewal can be a dominant factor.[3] The concentration profile between a bilayer of hydrogenated and deuterated polymers can be determined from the elastic recoil of deuterons and protons when the sample is irradiated with alpha particles. In this way Green and Kramer[4] have obtained a quantitative description of the effect of molecular weight on the tracer diffusion coefficient. For linear polymers, the agreement between theory and experiment is excellent.[4]

By introducing branches or closing a molecule into a ring, it should be possible to stop the snakelike motion by which linear polymers move, and thereby force the molecule to relax by other means. New diffusion experiments on cyclic and branched polymers have been reported,[5] but the theoretical description for these cases requires further development.

Elastic recoil detection has also been used to measure the mutual diffusion coefficient of chemically dissimilar but compatible polymers.[6] Of particular interest is the case in which the diffusion couple is composed of isotopes of the same polymer. Near the critical point, induced by the small positive interactions between deuterated and protonated monomers, interdiffusion is substantially slowed. The interaction coefficient determined from recent diffusion experiments by Green and Doyle[7] is in excellent agreement with results obtained from the equilibrium structure factor by Bates and Wignall.[8]

Another process that can compete with reptation is *tube length fluctuation*. The average length of the confining tube can be decreased by a breathing motion that pushes out unentangled loops into the surrounding matrix. This causes additional relaxation to occur at the chain ends. A basic prediction of the reptation model is that the viscosity of linear polymers depends on the cube of molecular weight M. The fluctuation mechanism can cause a stronger dependence on M, such as $M^{3.4}$, for intermediate molecular weights but changing to M^3 at high molecular weights.[9] Until recently viscosity measurements on polymers did not reach sufficiently high molecular weights to test this prediction. To remedy this, Colby, Fetters, and Graessley[10] prepared polybutadienes with molecular weights as great as 1.6×10^7. The viscosities start as a power law with an exponent greater than three, but the new high molecular weight data suggests an asymptotic approach to M^3. The magnitude of the viscosity in this region is depressed by an amount consistent with the tube renewal interpretation of results obtained from diffusion.[4]

When a polymer has closely spaced relaxation times, it is almost impossible to resolve them by mechanical measurements. However, since the stress in a polymer liquid is proportional to its orientation, optical measurements sensitive to orientation can be used to overcome this problem.[2] This is accomplished by selectively labeling a portion of a polymer chain with dichroic or birefringent units. A number of research groups[11] have done this and shown that relaxation occurs most rapidly at the end of a molecule, in agreement with the basic reptation mechanism. Further analysis of the experimental data is expected to provide evidence for the rapid relaxation associated with tube length fluctuations. Optical experiments on blends of homopolymers have provided new information on tube renewal over a wide range of concentration and molecular weight.[12]

If it appears that we have a good understanding of the viscoelasticity of linear and branched polymers, recent experiments by McKenna and Kovacs[13] and Roovers[13] on macrocyclic polymers suggest that our knowledge of entangled liquids is far from complete. As stated, closing a polymer into a ring should turn off the basic reptation mechanism. An alternate relaxation process suggested by Klein[14] predicts that the viscosity of such materials should increase exponentially with molecular weight. However, the experiments show that entangled rings have viscosities smaller than linear polymers of the same length. Obviously our knowledge of disentanglement mechanisms is incomplete and the ring results provide a challenge for further theoretical and experimental developments.

Dale S. Pearson, University of California at Santa Barbara

1. P.-G. De Gennes, Phys. Today **36**, 33 (June 1983).
2. M. Doi and S. F. Edwards, *The Theory of Polymer Dynamics* (Clarendon Press, Oxford, 1986).
3. J. Klein, Macromolecules **14**, 480 (1981); M. F. Marmonier and L. Leger, Phys. Rev. Lett. **55**, 1078 (1985); M. Antonietti, J. Coutandin, and H. Sillescu, Macromolecules **19**, 793 (1986).
4. P. F. Green and E. J. Kramer, Macromolecules **19**, 1108 (1986).

5. C. R. Bartles, B. Crist, L. J. Fetters, and W. W. Graessley, Macromolecules **19**, 785 (1986); E. J. Kramer (preprints).
6. R. J. Composto, J. W. Mayer, E. J. Kramer, and D. M. White, Phys. Rev. Lett. **59**, 1312 (1986); R. A. L. Jones, J. Klein, and A. M. Donald, Nature **321**, 161 (1986).
7. P. F. Green and B. Doyle, Phys. Rev. Lett. **57**, 2407 (1986).
8. F. Bates and E. Wignall, Macromolecules **19**, 932 (1986).
9. M. Doi, J. Polym. Sci., Polym. Lett. Ed. **19**, 265 (1981).
10. R. C. Colby, L. J. Fetters, and W. W. Graessley, Macromolecules (to be published)
11. J. F. Tassin, L. Monnerie, and L. J. Fetters, Polym. Bull. **15**, 165 (1986); A. Lee and R. T. Wool, Macromolecules **20**, 1924 (1987); K. Osaki (preprint).
12. G. Fuller and J. Kornfield (private communication).
13. G. B. McKenna, G. Hadziioannou, P. Lutz, G. Hild, C. Strazielle, C. Straupe, P. Rempp, and A. J. Kovacs, Macromolecules **20**, 498 (1987); J. Roovers (preprint).
14. J. Klein, Macromolecules **19**, 105 (1986).

VACUUM PHYSICS

Thin Film Aspects of High-T_c Superconductors

Although many have asserted that the new high-T_c superconductors LaSrCuO and YBaCuO can be synthesized by school children, no one has said that thin films of these materials are easy to fabricate. Eight groups have succeeded in obtaining T_c's ($R = 0$) greater than 80 K. But only two have achieved a T_c ($R = 0$) greater than 89 K as of this writing. This is due at least in part to the granular nature of these materials and to the stricter requirements for percolation of a superconducting path in two dimensions as compared with three.

Thin films are contributing to the basic understanding of these materials for many of the same reasons that thin films have proved useful in the past. Not the least of these reasons is the fact that these well-characterized materials are useful for studying general physical property determinations (optical transmission and absorption, transport, etc.) and specific superconducting properties (coherence lengths, penetration depths, critical fields and currents, energy gaps, and tunneling spectroscopy).

Future electronic applications of these superconductors will depend on the existence of good thin films. These include SQUID instruments, high-speed analog and digital signal processing, and sensitive infrared sensors. Even the high-field, high-current applications of superconductivity, including magnetic shields, and ac power lines, may depend on films of these materials in the form of tapes should other methods involving bulk wires prove unable to overcome the problem of weak links between the superconducting grains. So far, high critical current densities have only been obtained in thin films.

Most of the standard thin film synthesis techniques have been applied to these materials and to some extent been found successful. For both LaSrCuO and YBaCuO these include: three-element electron beam co-deposition (IBM,[1] Stanford,[2] Cornell,[3] Westinghouse,[4] and Argonne[5]); three-element co-deposition using magnetron sputtering (Stanford,[6] Cambridge University[7]); sequential layering (Peking University[8]); molecular beam epitaxy (Varian/Stanford,[9] AT & T[10]), sputtering from a single oxide target with a compensated composition to allow for loss of certain elements (Tokyo University,[11] Nippon Telephone and Telegraph,[12] Electrotechnical Laboratory,[13] Matsushita Electric[14]—all in Japan—and AT & T[15]); laser evaporation of a sintered target (Bellcore/Rutgers,[16] Johns Hopkins University/NBS[17]); and ion beam deposition from a sintered target (Rockwell[18]).

The important parameters determining T_c have been found to be composition, substrate interaction, and the temperature of deposition or the temperature of the post deposition oxygen annealing. The crystal structure and, in particular, the texture of thin films formed from these highly anisotropic materials are extremely important in determining their physical properties. The sharpest transition and the highest T_c ($R = 0$) have been obtained with $SrTiO_3$ substrates. The available evidence suggests that the other substrates studied so far yield lower T_c ($R = 0$) (but very similar onset transition temperatures) owing to intergranular diffusion. Values of T_c ($R = 0$) in the range 89–90 K and transition widths of 1–2 K have been obtained by IBM[1] and by Stanford using three approaches.[2,6,9]

Evidence for tunneling has been obtained using sandwich junctions only in the case of LaSrCuO, and even here the results are controversial.[19] Energy values that are unexpectedly large, and remain unexplained, although the large anisotropy of these materials remains a possibility. Similarly the point contact tunneling results on these materials still are not understood.[20]

Critical current measurements on thin films have removed early doubts about the current carrying capacity of

these materials and contribute to hopes for high-current applications.[1] The critical currents reported early on bulk sintered powders at 77 K were dismally low, 10^3 A/cm^2, whereas the best thin film results at this time are greater than 10^6 A/cm^2. This latter result was obtained at Nippon Telephone and Telegraph.[12] Similarly high values were found by the Stanford group: 1.2×10^7 A/cm^2 at 4.2 K.[21,22]

Other measurements such as critical field and infrared transmission and reflection are currently in progress at the time of this writing.[21] Preliminary results suggest that these studies, like those discussed above, will yield new and important insights into the understanding of the mechanism of superconductivity in these materials.

R.H. Hammond, Stanford University

1. P. Chaudhari, R. H. Koch, R. B. Laibowitz, T. R. McGuire, and R. J. Gambino, Phys. Rev. Lett. **58**, 2684 (1987).
2. M. Naito, R. H. Hammond, B. Oh, M. R. Hahn, J. W. P. Hsu, P. Rosenthal, A. F. Marshall, M. R. Beasley, T. H. Geballe, and A. Kapitulnik (to appear in J. Mat. Res.).
3. D. Lathrop, S. Russek, and R. A. Buhrman, *Proceedings of the International Workshop on Novel Mechanisms of Superconductivity*, edited by V. Kresin and S. A. Wolf (Plenum, New York, 1987); (private communication).
4. A. I. Braginski, *Proceedings of the International Workshop on Novel Mechanisms of Superconductivity*, edited by V. Kresin and S. A. Wolf (Plenum, New York, 1987).
5. O. F. de Lima, J. Mattson, C. H. Sowers, and M. B. Brodsky (Argonne National Lab preprint).
6. K. Char, A. D. Kent, A. Kapitulnik, M. R. Beasley, and T. H. Geballe (submitted to Appl. Phys. Lett.).
7. R. E. Somekh *et al.*, Nature **326**, 857 (1987).
8. Z. L. Bao *et al.* (Peking University preprint).
9. C. Webb, S. L. Weng, J. N. Eckstein, N. Missert, K. Char, D. G. Schlomn, E. S. Hellman, M. R. Beasley, A. Kapitulnik, and J. S. Harris, Jr. (submitted to Appl. Phys. Lett.).
10. J. Kwo, T. C. Hsieh, R. M. Fleming, M. Hong, S. H. Liou, B. A. Davison, and L. C. Feldman (AT & T Bell Lab preprint).
11. M. Kawasaki *et al.*, Jpn. J. Appl. Phys. **26**, L738 (1987).
12. Y. Enomoto, T. Murakami, M. Suzuki, K. Moriwaki (NTT preprint).
13. N. Terada *et al.*, Jpn. J. Appl. Phys. **26**, L508 (1987).
14. H. Adachi *et al.*, Jpn. J. Appl. Phys. **26**, L709 (1987).
15. M. Hong, S. H. Liou, J. Kwo, and B. A. Davidson (to be published in Appl. Phys. Lett.).
16. D. Kijkhamp, T. Venkatesan, X. D. Wu, S. A. Shaheen, N. Jisrawi, Y. H. Min-Lee, W. L. McLean, and M. Croft, Appl. Phys. Lett. **51**, 619 (1987).
17. K. Moorjani *et al.*, Phys. Rev. B **36**, 4036 (1987).
18. P. Kobrin, J. DeNatale, R. Housely, J. Flintoff, and A. Harker (Rockwell International Science Center preprint).
19. M. Naito *et al.*, Phys. Rev. B Rapid Commun. **35**, 7228 (1987).
20. M. D. Kirk *et al.*, Phys. Rev. Rapid Commun. (to be published).
21. I. Bozovic, D. Kirillov, A. Kapitulnik, K. Char, M. R. Beasley, T. H. Gaballe, Y. H. Kim, and A. J. Heeger (submitted to Phys. Rev. Lett.).
22. B. Oh, M. Naito, S. Arnason, P. Rosenthal, M. R. Beasley, T. H. Geballe, R. H. Hammond, and A. Kapitulnik, J. Appl. Lett.

Atomic Force Microscopy

The scanning tunneling microscope (STM)[1] is the most well known of a family of instruments[2] which generate three-dimensional images of a surface by sensing the proximity of a sharp tip to the surface. Binnig, Quate, and Gerber recently introduced a device of this type called the atomic force microscope (AFM),[3] which can resolve the surface atomic structure both of conductors and (unlike the STM) of insulators. In the AFM, tip-surface forces are imaged by translating a sample near a force-sensing tip at the end of a flexible cantilever.[3–7] The normal force of the surface on this tip generates a deflection of the cantilever, which in the original AFM[3] was measured by the tunneling current between a (second) nearby conducting tip and the cantilever. Both this tunneling method and interferometric deflection detection[4,5] are sufficiently sensitive to detect forces several orders of magnitude less than 10^{-8} N (10^{-6} g weight), which is the strength of a single chemical bond.

Atomic resolution images of repulsive tip-surface forces have been obtained in the air[8,9] and under an oil film,[6] using tips of microfabricated SiO_2[8,9] and fractured diamond.[6] Although STM images of graphite distinguish strongly between two electronically inequivalent types of surface atoms,[10] AFM images can show a more nearly symmetric honeycomb pattern characteristic of the expected physical interaction with the topmost atomic layer.[6,8,9] Images of monatomic steps on a NaCl surface,[6] and of the atomic structure of MoS_2 and BN surfaces[9] have also been recorded.

Frictional forces were observed to vary periodically at the graphite lattice spacing[11] by interferometrically detecting the deflection of a tungsten wire *parallel* to a graphite surface. In a study designed to clarify the role of forces in scanning *tunneling* microscopy,[12] the normal forces in an operating STM were measured directly while a constant current STM image of graphite was recorded.[13] Such forces can also be deduced in a conventional STM from the frequency spectrum of current fluctuations due to the thermally induced vibration of a flexible sample.[14]

To attain the ultimate sensitivity limit imposed by thermal excitation of the lever,[3,4,5,14] for measuring small forces, it is useful to oscillate the cantilever of an AFM at its resonance frequency. This resonance technique has been combined with laser heterodyne interferometry to profile the weak long-range attractive dispersion force between the tip and sample.[5]

Ferromagnetic tips have been used to image with 100 nm resolution magnetic fields above a magnetic recording head[15] and above optically recorded domains in a TbFe film,[16] and preliminary magnetic images of a Ni film have been reported.[17] Capacitative profiling of conductors has been achieved by sensing the electrostatic force between an electrically biased tip and a surface.[13]

In the near future we can expect the AFM to be applied to well-characterized surfaces in ultrahigh vacuum, and to continue to be used not only as a structural tool, but also as a method for understanding the nature of electromagnetic, chemical, and frictional forces on a microscopic scale.

Gary M. McClelland, IBM Almaden Research Center

1. G. Binnig and H. Rohrer, IBM J. Res. Dev. **30**, 355 (1986); Calvin Quate, Phys. Today **39**, 26 (August 1986).
2. R. Young. J. Ward, and F. Scire, Rev. Sci. Instrum. **43**, 999 (1972); D. W. Pohl, W. Denk, and M. Lanz, Appl. Phys. Lett. **44**, 651 (1984); C. C. Williams and H. K. Wickramasinghe, Appl. Phys. Lett. **49**, 1587 (1986); P. Muralt and D. W. Pohl, Appl. Phys. Lett. **48**, 514 (1986); J. R. Matey and J. Blanc, J. Appl. Phys. **57**, 1437 (1985).
3. G. Binnig, C. F. Quate, and Ch. Gerber, Phys. Rev. Lett. **56**, 930 (1986).
4. G. M. McClelland, R. Erlandsson, and S. Chiang, *Review of Progress in Quantitative Nondestructive Evaluation* edited by D. O. Thompson and D. E. Chimenti (Plenum, New York, 1987), Vol. 6B, p. 1307.
5. Y. Martin, C. C. Williams, and H. K. Wickramasinghe, J.Appl. Phys. **81**, 4723 (1987).
6. O. Marti, B. Drake, and P. K. Hansma, Appl. Phys. Lett. **51**, 484 (1987).
7. H. Heinzelmann, P. Grütter, E. Meyer, H. Hidber, L. Rosenthaler, M. Ringger, and H.-J. Guntherodt, Surf. Sci. (to be published).
8. G. Binnig. Ch. Gerber, E. Stoll, T. R. Albrecht, and C. F. Quate, Europhys. Lett. **3**, 1281 (1987).
9. T. R. Albrecht and C. F. Quate (submitted to J. Appl. Phys.)
10. I. P. Batra, N. Garcia, H. Rohrer, H. Salemink, E. Stoll, and S. Ciraci, Surf. Sci. **181**, 126 (1987).
11. C. M. Mate, G. M. McClelland, R. Erlandsson, and S. Chiang (submitted to Phys. Rev. Lett.).
12. J. H. Coombs and J. B. Pethica, IBM J. Res. Dev. **30**, 455 (1986); J. B. Pethica and W. C. Oliver (submitted to Phys. Scr.).
13. R. Erlandsson, G. M. McClelland, C. M. Mate, and S. Chiang (submitted to J. Vac. Sci. Tech.).
14. U. Dürig, J. K. Gimzewski, and D. W. Pohl, Phys. Rev. Lett. **57**, 2403 (1986).
15. Y. Martin and H. K. Wickramasinghe, Appl. Phys. Lett. **50**, 1455 (1987).
16. Y. Martin, H. K. Wickramasinghe, and D. Rugar (submitted to Appl. Phys. Lett.).
17. J. J. Sáenz, N. Garćia, P. Grütter, E. Meyer, H. Heinzelmann, R. Wiesendanger, L. Rosenthaler, H. R. Hidber, and H.-J. Güntherodt (submitted to Appl. Phys. Lett.).

Laser Surface Chemistry

Laser light has been used in several innovative ways for the materials processing or microfabrication of microelectronics components. A particularly exciting approach involves optical stimulation or control of chemical reacations needed for materials growth, etching, or deposition. The importance of laser chemistry has been demonstrated for techniques ranging from ultrahigh-rate writing by microscopic thermal reactions to the more subtle low-temperature, chemically selective, epitaxial growth over large areas.

During this last year, important breakthroughs have been made in the applications of laser writing. This technique uses a tightly focused laser beam to cause a micrometer-scale chemical reaction. Deposition or etching processes are driven as the beam is scanned across a substrate. One major advance is the demonstration of the direct writing of metal interconnects, and the etching of components on a working GaAs wafer.[1] These techniques permit the ready reconfiguration for design and testing of an experimental MESFET circuits. In one case,[2] a sequence of laser-etching of amorphous silicon, followed by reactive ion etching of gold has resulted in such high writing rates that customization for bipolar logic integrated circuits can be generated in less than an hour.

Other more basic improvements in laser writing are in store. For example, two groups have used focused laser chemistry to write GaAs structures epitaxially on GaAs wafers.[3] This procedure would allow *in situ* patterning of small and compact features during the epitaxial growth of, for example, monolithic type *III–V* chips.

The interest in the practical results of laser-surface chemistry has also generated a substantial amount of research on fundamental phenomena in photon-driven chemical reactions. For example, recent photofragmentation studies using time-of-flight mass spectrometry have begun to delineate the physics of photodecomposition on surfaces for the first time. In one type of study, ultraviolet radiation from an excimer laser dissociated CF^3Br molecules on LiF, a relatively passive substrate.[4] The study found that while the energetics of decomposition were in many ways similar to the gas-phase process, collisions of the laser-produced species with the surface and other adsorbed molecules altered the fragment energy distribution.

Further, on semiconductor surfaces, it is now becoming clear that ultraviolet light can also greatly influence surface reactions. The effects are manifest, for example, in photon-assisted semiconductor oxidation. Several previous experiments using ultrahigh vacuum had clearly demonstrated that photogenerated electron–hole pairs on semiconductor surfaces can accelerate oxidation rates on GaAs.[5] Related investigations had also shown that photogenerated carriers also play an important role in the related process of semiconductor photohalidization.[6] Within the last year, anomalously high oxidation rates were observed when deep-UV light (250 nm) was used in the photooxidation process.[7] This effect, which appears only at high oxide coverage, is photochemical in origin since a very low photon flux is needed to observe it. The details of this mechanism, including the possibility of "hot" carrier injection into the oxide, are being studied.

Laser techniques are also being used to study the basic electronic structure of surfaces. For example, picosecond UV lasers have also been used for the first time to probe the dynamics of surface states above the Fermi level. In these experiments, a pulsed, two-wavelength, pump/probe system was used to investigate the surface states of InP and GaAs.[8]

An important result of such fundamental studies is the development of other new semiconductor processing techniques. An excellent example is the recently developed maskless method for the patterning of aluminum on semiconductors and other substrates.[9] This development greatly simplifies the process of IC metallization. The approach is based on an earlier discovery that laser photodissociation of organometallic molecular layers on the substrate can initiate the nucleation of metal films upon which subsequent film growth is selectively enhanced.[10]

R.M. Osgood, Columbia University

1. J. Black *et al.*, Appl. Phys. Lett. **50**, 1016 (1987).
2. F. Mitlitsky *et al.*, Abstract, CLEO-87, Baltimore (1987).
3. N. H. Karam *et al.*, Appl. Phys. Lett. **49**, 14 (1986); B. Dai *et al.*, Appl. Phys. Lett. **49**, 785 (1986).
4. E. B. D. Boudon *et al.*, J. Phys. Chem. **88**, 6100 (1984); E. L. Tabarbes *et al.*, J. Phys. Chem.; J. Cowin *et al.*, J. Chem. Phys. **86**, 739 (1987).
5. W. G. Petro *et al.*, J. Vac. Sci. Tech. **21**, 405 (1982); F. Bartels *et al.*, Surf. Sci. **143**, 315 (1986).
6. F. Houle, Chem. Phys. Lett. **95**, 5 (1983).
7. C. F. Yu *et al.*, J. Vac. Sci. Tech. (Aug. 1987).
8. R. Haight *et al.*, Phys. Rev. Lett. **54**, 1302 (1985); R. Haight *et al.*, Phys. Rev. Lett. **56**, 2846 (1986).
9. G. Blonder *et al.*, Appl. Phys. Lett. **50**, 766 (1987).
10. D. J. Ehrlich *et al.*, Appl. Phys. Lett. **38**, 1 (1981); J. Y. Tsao *et al.*, Appl. Phys. Lett. **45**, 617 (1984).

NOBEL PRIZE IN PHYSICS

J. Georg Bednorz and K. Alex Müller of IBM were awarded the 1987 Nobel Prize in physics for their discovery of superconductivity in a new class of materials. This marks the second year in a row that scientists from IBM's Zürich Research Laboratory have won the physics Nobel Prize. Last year Heinrich Rohrer and Gerd Binnig were honored for their work on the scanning tunneling microscope.

Ever since 1911, when Kammerlingh Onnes first observed superconductivity, in a sample of mercury at a temperature of 4 K, scientists have tried to discover materials that became superconducting at less severe temperatures. After decades of research, however, the record for highest transition temperature (T_c), as late as 1973, was no more than 23 K. Superconductivity research at that time and since centered primarily on transition-metal compounds, such as niobium–germanium. Efforts to find higher T_c materials proved so frustrating that some theorists came to suspect that some kind of natural limit had been reached, at least if superconductivity were indeed moderated by the exchange of phonons (distortions propagating through the lattice of atoms in the sample) between pairs of electrons, as prescribed by the Bardeen–Cooper–Schrieffer (BCS) theory.

This situation changed dramatically last year. In January 1986 Bednorz and Müller, working not with intermetallics but with oxides, observed a transition to superconductivity above 30 K for a compound made of lanthanum, barium, copper, and oxygen.[1] Later in 1986, after news of the Bednorz–Müller work had spread, scientists in Japan, China, and the U. S. quickly sought to explore the new class of ceramic superconductors. By February 1987 Paul Chu at the University of Houston and other groups had succeeded in pushing T_c above 90 K in compounds of yttrium, barium, copper, and oxygen. Such an achievement was important not only because superconductivity at temperatures above that of liquid nitrogen (which is relatively cheap to produce) may facilitate a greater and more economical use of superconducting devices, but also because it may herald a new phenomenon, a form of superconductivity not accounted for by the BCS theory.

The frantic pursuit of ever higher T_c's and improved material samples in early 1987 culminated in the so-called Woodstock of Physics, an all-night session at the March meeting of The American Physical Society in New York,[2] at which more than 50 speakers from around the world delivered papers. Since that time, the highest T_c has not changed much, but other figures of merit, such as the maximum current density and the maximum magnetic field strength that can be tolerated by the superconducting oxides, have been greatly increased. Details of recent work in this area can be found in the chapters on condensed matter physics, crystallography, vacuum physics, and industrial physics.

Phillip F. Schewe, American Institute of Physics

1. J. G. Bednorz and K. A. Müller, Z. Phys. B **64**, 189 (1986).
2. Phys. Today **40**, 17 (April 1987).